SNAP-23A PROGRAM POST-TEST ANALYSIS PLAN AND REPORT

VOLUME II
ANALYSIS REPORT

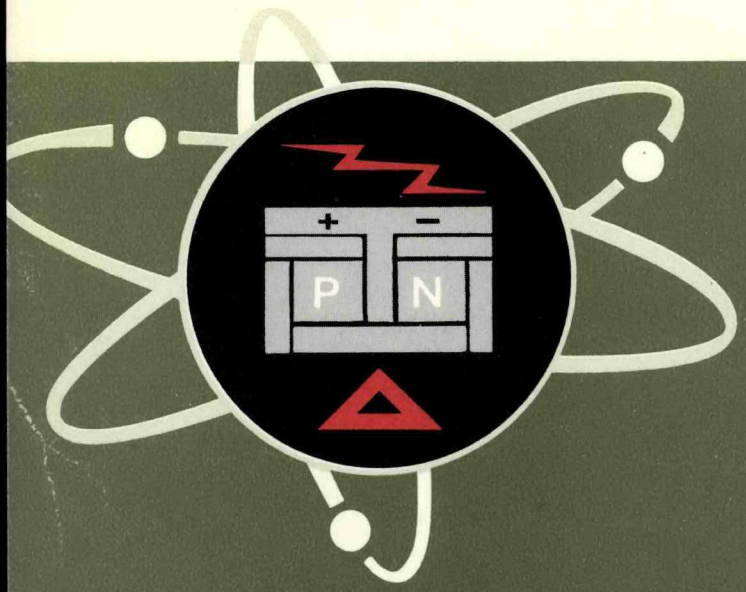

3M Isotope Power Products
MINNESOTA MINING & MANUFACTURING CO.
2501 HUDSON ROAD, ST. PAUL, MINN. 55119 PH. 631-2500

DISCLAIMER

Report No. MMM 3824-0002

AEC RESEARCH AND DEVELOPMENT REPORT

SNAP-23A PROGRAM
POST-TEST ANALYSIS PLAN AND REPORT

VOLUME II
ANALYSIS REPORT

NOVEMBER 1967

Prepared by
D.R. Field
Physicist

Approved by
G.W. Bunde
Test Supervisor
D.D. Schley
SNAP-23A
Program Manager

Issued by

SPACE AND DEFENSE PRODUCTS

MINNESOTA MINING AND MANUFACTURING COMPANY
ST. PAUL, MINNESOTA 55119

page blank

FOREWORD

The following document reports the plan for and work conducted under the SNAP-23A Program, Task III, SNAP-23 post-test analysis effort. The report consists of two volumes. Volume I contains the post-test analysis plan and Volume II contains the report of the post-test analysis disassembly, observations, results and conclusions drawn from the results.

page blank

TABLE OF CONTENTS

TABLE OF CONTENTS (Continued)

TABLE OF CONTENTS (Continued)

TABLE OF CONTENTS (Continued)

LIST OF FIGURES

LIST OF FIGURES (Continued)

LIST OF FIGURES (Continued)

LIST OF TABLES

LIST OF TABLES (Continued)

1.0 INTRODUCTION

1.1 GENERAL

The SNAP-23 six-couple Module A-2 and 252-couple prototype Converter P-1 were disassembled for post-test analysis. The post-test examination was conducted in accordance with Section 5.4.3.1 of the SNAP-23A Phase I Program Plan, Volume I, Report No. MMM 3824-0005. The general post-test procedures are described in Volume I - Analysis Plan of this report. The two thermopiles were disassembled and their components analyzed to determine any change in the thermoelectric materials, other materials or components to the extent that such changes would affect device performance.

Module A-2 was composed of six couples electrically connected in series within a parallel plate configuration using a nominal contact pressure of 150 psi at each hot electrode interface. A nominal hot electrode temperature of 1100°F and cold electrode temperature of 190°F was maintained throughout the module's life (18,100 hours). The six-couple module was designed and built to evaluate the performance of the SNAP-23 thermoelectric couple geometry, and to determine its long-term stability. Except for the cold electrodes and barrier discs between the hot and cold P-type segments, the couples were of the same geometric configuration as used in the P-1 and P-2 converter prototypes. The cold electrodes were different, being of a different geometry, and were not nickel plated as in the prototypes. During the 18,100 hours of thermoelectric performance, the module output power had degraded to 85 percent of the original power value (an approximate power degradation rate of one percent per 1000 hours).

The converter prototype was a full-size, 252-couple SNAP-23 thermopile. The 252 couples were connected in series in a cylindrical design with a nominal contact

pressure of 250 psi at each hot electrode interface. The couples used copper electrodes which were nickel plated to retard diffusion of the electrode base metal into the thermoelectric material.

The converter operated at a nominal hot electrode temperature of 1065°F, and cold electrode temperature of 200°F. During the 10,800 hours of test operation, the output power appeared relatively stable (within the resolution of measurement accuracy).

1.2 OBJECTIVES

The primary objective of the post-test examination was to attempt to establish potential failure or degrading mechanisms within the converter and module. Both the converter prototype and the module had anomalies in their thermoelectric performances during life testing. These anomalies dictated the principal areas of investigation during the post-test tear-down and analyses of the converter and module.

1.3 SCOPE

The principal areas of investigation were:

- Changes in gas environment (Leak and Gas Analyses)
- Visual changes in components (Visual Analysis)
- P and N legs-hot junction electrical contact resistance (Extraneous Resistance Analysis)
- Deformation of the couples (Converter P-1 Alignment Analysis, Spring Pressure Analysis, and Dimensional Analysis)
- Cold end thermal conductance changes (Thermal Conductance Analysis)
- Thermoelectric N and P leg performance changes (Thermoelectric Analysis)
- Metallurgical changes within the P-N thermoelectric hardware (Chemical Analyses of Couples)

Each of the principal areas of investigation are discussed in the subsections shown in parenthesis following the area in the above listing. Each subsection is self-supporting and can be read without reference to other sections of the report.

2.0 SUMMARY

Module A-2 had large fluctuations in output power. The output increased over the first 2000 hours from 1.46 to 1.75 watts but decreased thereafter.

The initial increase in power was due to a decrease in resistance across the P leg-hot electrode contact regions. The final power degradation was due to a decrease in Seebeck voltage for the P legs and an increase in resistance across the N leg-hot electrode contact regions. P leg Seebeck voltage degradation was due to copper migration into the cold end segment material ($(BiSb)_2Te_3$-TPM-29) and a loss of manganese from near the hot end segment material (PbTe-SnTe – TPM-76).

Converter P-1 operated stably for 10,800 hours. The higher spring pressure and lower hot electrode temperatures were probably major contributing factors to the stable performance.

There was significant misalignment of legs within the converter. The legs near the bottom of the converter had their hot electrodes misaligned approximately 0.066 inch during operation. The misalignment had no apparent affect on the converter performance.

There was an increase in thermal impedance between the cold caps and cold frame of the converter during operation. The increase in thermal impedance was caused by the inability of the heat transfer grease to maintain good thermal contact between the cold caps and followers.

A coating of nickel on the cold caps appears to restrict the copper migration into the cold segment material.

3.0 DESCRIPTION OF SPECIMEN

This section describes prototype Converter P-1 and Module A-2, including their performance histories.

3.1 PROTOTYPE CONVERTER P-1

3.1.1 PHYSICAL DESCRIPTION

Prototype Converter P-1 (Figure 2-1, Volume I) consists of 252 couples, connected in series through mild steel hot electrode caps and iron-plated copper hot shoes at the hot end, and nickel-plated copper cold caps and copper jumper wires at the cold end. The thermopile is designed in a cylindrical configuration with the thermoelectric legs positioned between two concentric cylinders. The thermoelectric couples utilize pressure contacts at the hot electrode caps. This pressure contact is provided by a spring and follower arrangement from the cold cap into the aluminum outer cylinder cold frame. The inner cylinder hot frame and converter outer case are constructed of 304 stainless steel. Hot side electrical insulation is boron nitride; internal thermal insulation is powdered Min-K 1301. The followers are aluminum with a hard coat of aluminum oxide. The converter is hermetically sealed and backfilled with xenon gas. The heat required to operate the converter is provided by the heat source which is mated to the tapered hot frame surface. In practice, heat would be provided by the system; however, for operation of Converter P-1 which was tested as a system component, heat was provided by a bench top heat source simulator (resistance heater cartridges located within a copper accumulator inside the inner hot frame cylinder).

3.1.2 DEFINITION OF TERMS

In order to adequately describe the performance characteristics of the converter, it is necessary to define a few terms:

1) Axial Row is a row of legs confined in the same plane as the vertical axis of the hot frame. There are a total of 36 axial rows. The output terminal P and N legs are located in rows 17 and 18 respectively. All of the rows are numbered in consecutive order.

2) Radial Row is a row of legs encircling the hot frame in a plane normal to the vertical axis. There are a total of 14 radial rows starting with number one at the top of the converter. The output terminal P and N legs are located in radial row one.

3) Notation - The following notation will be used in this report:

   - Leg Position (e.g. R1A18) identifies the position of a leg in the converter. R1A18 would be the leg in radial row 1 and axial row 18, and is the output terminal N leg.

   - Parameter (e.g. P_{cn}) identifies the particular thermoelectric parameter in question. Resistance, open circuit (Seebeck) voltage, and matched load power will be identified by the letters R, E, and P respectively. Each letter will have two indices. The first index (either x or c) identifies the parameter as either a quantity measured during life testing (x), or a quantity anticipated (calculated) according to design estimates at a given measured hot and cold electrode temperature (c). The second index (N, P, C, or O) identifies what is being measured as an N leg (N), P leg (P), Couple (C), or circuit (O). Therefore, P_{cn} would be the anticipated design match load power output for an N leg at a given measured hot and cold electrode temperature. Hot electrode temperatures, cold electrode temperatures, cold frame temperatures, and power input to converter thermopile will be identified as T_h, T_c, T_{cf}, and P_{in} respectively.

3.1.3 INSTRUMENTATION

This section discusses how the converter was instrumented.

3.1.3.1 Pressure Transducer

A pressure transducer located at the side of the converter above the fins measured the internal pressure of the converter.

3.1.3.2 Temperature Measuring Thermocouples

Two couples (both N and P legs) were instrumented with iron-constantan thermocouples at both the hot and cold electrodes. The instrumented P and N legs were located at the extreme top and bottom of the thermopile (i.e., radial row 1 and radial row 14). The iron-constantan thermocouples were either welded to the hot buttons or soldered to the cold caps.

In addition, there were thermocouples positioned at various locations throughout the thermopile and outer casing for the purpose of evaluating the converter and fin system thermally. The thermocouples were located at the inside and outside surfaces of the cold frame, inner and outer portions of the radiator fins, and in the hot frame near the top of the thermopile.

3.1.3.3 Voltage Instrumentation

The output open circuit (Seebeck) voltage and load voltage were measured from voltage taps located at the cold caps of the output P and N terminal legs. The individually monitored couples were measured via iron thermocouple leads. The load current was determined by measuring the voltage drop across a calibrated resistance (shunt) in series with the output load.

3.1.3.4 Power Instrumentation

An AC wattmeter was used to monitor the input power to the heat accumulator.

3.1.4 PERFORMANCE EVALUATION

During heat-up and the remainder of the thermal gradient testing, the electrical performance of the two monitored couples (and their legs), along with the whole circuit, was evaluated.

To evaluate the electrical performance, the open circuit (Seebeck) voltage, load voltage, and load current were measured. From these measurements, internal resistance and power output were calculated.

All strategically placed thermocouples were monitored and recorded.

3.1.5 DATA MONITORING

The data was monitored approximately as follows:

- First three days – three times daily.
- Next three days – daily.
- Thereafter – monitored at irregular intervals ranging from one to three weeks.

There were four periods when the converter was not in operation (cold). They were:

- A one-week period after 50 hours of operation. This was caused by a heater failure.
- A four-day weekend period after 100 hours of operation.
- A four-week period after 4300 hours. Caused by a heater failure.
- A five-month period after 6800 hours of operation.

After each dormant period, the converter was energized and monitored daily for approximately a week. Thereafter, the converter was monitored irregularly, from one to three weeks.

All thermal and electrical performance parameters monitored during the thermal gradient tests are shown in Table 3-1.

Table 3-1. Monitored Parameters

Parameter	Comment
Open circuit and load voltage	A primary measurement: circuit, couple and each N and P leg of two couples from radial row one and radial row fourteen.
Load Current	A secondary measurement: for circuit.
Internal Resistance	A calculation: circuit, couple and each N and P leg of two couples from radial row one and radial row fourteen.
Power Output	A calculation: circuit and two couples from radial row one and radial row fourteen.
Power Input	A primary measurement.
Temperature	The following temperatures are measured: hot frame, inside and outside cold frame, six fin positions, hot and cold electrodes of two couples.

3.1.6 ENVIRONMENTAL CONDITIONS

The variables which influence the operating conditions of the converter are:

- Electrode temperatures.
- Backfill gas type and pressure.
- Hot electrode contact pressure.
- Electrical loading.

3.1.6.1 Electrode Temperatures (Figure 3-1)

During test operations, the hot electrode temperatures fluctuated from 1000°F to 1160°F at the bottom (row 14), and 950°F to 1100°F at the top (row 1). The temperature-time characteristics can be divided into two parts:

- First 3500 hours were temperature stable. The converter was carefully monitored and maintained at a nominal hot electrode temperature of 1045°F (top) and 1095°F (bottom).
- The converter was not monitored as closely during the remaining period of operation which resulted in large thermal drifts at the hot electrode.

The cold electrode temperature was controlled only by the radiator; therefore, the cold electrode temperature was subject to variations caused by changes in hot electrode temperature, cold-end thermal impedance, and variations in the test room environment. However, the cold electrode temperature remained relatively stable (nominal 200°F) throughout the test operation.

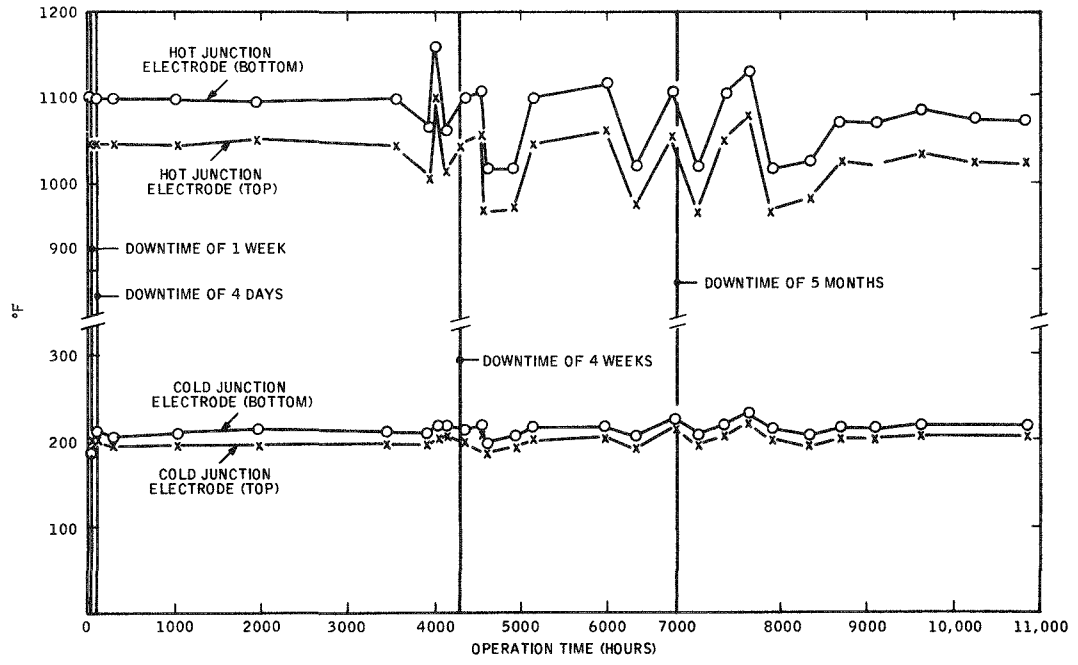

Figure 3-1. SNAP-23 Converter P-1 Hot and Cold Electrode Temperatures

3.1.6.2 Backfill Gas and Pressure

The internal gas environment was xenon at a pressure of approximately 27 psia at operational temperatures. The initial gas composition was 100 percent xenon (ultra-pure grade).

3.1.6.3 Hot Electrode Contact Pressure

The hot electrode mechanical contact pressure was approximately 250 psi for each thermoelectric leg.

3.1.6.4 Electrical Load

During the entire period of testing, the circuit was maintained at matched load conditions. This corresponded to a load voltage of approximately 25 volts and a load current of 2.7 amperes.

3.1.7 PERFORMANCE

Prototype Converter P-1 was placed on test 21 June 1965. The test was terminated on 12 April 1967. A total of 10,847 hours of test time was accumulated. The converter was stable throughout the test period except for small thermal changes, and an initial power decrease of 5 percent and then a return to the beginning-of-life level by approximately 3000 hours of operation.

A summary of the thermoelectric performance characteristics for the converter is shown in Figure 3-3 and Table 3-1 of Volume I and Figures 3-2 through 3-6 of this volume. To facilitate analysis regardless of hot and cold electrode temperature fluctuations, the power output, internal resistance, and open circuit voltage data for the circuit have been normalized in the Volume II presentation. The three parameters are expressed as a ratio of measured value to calculated value at the measured temperatures. The calculated value is based on experimental tests and does not include any extraneous resistances from jumper straps or hot junction electrical contacts. The results are shown in Figure 3-2. Seebeck voltage and resistance characteristics of individually monitored thermoelectric legs, are in Figures 3-3 and 3-4. The measured resistances in Figure 3-4 include portions of the hot and cold electrodes, thermoelectric leg, and the thermoelectric leg-hot button contact.

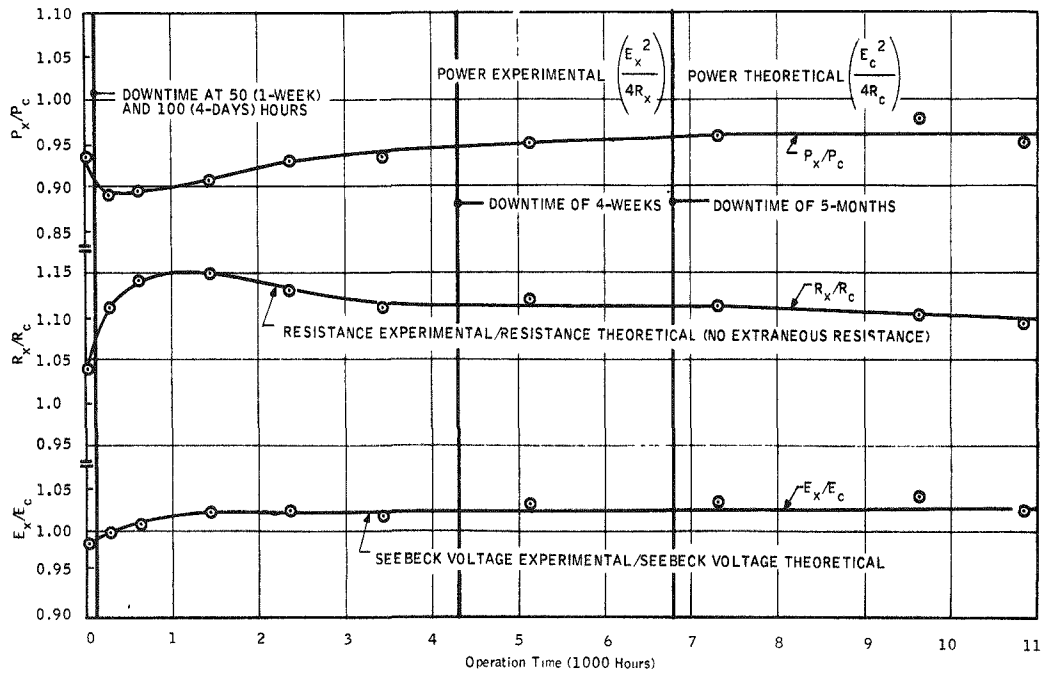

Figure 3-2. SNAP-23 Converter P-1 Performance (3M-39-P1) — Experimental/Theoretical Data

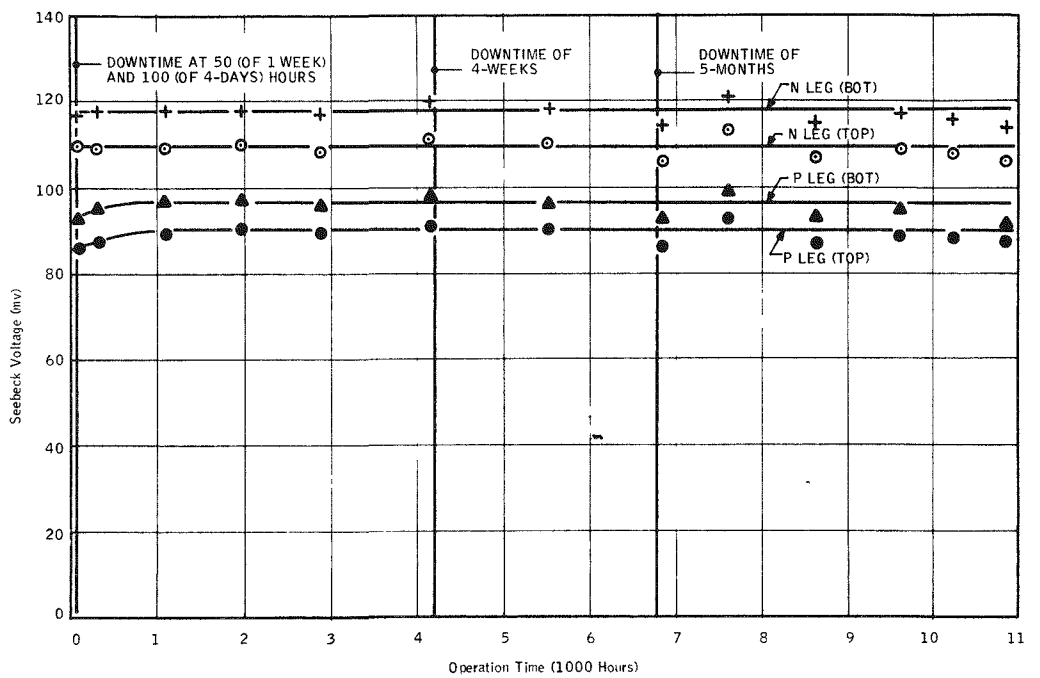

Figure 3-3. SNAP-23 Converter P-1 Seebeck Voltage of Individually Monitored Thermoelectric Elements

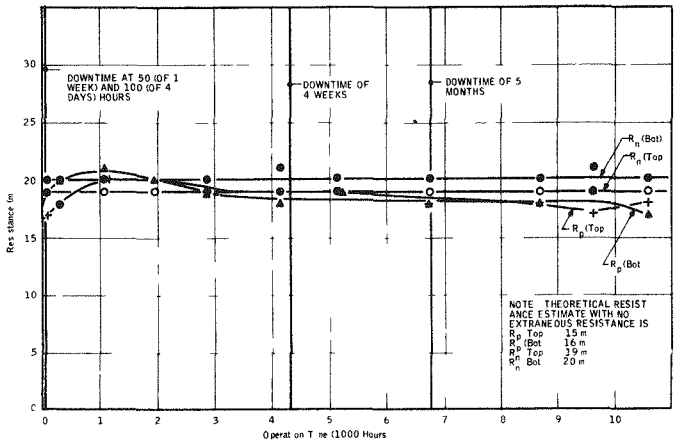

Figure 3-4. SNAP-23 Converter P-1 Resistance of Individually Monitored Thermoelectric Elements

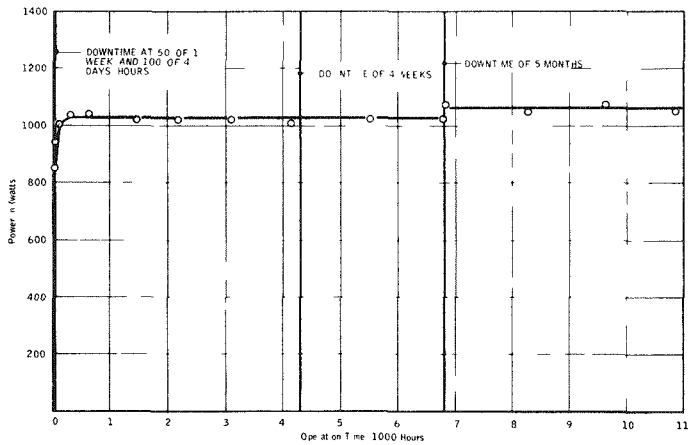

Figure 3-5. SNAP-23 Converter P-1 Input Power to Converter versus Time

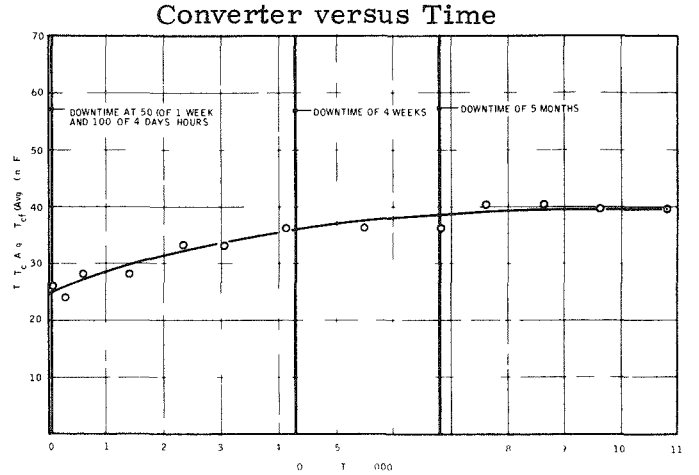

Figure 3-6. SNAP-23 Converter P-1 Temperature Differences Between Cold Cap (Avg) and Cold Frame (Avg)

Power input into the converter versus time is plotted in Figure 3-5. It should be noted that additional power was required to maintain the same hot electrode temperatures after the converter was again energized following the five-month dormant period. In addition, there was some thermal instability that occurred during the first 200 hours of life testing that required additional input power to maintain constant hot electrode temperatures.

The thermal impedance between the cold cap and cold frame was studied during the course of converter life testing. The difference in temperature between the average cold cap temperatures and average cold frame temperatures ($T_c - T_{cf}$) is plotted in Figure 3-6. An increase of 15°F occurred across the cold cap - cold frame region during testing. It should be noted that a portion of this increase (4°F) occurred between the time the converter was turned off (dormant for five months) and heated up again for continuous long-term testing. A 4°F temperature change is considered significant since relative temperature changes can be measured within ±2°F.

3.2 MODULE A-2

This section contains a description of Module A-2, including performance history. The module is shown in Figures 2-1 and 3-2 of Volume I.

3.2.1 PHYSICAL DESCRIPTION

The SNAP-23 Module A-2 contained six thermoelectric couples, connected in series, with thermoelectric legs similar to those used in the converter. The couples and adjacent hardware differ from the converter in the following items:

- Barrier disc between hot and cold P segments.
- Different shape hot electrode straps and cold caps.
- The cold caps in the module were not nickel plated.
- Internal gas environment was argon rather than xenon.
- Hot block electrical insulation was natural mica rather than boron nitride.

The thermopile was in a parallel plate hot frame - cold frame configuration. The springs, followers, internal thermal insulation (Min-K 1301), hot frame, and cold frame were the same material as that used in the converter.

3.2.2 INSTRUMENTATION

The following is a description of the instrumentation within the module.

3.2.2.1 Temperature

Two couples within the thermopile were instrumented with iron-constantan thermocouples. Refer to Figure 3-7.

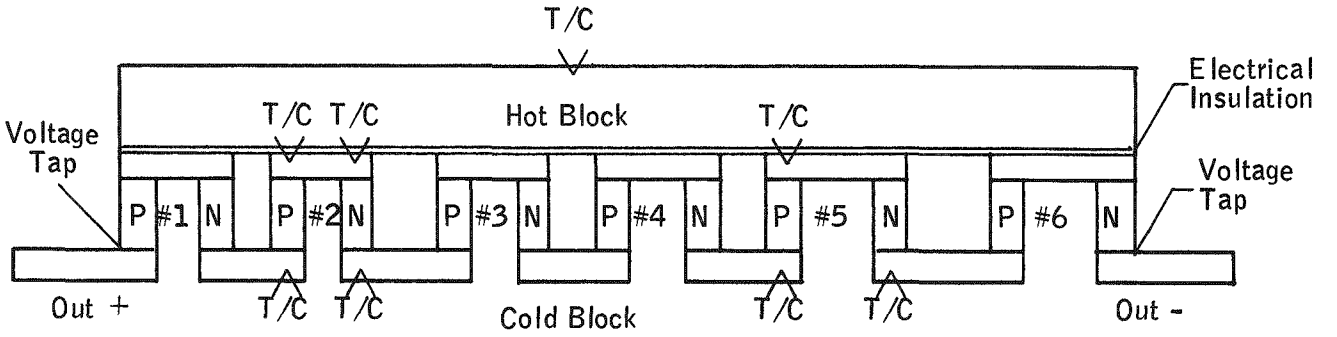

Figure 3-7. Schematic of SNAP-23 Module A-2 Thermopile with Thermocouple Instrumentation

The hot electrode instrumentation consisted of 30 gage iron and constantan wires welded to the hot junction button of two P legs and one N leg, 30 gage iron-constantan wires were also soldered to the cold electrodes of couples numbers two and five. In addition, a heavy duty, 24-gage, iron-constantan thermocouple was welded to the hot block for temperature monitoring and use as a reference for the hot electrode temperatures.

3.2.2.2 Voltage

Iron leads from the iron-constantan thermocouples were used to monitor the individual P and N elements of couples numbers 2 and 5. Voltage taps at the N and P terminal elements monitored the module circuit (Figure 3-7). Voltage taps across a standard calibrated shunt in series with the output load monitored the current through the module circuit.

3.2.2.3 Power Input

A wattmeter monitored the input power to the hot block heater. Variacs controlled the input power to both the hot and cold heater blocks.

3.2.3 DEFINITION OF TERMS

The following nomenclature will be used to identify the individual N and P legs, and to identify the various parameters measured within the module:

3.2.3.1 N- and P-Leg Identification

Individual N and P legs are identified with respect to their couple numbers. Therefore, the 2P leg is the P leg from couple number 2.

3.2.3.2 Parameter Identification

The parameters are identified similarly to the converter as defined in paragraph 3.1.2. For example, E, R, P, T_h, T_c are the same as in the converter. The indicies on E, R, P also apply.

3.2.4 PERFORMANCE EVALUATION

The electrical performance was evaluated the same as for the converter as previously covered in paragraph 3.1.4. All thermocouples were monitored and recorded.

3.2.5 DATA MONITORING

The data was monitored approximately to the following approximate schedule:

- First day - six times.
- Next three days - daily.
- Next three weeks - every other day.

- Next eight months - once a week.
- Next ten months - every other week.
- Remaining six months - irregular monitoring, ranging from one to four weeks.

The module was in continual operation throughout the entire life test period.

3.2.6 ENVIRONMENTAL CONDITIONS

3.2.6.1 Electrode Temperatures

The hot electrodes were maintained at a nominal temperature of 1100 ± 15°F throughout most of the test operation. Because the 30-gage, iron-constantan thermocouple wire at the hot electrode is highly susceptible to attack and degradation in the 1100°F environment, it was necessary to use the heavy duty 24-gage wire on the hot block as a reference, and finally as the ultimate criterion for determining the hot electrode temperatures. This was done by first establishing the difference in temperature between the hot block and hot electrode temperatures during the first 300 hours. For Module A-2, this turned out to be 34°F. Thereafter, the hot block was maintained at a nominal temperature of 1134°F. There was no evidence that the hot block thermocouple had degraded during life testing. However, after 2000 hours of operation, the hot electrode thermocouples instrumenting the P legs were measuring less than 1000°F. A decrease of 100°F on the hot electrodes cannot be supported by the performance data of Module A-2, since the output power of Module A-2 actually increased during the first 2000 hours. Refer to Figure 3-8. The thermocouple instrumentation on 5N hot electrode remained stable for nearly 6000 hours; however, monitoring of hot electrode temperatures was discontinued after 6000 hours of testing because of apparent instrumentation degradation and failure.

3.2.6.2 Backfill Gas

The internal gas environment was initially 100 percent argon (ultra-pure grade). Initial gas pressure was 1.0 atmosphere. Final gas pressure is not known as no provisions were included for measurement of internal gas pressure.

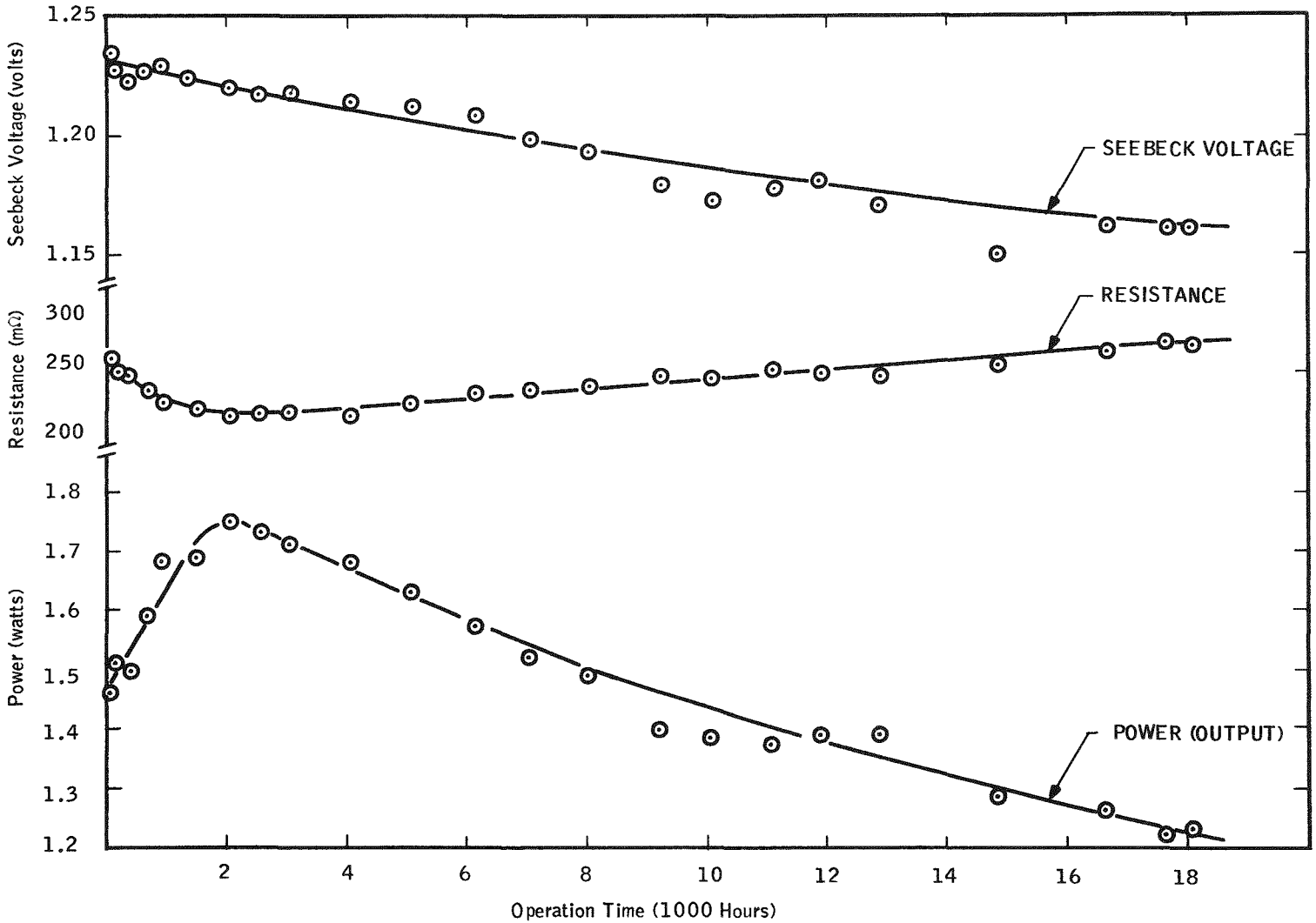

Figure 3-8. SNAP-23 Module A-2 Performance Data

3.2.6.3 Hot Electrode Contact Pressure

The hot electrode mechanical contact pressure was approximately 150 psi for each thermoelectric leg.

3.2.6.4 Electrical Load

The circuit was maintained at approximately matched load conditions during the entire test.

3.2.7 PERFORMANCE

Module A-2 was put on test March 8, 1965. The test was terminated April 7, 1967. A total of 18,100 hours of running time was accumulated.

A summary of the thermoelectric performance characteristics for the module is shown in Figures 3-8 through 3-12 of this volume and Figures 3-4 and 3-5 and Table 3-2 of Volume I. Because the operating temperatures were maintained throughout the test, it was not necessary to normalize the data to performance ratios as had been done with Converter P-1. All resistance data includes extraneous resistance from jumper straps and hot junction contacts.

Output power varied widely during operation. The output power increased over the first 2000 hours from 1.46 watts to 1.75 watts. Thereafter, the power decreased to 1.23 watts at the end of test.

Three comments can be made about the individually monitored N and P legs:

1) The N legs increased in resistance over the total period of operation; the average increase was 13 milliohms (Figure 3-11).

2) The P legs decreased in Seebeck voltage over the total period of operation. The average decrease was 11 millivolts.

3) The P legs decreased in resistance during the first 2000 hours, stabilized thereafter. The average decrease was 9 milliohms.

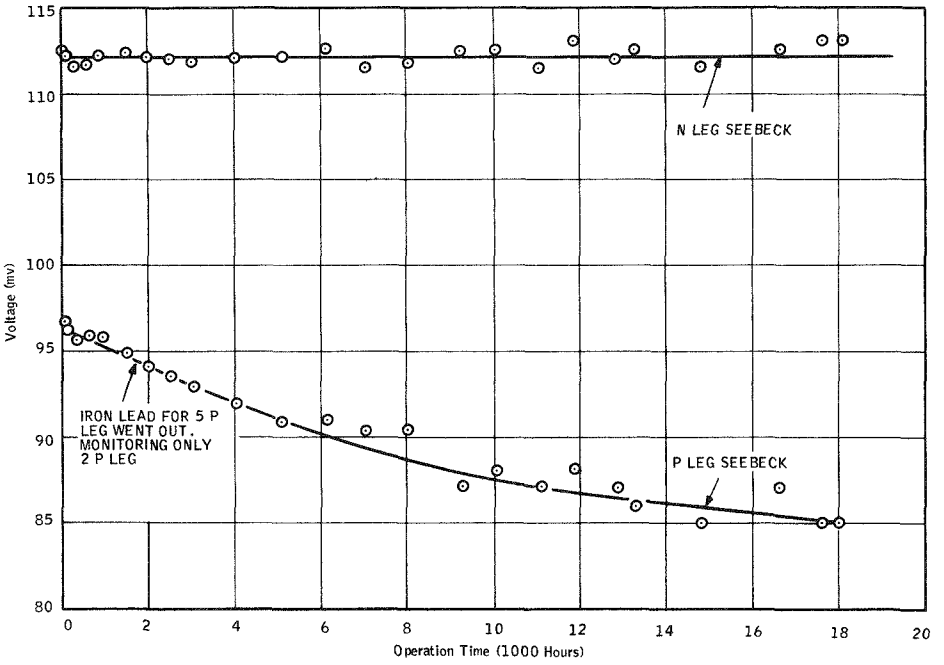

Figure 3-9. SNAP-23 Module A-2 P and N Leg Seebeck Average (from Couples No. 2 and 5) Voltage vs Time

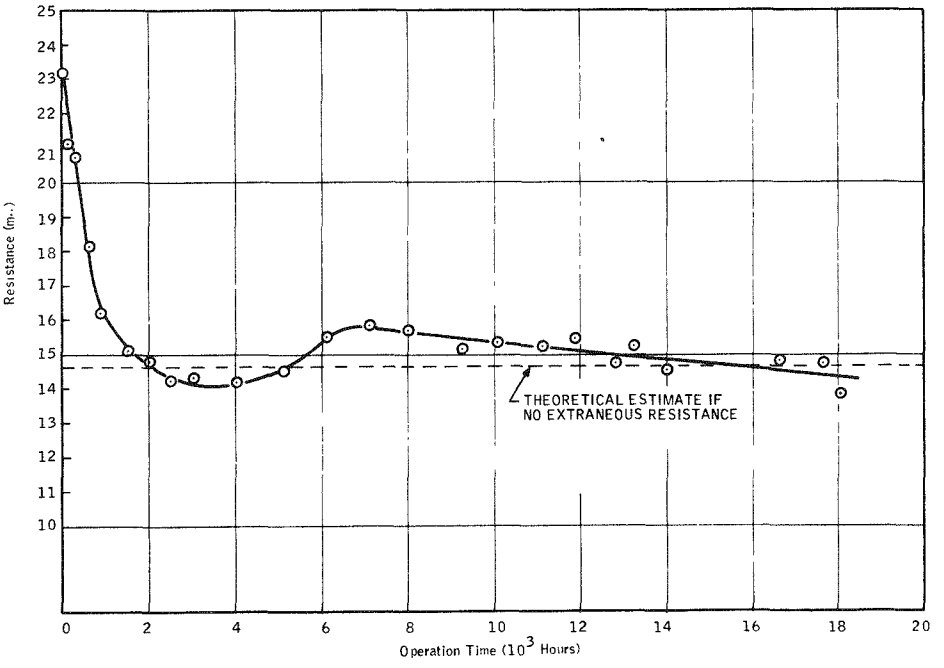

Figure 3-10. SNAP-23 Module A-2 P Leg Resistance vs Time (Average of 2 P and 5 P)

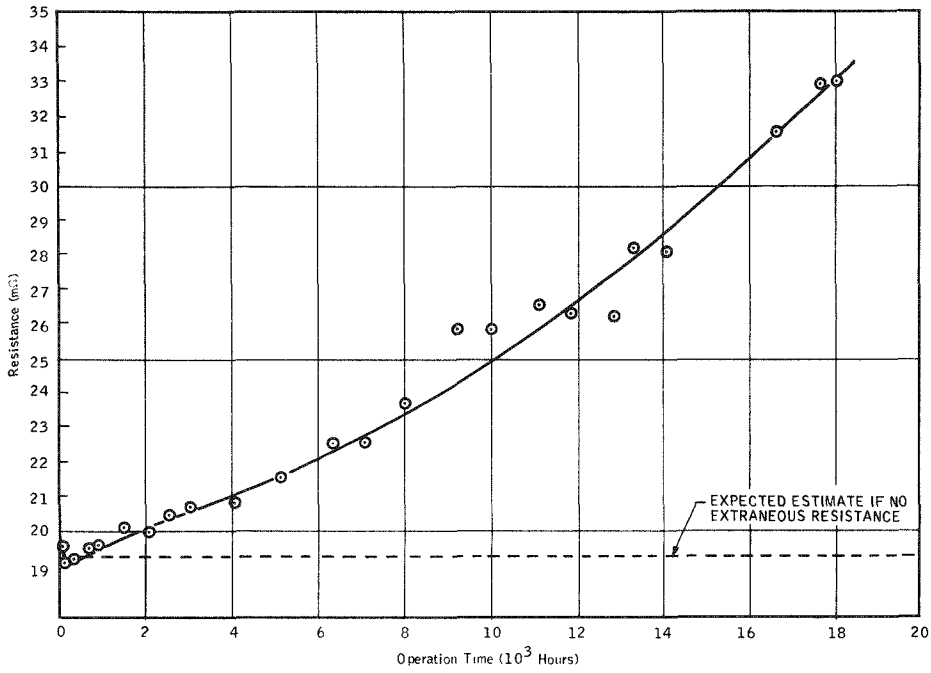

Figure 3-11. SNAP-23 Module A-2 N Leg Resistance vs Time (Average of 2 N and 5 N)

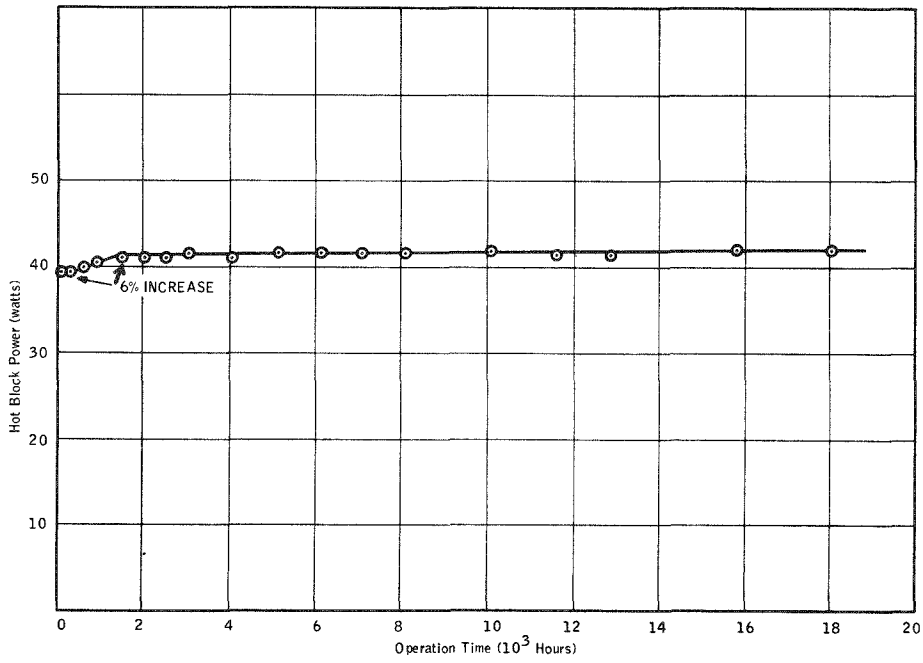

Figure 3-12. SNAP-23 Module A-2 Input Power vs Time

The first two comments refer to major problem areas that were investigated during the post-test analyses.

Input power is plotted in Figure 3-12. An increase of 6 percent in the input power was required to maintain the same hot electrode temperatures. The majority of the input power increase occurred during the first 1000 hours of operation.

4.0 POST-TEST ANALYSES

This section is divided into several analytical subsections, as previously outlined in paragraph 1.2. Each analytical subsection will have the following:

- General Background
- Analytical Procedures
- Results
- Discussion

4.1 LEAK CHECK ANALYSIS

After cooling both the converter and module to room temperature, they were leak checked. Particular emphasis was made to detect any leaks in the instrumentation feedthroughs and welded interfaces.

No leaks were detected in either module or converter. A Veeco leak detector was used sensitive enough to detect a leak of 2×10^{-8} cc/sec of helium.

4.2 VISUAL EXAMINATION OF POST-TEST COMPONENTS

4.2.1 BACKGROUND

During various stages of disassembly, photographs and notes were taken of any significant observations that could be linked to the output performance and stability of the thermopiles. Many of the significant observations dictated the direction of the post-test analysis. Results and conclusions are delineated in the various analytical subsections which follow; this subsection is a condensation of the observations made during disassembly of the module and converter which point out the areas of interest for further investigation.

4.2.2 MODULE A-2

The following is a summary of the visual observation for Module A-2:

1) Metallic sublimate was noted on the surface of the Min-K 1301 blocks nearest the thermoelectric legs. The sublimate was suspected to be lead telluride.

2) Silicon heat transfer grease appeared to have reacted with the Min-K 1301 near the base of the cold caps and on the sides of the followers forming a white powder.

3) There was a heavy metallic sublimate mixed with the powdered Min-K 1301 around both N and P legs approximately 0.1 inch from hot electrodes. Though the sublimed material formed a bridge through the Min-K 1301 between the hot N and P ends of the couples, there was no evidence of any current leakage through the Min-K 1301 via the sublimed material.

4) All hot electrode thermocouple instrumentation was brittle and broke when touched.

5) There was a distinct methane-like odor from the module.

6) There was a dark purple region on all the P legs approximately 0.04 inch long and adjacent to the cold caps. Chemical analysis revealed it to be a Cu-Bi-Sb-Te phase. Refer to paragraph 4.10.

7) Output terminal P leg had a hairline fracture located from the base of the leg adjacent to the cold cap and traveled diagonally to the side of the leg adjacent to the hot-cold segment interface (Figure 4-1).

8) The Min-K 1301 powder was densely packed around the legs.

9) In general, the thermopile seemed free of oxides.

10) The iron plating on all the hot electrode straps was blistering as shown in Figure 4-2.

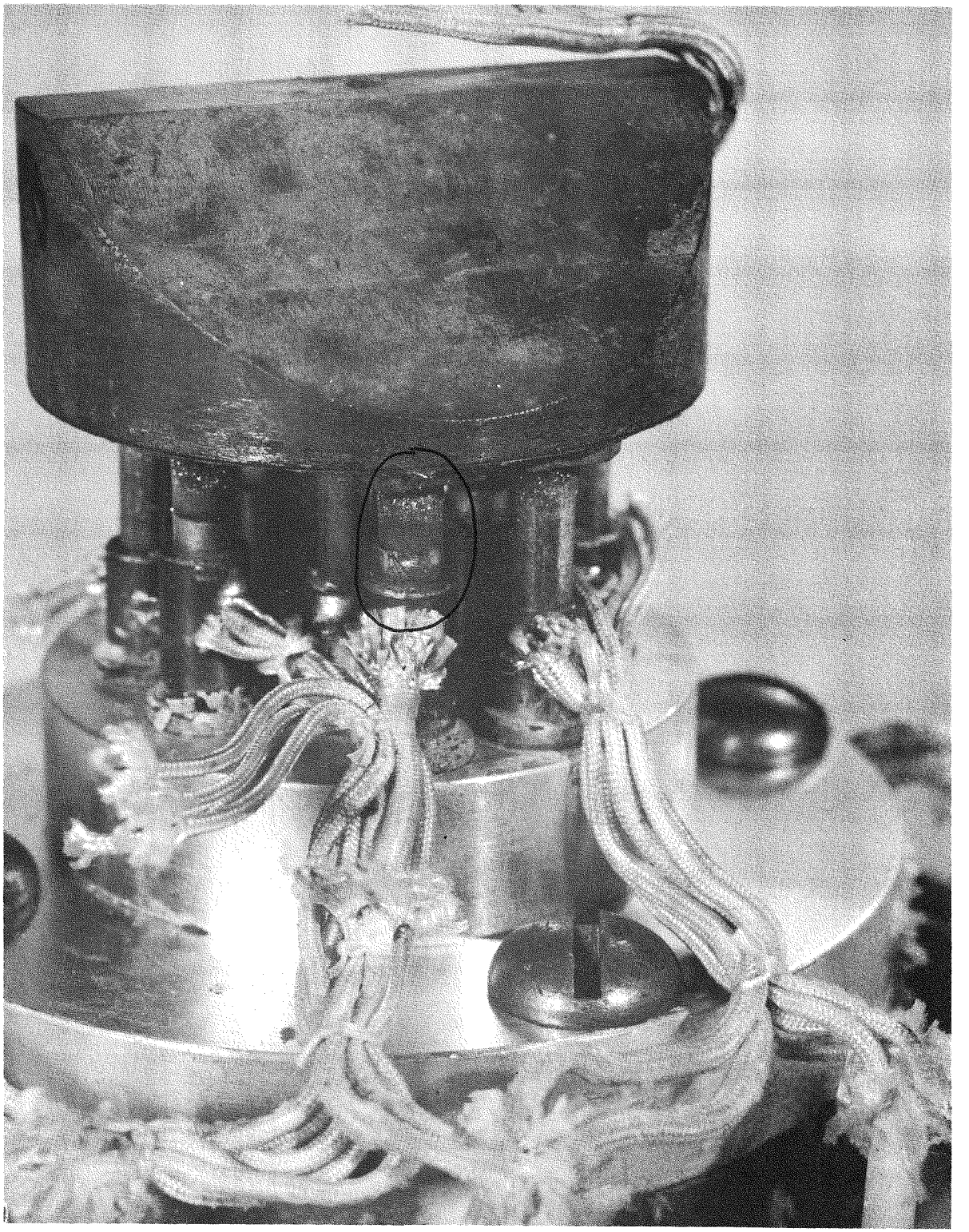

Figure 4-1. Module A-2 Showing Cracked Terminal P Leg

4.2.3 CONVERTER P-1

The following are significant observations made throughout the disassembly of the converter:

- A gradual darkening of the Min-K extending from the cold frame to the hot frame was noted. A very dark (purple) zone, about 1/8 inch in depth, existed immediately adjacent to the hot frame. It was also observed that the Min-K was densely packed in this region and at the leg hot ends.

- White flakes of material were apparent in the Min-K adjacent to boron nitride strips, suspected to be boric oxide (8 percent boric oxide in boron nitride strips).

- Lead telluride crystals were observed throughout the Min-K (all the way outward to the outer case above and below the cold frame).

- With few exceptions, both N and P legs were very clean, with pre-test measurements of R versus L scribe lines readily visible. Both N and P legs had a sublimate buildup at their hot ends and the N legs bore evidence of a reddish film on their surfaces toward the hot end. It was observed that a sublimate buildup formed a bridge through the Min-K 1301 between the hot N and P ends of the couples (Figure 4-2).

  The reddish film existed in a very thin deposit on the inside surface of N legs on the outside rows. Legs within the pile displayed the red coloration about their entire lower hot end circumference.

- Leg hot end – button bonds were very strong in the upper rows (1, 2, 3, etc.) and very weak at the opposite end (rows 14, 13, 12, etc.). The N output leg – button bond at radial row 1 was so durable that in an attempt to remove the leg, the hot electrode was bent without breaking the bond.

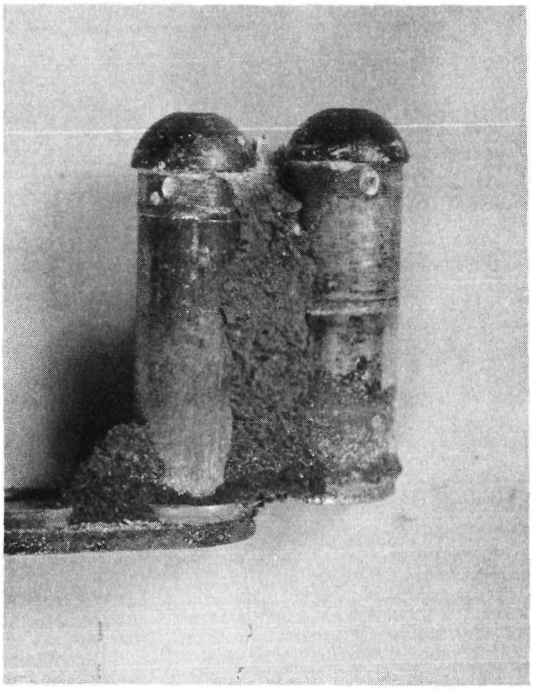

Figure 4-2. Converter P-1 Sublimate Buildup Near Couple Hot End

- Many P legs throughout the pile came apart at the leg-cap solder region when follower pressure was removed. Solder bonds were, in many cases, minimal, and in still others, completely absent. However, electrical continuity checks indicated little or no resistance across the leg-cold cap interfaces (paragraph 4.4).

- While an explanation is not easily arrived at, it was noted that followers on N legs moved harder in most cases than P leg followers.

- In most cases, cold cap-follower interfaces were clean and shiny with evidence of Min-K in only one interface. There were traces of grease in the follower spherical surfaces and the cold cap solder drill-holes. The grease no longer had the greasy texture of unused grease (paragraph 4.6).

- Instrumented and output legs displayed exceptionally clean cold caps, being shiny and silvery, displaying no tarnishing of their nickel plate.

- Legs were displaced from design locations both axially and radially. Support cone removal at a later stage of disassembly allowed the legs to return radially, but axial displacement was unaffected by this step. Axial displacement was only slightly evident at radial row 1, with displacement (vertical, downwards) increasing slightly with each subsequent radial row. Displacement was greatest at radial row 14. Measurements disclose this to be reasonably correct (refer to paragraph 4. 5).

- All boron nitride strips were broken into 8-12 pieces with the breaks occurring at approximately right angles to the strips' longest axes and, in all cases, through the machined depressions either underneath or between leg ends. A typical example is shown in Figure 4-3. No radial or axial row-to-row relationships of cracks could be established with the exception of the fact that all strips were broken at the top end, across their machined recess at the retaining ring location.

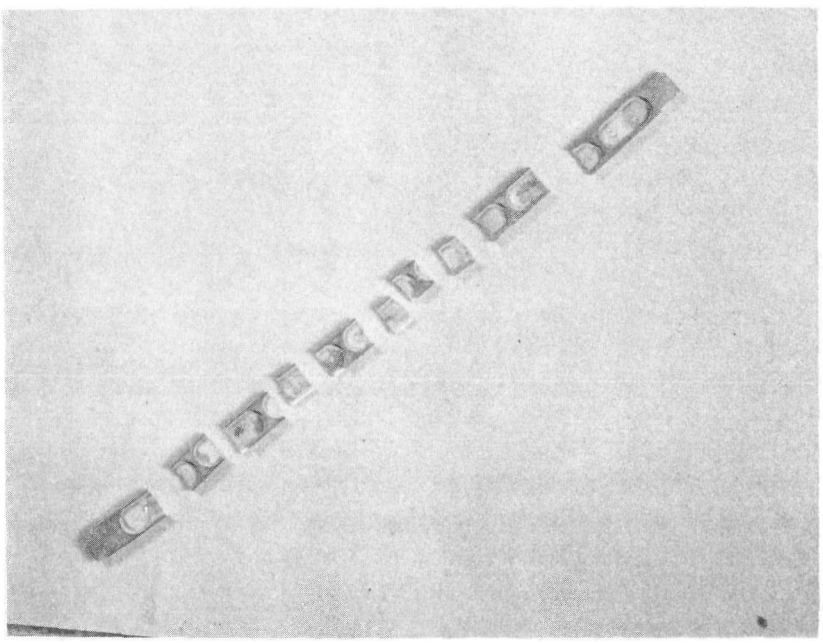

Figure 4-3. Converter P-1 Broken Boron Nitride Strip

- Boron nitride strips from axial rows 8 through 18 had a pink-red color in their machined depressions. Strips from rows 19 through 36 through 7 do not display this characteristic. The hot frame displayed a surface variation phenomenon coincidental with the defined areas of strip discoloration as shown in Figure 4-4. The hot frame surface beneath rows 8 through 18 was relatively clean and "unshaded", while the remaining area had a distinctive shading or shadow effect which discloses exactly where leg ends were situated upon it. The shadow effect was caused by the presence of a white material in the machined depressions of the hot frame surface.

- Vertical striations were noted in the Converter P-1 follower coatings as shown in Figure 4-5. The coating imperfections were not noticed in the pretest followers.

4.3 GAS ANALYSIS

4.3.1 BACKGROUND

The purpose of making a gas analysis was:

1) To detect the presence of any gas or vapor that could seriously affect the electrical performance. Of particular concern were highly corrosive gases and potential thermoelectric doping agents.

2) To detect any gas or vapor that could affect the thermal characteristics of the thermopiles. Of particular concern were highly mobile gases with low molecular weights (e.g., H_2, He, CH_4, etc.).

4.3.2 ANALYTICAL PROCEDURE

The following steps were taken:

1) Both converter and module were allowed to cool to room temperature.

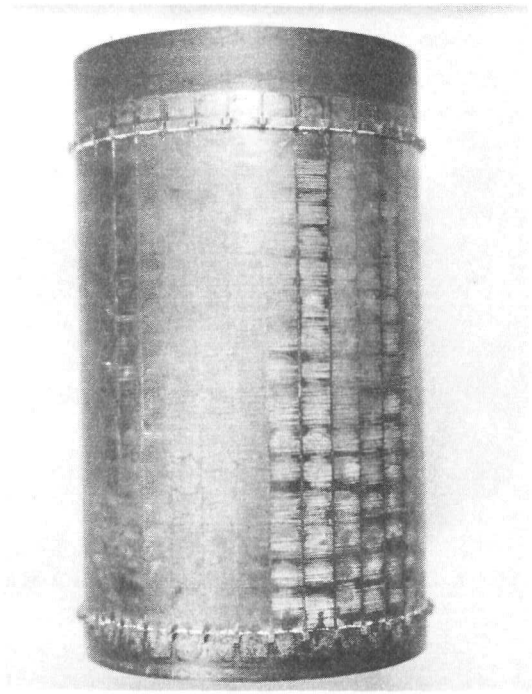

Figure 4-4. Converter P-1 Hot Frame Surface Condition

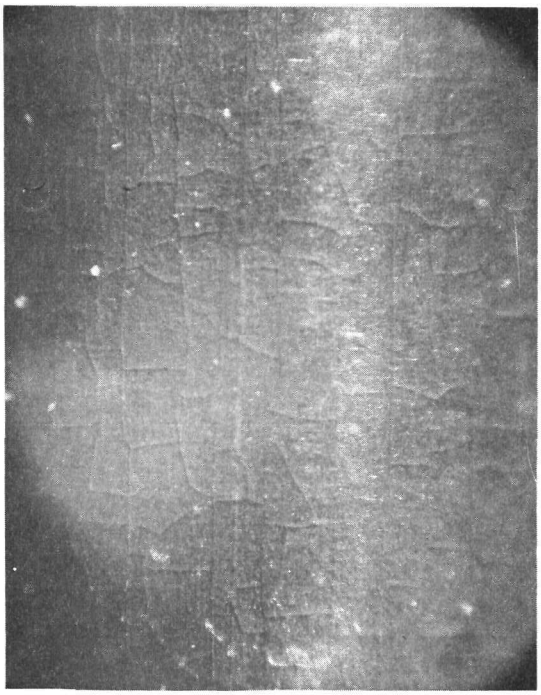

Figure 4-5. Converter P-1 Follower Coating Vertical Striations

2) The basic converter and module designs did not contain provisions for extraction of a gas sample; therefore, special gas sampling adapter was designed and attached to the outer case of each thermopile. A sketch is shown in Figure 4-6.

3) The gas sampling bulb and vacuum station were connected, and the entire system was evacuated and leak checked.

4) After no leaks were detected, the vacuum station was closed off from the adapter and a gas sample taken.

5) The gas samples were then analyzed with the mass spectrograph.

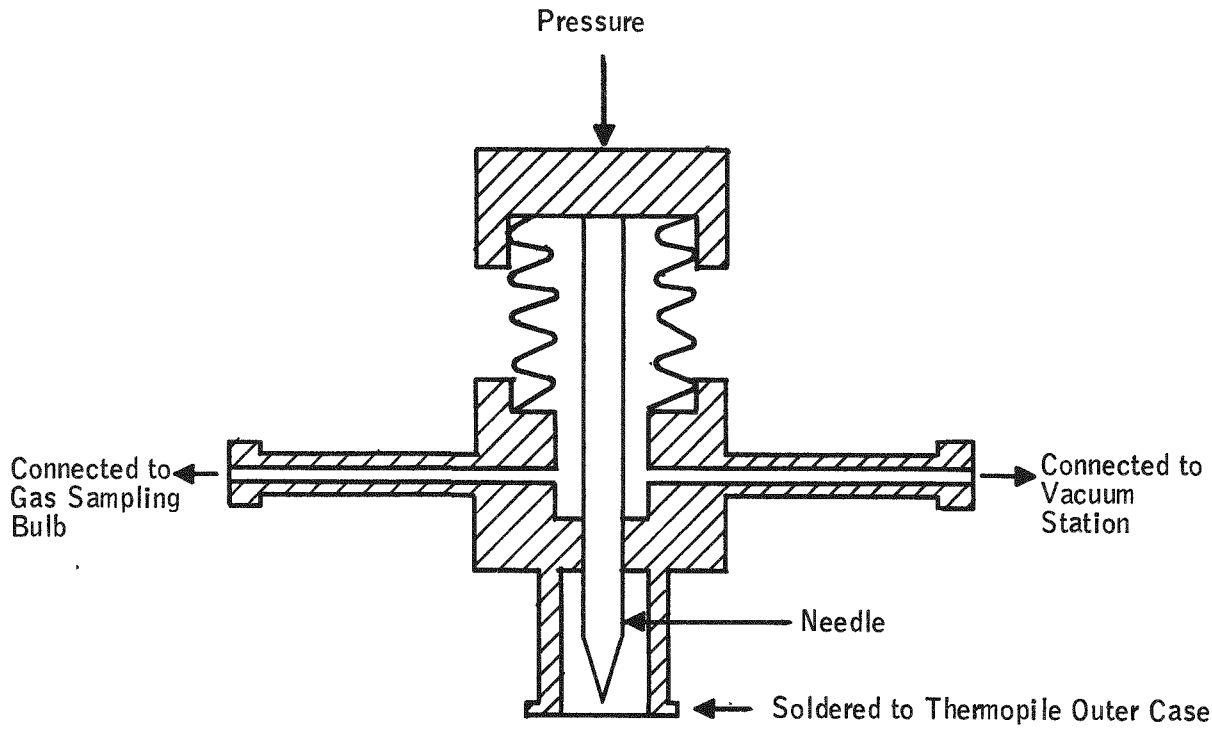

Figure 4-6. Sketch of Gas Sample Adapter

4.3.3 RESULTS

During the process of taking a gas sample for Module A-2, the solder joint between the outer case and fixture broke loose resulting in the internal gas environment of the module to be released to the atmosphere. As a result, the Module A-2 gas sample was contaminated with air and the results are, for the most part, not usable.

The results of the gas analysis for Module A-2 and Converter P-1 are given in Tables 4-1 and 4-2.

Table 4-1. Gas Analysis for Module A-2 (Original Gas was Argon)

All Components in Mole Percent

Xe	N_2	CO	CO_2	CH_4	H_2	O_2	H_2O	Ar
0.0	65.1	0.0	0.2	0.0	2.6	17.5	0.09	14.5

Table 4-2. Gas Analysis for Converter P-1 (Original Gas was Xenon)

All Components in PPM Except Xenon, Which is Given in Mole percent

O_2	N_2	H_2O	Xe	Ar	H_2	He	CO_2	CO	SO_2	CH_4
60	1300	20	93.6%	20	28,000	0	0	0	0	6000

H_2S	CS_2
0	*

*Detection obscured by interference from other peaks.

4.3.4 DISCUSSION OF RESULTS

4.3.4.1 Module A-2

The majority of the gas sample was air (83 percent), introduced during the gas sampling procedure. The other two components, 2.6 percent hydrogen and 14.5 percent argon, probably originated from the module. Release of hydrogen from Min-K 1301 thermal insulation during test may account for the fact that the input power to the module had to be increased by 6 percent over the first 1500 hours.

4.3.4.2 Converter P-1

Besides the 93.6 percent xenon, three other components were present in quantities large enough to be considered significant. They are: nitrogen, hydrogen, and methane.

The nitrogen content suggests the presence of a small quantity of air within the converter. The fact that very little oxygen was present is no deterrent to the possibility of air being present, since free oxygen would be expected to be either "gettered" by the free silicon in the Min-K thermal insulation or by the hot metal surfaces within the thermopile.

Another possible source of nitrogen is from the forming gas used to process Min-K 1301.

Min-K 1301 binder is the most probable source of methane because methane of 1 percent or greater has been observed in the SNAP-27 Min-K 1301 thermal insulation stability tests. (Reference Section 5.0 of the SNAP-27 Program, Phases II, III, and IV, Quarterly Report No. 7, dated July 1967, Report No. MMM 8406-1606.)

4.4 EXTRANEOUS RESISTANCE ANALYSIS

4.4.1 BACKGROUND

Extraneous resistance is defined in this report as being any resistance within the thermopile that does not include the resistance of the thermoelectric leg materials. With this definition, the hot and cold electrodes are included as an extraneous resistance. However, electrode resistances are small (less than 1 mΩ/couple) and have been neglected in the analysis. The remaining portion of the extraneous resistance includes:

- Resistance across the leg-cold electrode bonded interface.
- Resistance across the leg-hot electrode pressure contact interface.
- Resistance across the hot and cold segment bonded interface.
- Resistance across any observable cracks in the thermoelectric legs.

In order to evaluate the extraneous resistance, it is necessary to know the material resistance of the thermoelectric legs. At room temperature, based on R versus L measurements conducted on P and N legs prior to assembly into the converter and the module, resistances were:

R_n = 3.2 milliohms ± 20%

R_p = 3.4 milliohms ± 20%

In a thermal gradient (T_h = 1100°F, T_c = 190°F), the calculated material resistances, based on material property data, are:

R_n = 19.4 milliohms

R_p = 14.7 milliohms

4.4.2 ANALYTICAL PROCEDURES

4.4.2.1 Module A-2

An electrical continuity test was conducted on the module. The procedures used are described in TPO-110, paragraph 6.3 of Volume I.

The electrical continuity test was conducted at four different stages of disassembly in order to determine the effects of various disturbances on the electrical resistance. This test was conducted at the following times:

- After the module was cooled to room temperature.
- After the gas sample was taken.
- After the outer case was removed.
- After all the Min-K 1301 thermal insulation was removed.

The first three electrical continuity checks measured the resistance of legs and couples using the iron leads of the diagnostic couple as probes, which limited these tests to resistance measurement of the circuit, couples numbered 1, 2, 5, 6, and legs numbered 2P, 2N, 5P, and 5N.

The fourth continuity test included resistances of various regions of the legs and adjacent electrodes. The various regions are identified in Table 4-4.

4.4.2.2 Converter P-1

Several electrical continuity tests were conducted on Converter P-1 using the procedure outlined in TPO-110, paragraph 6.3 of Volume I.

The continuity tests were performed at four different stages of disassembly. As in Module A-2, this was necessary to determine possible changes in the electrical resistances during the tear down sequence. The tests were performed at the following points:

- After the converter was cooled to room temperature.
- After the lower cover was removed.
- After support cone and outer case were removed.
- After all Min-K 1301 thermal insulation was removed.

The first three tests measured resistance of the instrumented couples and legs using the iron lead of each diagnostic thermocouple as a probe. Circuit resistance was also checked by this method, including total circuit resistance, one couple in radial row 1 (legs A35P and A36N) and one couple in radial row 14 (legs A36P and A1N).

The fourth continuity test consisted of resistance measurements of various leg regions at predetermined locations within the thermopile. Locations of legs checked were:

- All legs in radial row 1.
- All legs in radial row 14.
- All legs in axial rows 7, 19, and 31.

Leg regions checked at these locations are identified in Figure 4-7.

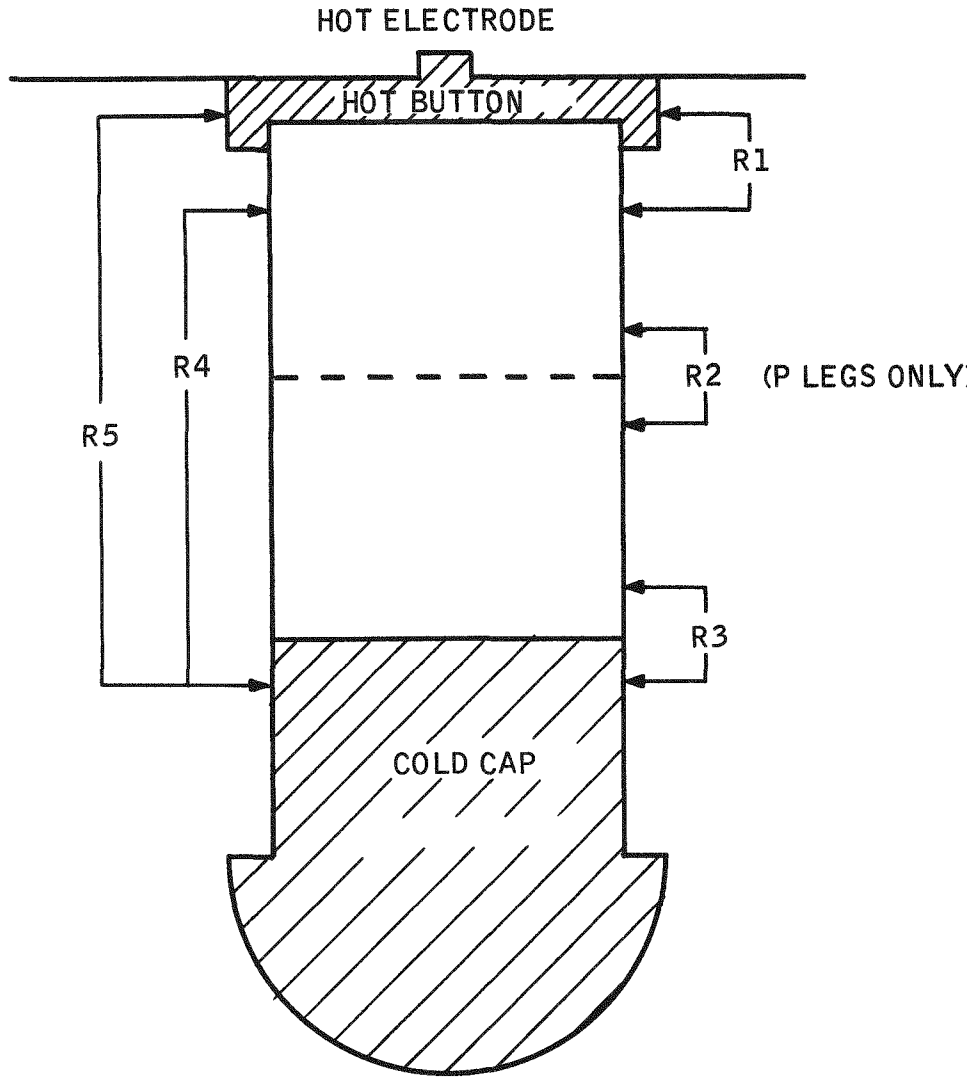

Figure 4-7. Converter P-1 Thermoelectric Legs Resistance Measurement Points

4.4.3 RESULTS

4.4.3.1 Module A-2

The results for the first three continuity tests are given in Table 4-3.

Table 4-3. Module A-2 Resistance Measurements (Milliohms)

Description	After Cool Down	After Gas Sample	After Case Removal
Circuit Total	207.0	331.0	559.0
Couple #1	57.5	89.4	123.0
Couple #2	15.0	33.1	69.8
Couple #5	37.9	48.8	87.2
Couple #6	43.5	65.9	110.0
#2 P leg	4.6	4.6	5.2
#2 N leg	10.4	28.0	64.5
#5 P leg	3.9	4.0	4.0
#5 N leg	31.5	42.1	81.2

The resistances measured at the various leg regions are given in Table 4-4.

Table 4-4. Module A-2 Resistance Measurements After Min-K Thermal Insulation was Removed (Milliohms)

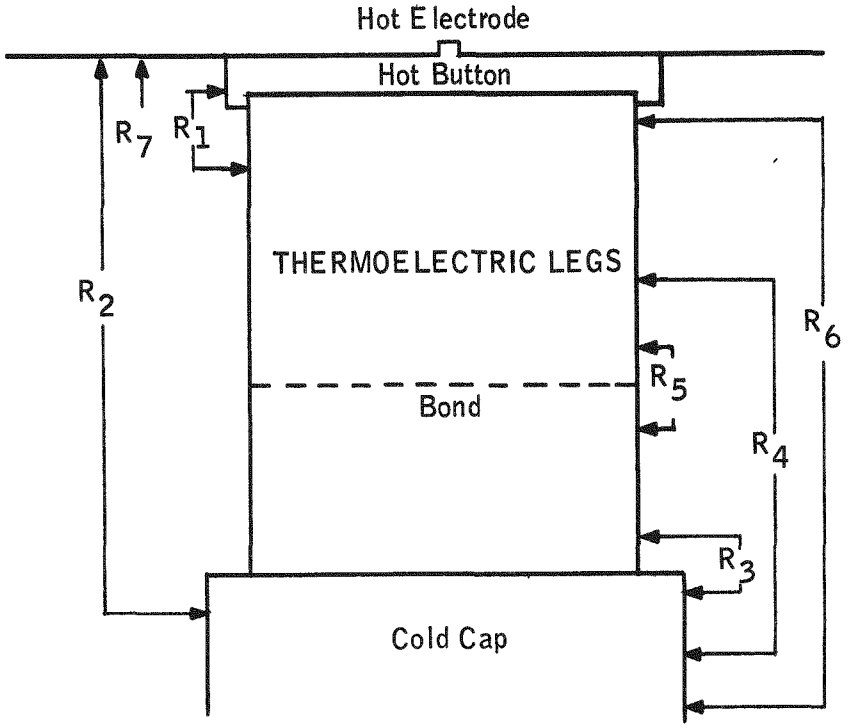

Description	Couple Resistance	Hot Contact R_1	Total R_2	Cold Contact R_3	R_4	R_5 P-legs only	R_6	R_7
Couple #1	90.0							
P leg	-	3.25	7.2	<0.28	2.0	<0.8	3.6	<0.1
N leg	-	77.0	84.0	<0.42	2.25	-	3.0	1.44
Couple #2	69.2							
P leg	-	1.5	5.3	<0.21	1.48	<0.48	3.1	0
N leg	-	60.0	64.0	<0.73	2.34	-	3.5	<0.65
Couple #3	96.0							
P leg	-	1.83	4.8	<0.25	1.62	<0.78	2.84	0
N leg	-	84.0	89.4	<0.57	2.4	-	3.4	<0.25
Couple #4	64.9							
P leg	-	2.8	6.3	<0.23	1.35	<0.57	2.8	0
N leg	-	53.8	57.2	<0.55	2.1	-	3.2	1.3
Couple #5	85.9							
P leg	-	2.42	5.2	<0.32	1.47	<0.50	2.65	0
N leg	-	74.0	79.0	<0.65	2.20	-	3.1	<0.87
Couple #6	212.0							
P leg	-	2.10	4.85	<0.75	1.43	<0.52	2.75	0
N leg	-	205.0	206.0	<0.45	2.80	-	3.40	0.10

4.4.3.2 Converter P-1

The results of the first three continuity tests are shown in Table 4-5.

Table 4-5. Converter P-1 Resistance Measurements (Milliohms)

Description	After Cool Down	After Bottom Removal	After Case Removal
Generator	4800	4380	5200
Top Couple	9.1	10.06	14.40
A35P	5.3	6.28	7.90
A36N	3.6	3.82	6.50
Bottom Couple	19.2	20.02	23.25
A36P	17.0	10.03	11.0
A1N	1.8	9.74	12.25

The resistances for the various regions in radial rows 1 and 14 are given in Tables 4-6 and 4-7 respectively.

A schematic diagram showing resistances for axial rows 7, 19, 31, and radial rows 1 and 14 is presented in Figure 4-9.

Extraneous resistance measurements for axial rows 7, 19, and 31 are summarized in Figure 4-8.

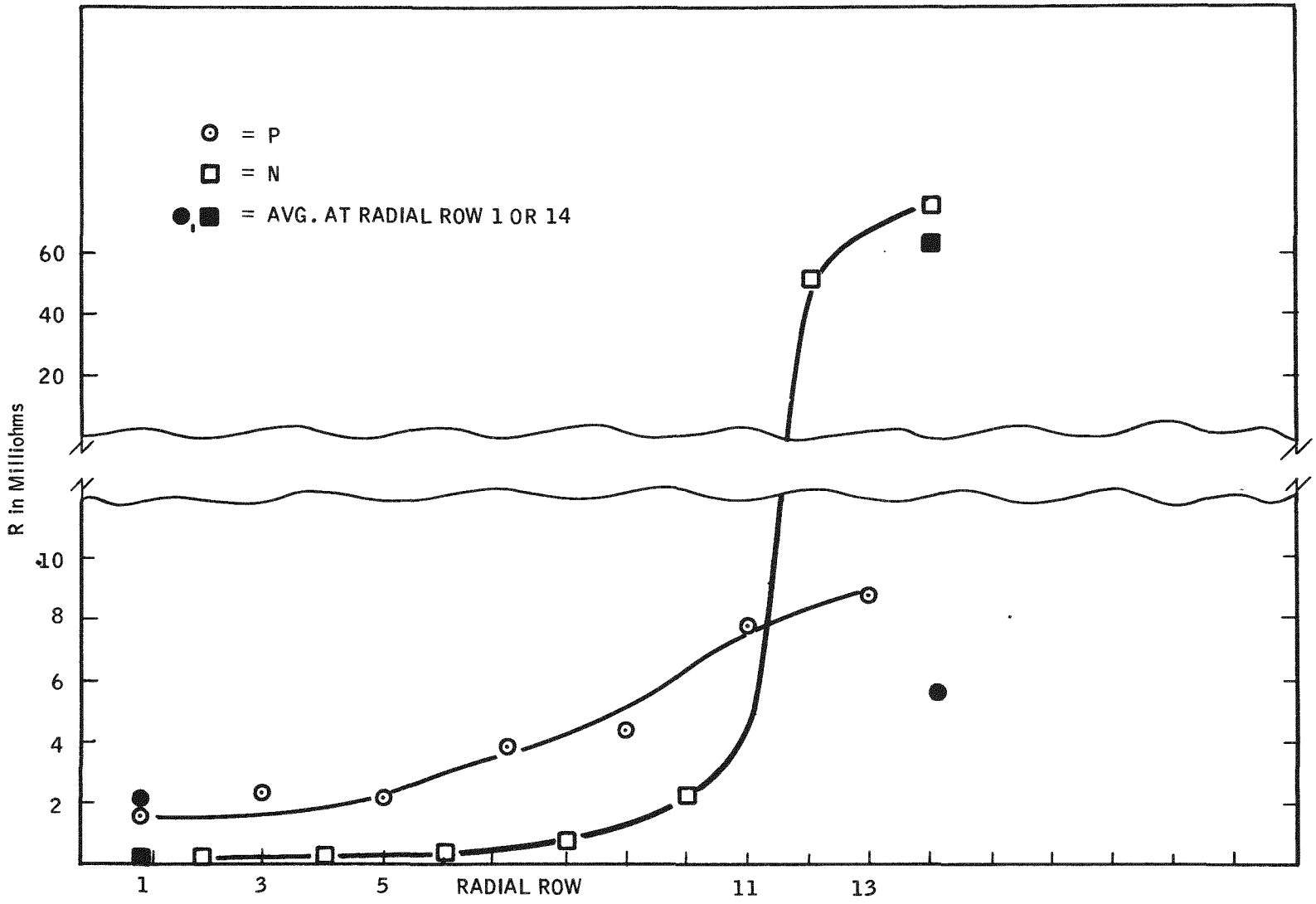

Figure 4-8. Converter P-1 P- and N-Leg Average Contact Resistance

Table 4-6. Resistance Measurements During Disassembly of Converter P-1 – Radial Row 1 (Milliohms)

Radial Row 1					
Axial Leg Location and Type	R_1	R_2	R_3	R_4	R_5
A1-P	2.68	<0.53	0.0	4.38	6.62
A2-N	<0.2	-	0.0	3.90	4.10
A3-P	1.82	<0.30	0.0	4.80	7.60
A4-N	<0.30	-	<0.30	3.50	3.80
A5-P	2.60	<0.25	0.0	4.50	7.10
A6-N	<0.30	-	<0.38	3.40	3.70
A7-P	2.00	<0.45	<0.25	5.10	7.20
A8-N	<0.22	-	<0.30	3.50	3.70
A9-P	1.20	<0.50	0.0	4.30	5.80
A10-N	<0.35	-	<0.35	3.50	3.80
A11-P	1.30	<0.60	<0.20	4.80	6.40
A12-N	<0.35	-	<0.20	3.60	4.00
A13-P	1.50	0.84	<0.30	5.80	7.60
A14-N	<0.38	-	<0.26	3.40	3.90
A15-P	1.75	1.10	<0.20	5.10	6.90
A16-N	<0.30	-	<0.28	3.60	3.90
A17-P	3.20	0.94	<0.53	6.40	9.40*
A18-N	<0.78	-	<0.28	3.50	4.40*
A19-P	1.35	<0.55	<0.13	4.96	6.51
A20-N	<0.36	-	<0.18	3.53	3.90
A21-P	2.35	<0.59	<0.23	4.62	7.02
A22-N	<0.46	-	<0.30	3.60	4.00
A23-P	1.70	<0.49	<0.31	5.10	7.00
A24-N	<0.24	-	<0.28	3.40	3.70
A25-P	1.70	<0.56	<0.25	5.10	6.80
A26-N	<0.42	-	<0.23	3.60	4.10
A27-P	3.30	<0.58	<0.30	5.40	8.50
A28-N	<0.30	-	<0.39	3.50	3.80
A29-P	2.05	<0.44	<0.20	4.70	6.80
A30-N	<0.33	-	<0.37	3.50	3.94
A31-P	1.65	<0.45	<0.29	4.90	6.50
A32-N	<0.50	-	<0.52	3.70	4.20
A33-P	1.95	<0.62	<0.25	5.50	7.30
A34-N	<0.44	-	<0.33	3.40	3.90
A35-P	2.60	<0.41	<0.27	5.30	7.90**
A36-N	3.20	-	<0.22	3.30	6.50**

*Output

**Instrumented Legs

Table 4-7. Resistance Measurements During Disassembly of Converter P-1 – Radial Row 14 (Milliohms)

Radial Row 14

Axial Leg Location and Type	R_1	R_2	R_3	R_4	R_5
A1-N	8.43	-	<0.26	3.64	12.25*
A2-P	6.90	<0.50	<0.35	5.35	12.20
A3-N	123.0	-	3.3	3.90	127.0
A4-P	5.70	<0.55	<0.21	5.50	11.2
A5-N	77.0	-	<0.25	4.30	83.0
A6-P	5.10	<0.43	<0.15	4.90	10.3
A7-N	37.0	-	<0.28	4.4	42.0
A8-P	6.10	<0.68	<0.42	5.80	11.9
A9-N	30.0	-	<0.19	4.50	35.0
A10-P	6.60	<0.70	<0.28	4.90	11.5
A11-N	15.50	-	<0.46	4.00	19.5
A12-P	5.90	<0.50	<0.26	5.30	11.1
A13-N	1.00	-	<0.32	3.70	4.8
A14-P	4.10	<0.52	<0.22	6.40	10.5
A15-N	17.8	-	<0.35	3.80	21.5
A16-P	4.90	<0.57	<0.16	4.40	9.80
A17-N	17.0	-	<0.34	3.90	20.8
A18-P	5.0	<0.75	<0.14	5.0	9.80
A19-N	39.0	-	<0.16	3.80	43.0
A20-P	5.78	<0.71	<0.38	5.20	11.0
A21-N	72.5	-	<0.15	3.95	77.5
A22-P	5.30	<0.61	<0.16	4.90	10.2
A23-N	117.0	-	<0.20	3.90	122.0
A24-P	4.78	<0.43	<0.20	4.70	9.60
A25-N	90.0	-	<0.37	4.65	95.5
A26-P	5.65	<0.42	<0.77	6.0	11.5
A27-N	106.0	-	<0.22	3.80	110.0
A28-P	4.70	<0.57	<0.14	4.65	9.35
A29-N	128.0	-	<0.32	4.60	133.0
A30-P	5.60	<0.55	<0.29	4.40	9.90
A31-N	163.0	-	<0.32	4.00	167.0
A32-P	4.90	<0.35	<0.12	5.05	10.05
A33-N	81.0	-	<0.44	4.50	87.0
A34-P	7.15	<0.50	<0.45	5.10	12.40
A35-N	44.0	0	<0.59	3.50	46.8
A36-P	6.30	<0.54	<0.25	4.70	11.0*

*Instrumented Legs.

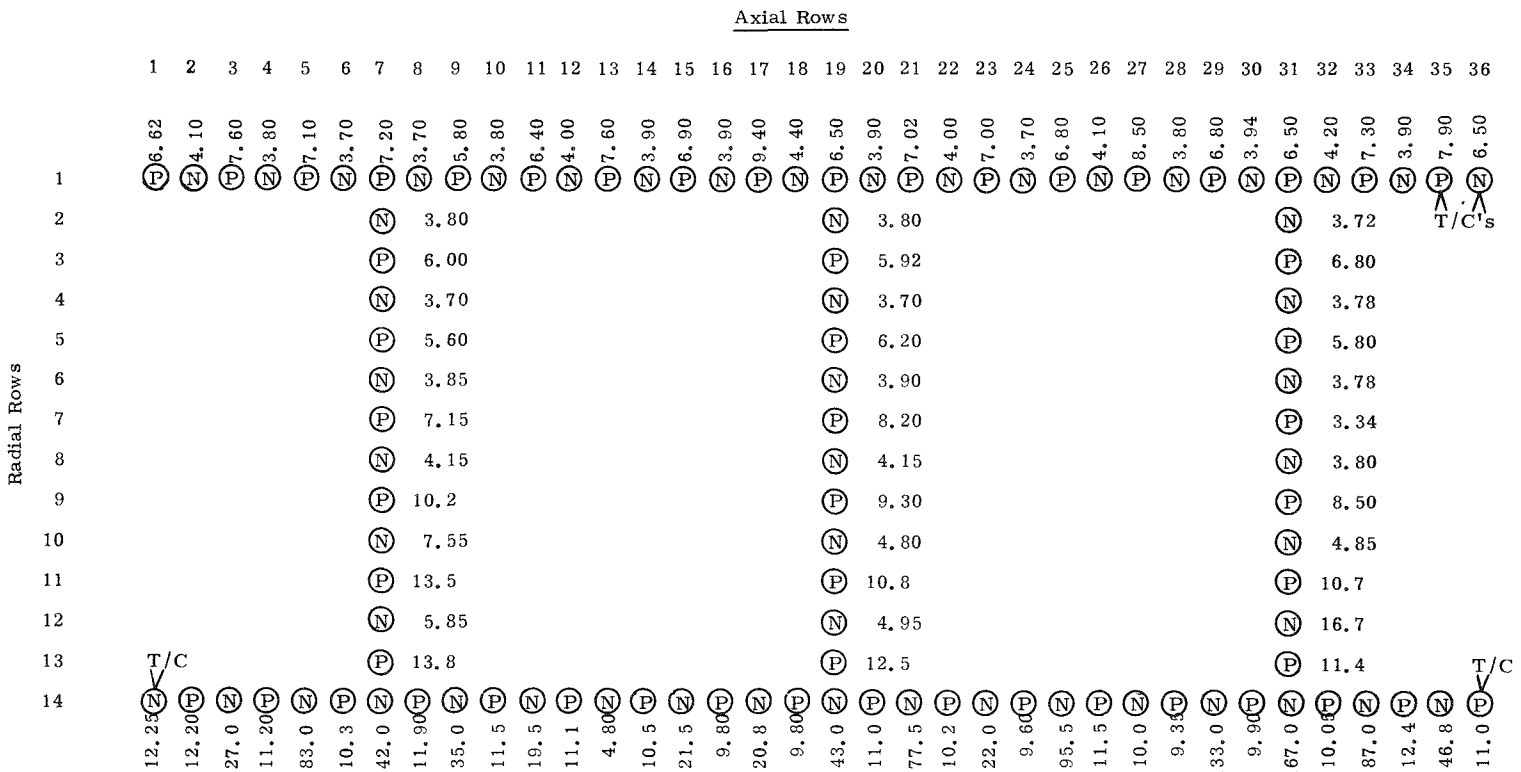

Figure 4-9. Converter P-1 Leg Resistance (R_5) Data and Locations

4.4.4 DISCUSSION OF RESULTS

4.4.4.1 Module A-2

4.4.4.1.1 General Discussion of Module A-2 Contact Resistances

Table 4-3 shows changes in circuit, couple, and leg resistances during various stages of module disassembly. It is suspected that these changes were caused by mechanical perturbations induced during the disassembly process.

Resistance probing of various regions within the legs and couples revealed no significant extraneous resistance except at the thermoelectric leg – hot electrode contact interface. The hot electrode contact resistance was considerably greater for the N legs than for the P legs. The contact resistance ranged from 1.5 milliohms to 3.25 milliohms for the P legs and 53.8 milliohms to 205 milliohms for the N legs. The N-leg contact resistance values are considerably greater than could have existed after thermal gradient testing or after the first resistance check.

The contact resistance during thermal gradient testing can be estimated by subtracting the expected (calculated) material resistance from the actual measured values. However, for monitored N and P legs, the actual resistance values were less than the expected material values at sometime during operation. For the N legs, the minimum resistance values occurred during the first 1000 hours of operation.

Therefore, a more realistic estimate of the contact resistance can be obtained by subtracting the minimum resistance during operation from the measured resistance. For the P legs, the measured resistances were 50 percent greater than the expected material values at the start of test, and then decreased to below expected material values at the time the module was torn down. Since the extraneous resistance for the P legs was significant only across the hot electrode contact interface, it is suspected that the majority of the initial decrease in resistance was across that interface. It is estimated that the initial P leg contact resistance was about 8 mΩ/leg at the start of test and then near ohmic contact after 2000 hours of operation.

Contact resistance during operation for the P legs was more difficult to determine than for the N legs because of an apparent change in thermoelectric properties of the P legs during operation. The material resistivity of the P legs appeared to undergo a decreasing trend as described in paragraph 4.8.4.1.

The estimated contact resistances of the monitored N legs at the end of test operation were:

- For #2 N, 17.1 milliohms
- For #5 N, 10.7 milliohms

4.4.4.1.2 Cause for N-Leg Contact Resistance

There was a strong correlation between contact resistance and contact area at the hot electrode interface. Heavy sublimation of the N legs was observed during post-test disassembly. The edges of the hot end of the N legs were rounded off (Figure 4-10) from sublimation causing a reduction in hot end contact surface area. The P legs were also rounded off but to a lesser degree.

The actual contact area was determined by measuring the diameter, r_1, of the N-leg imprint in the hot electrode as shown in Figure 4-11.

The results were:

- For 2 N, r_1 = 0.056 inch
- For 5 N, r_1 = 0.068 inch

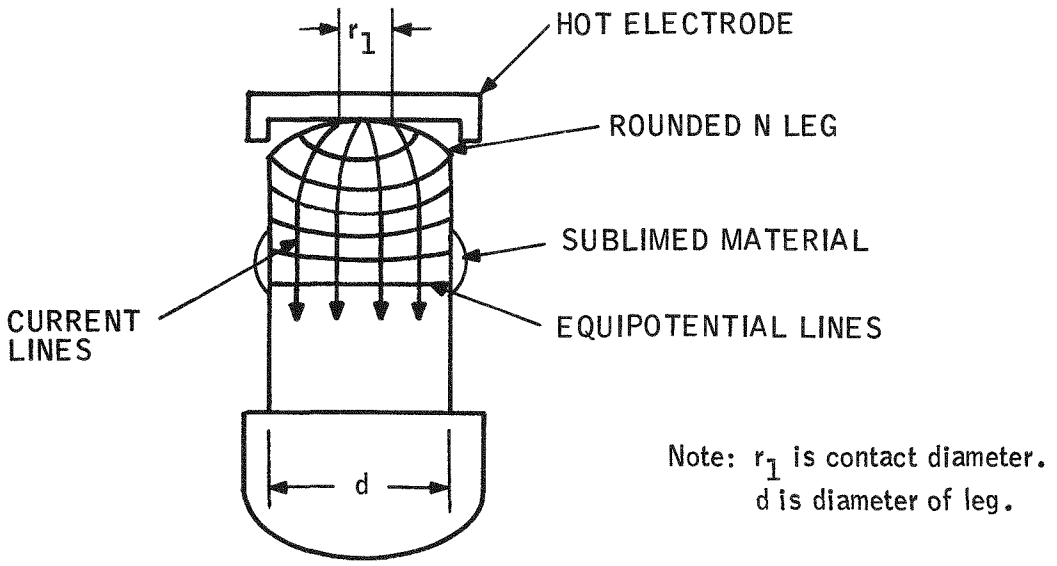

Figure 4-10. Sketch of SNAP-23 Module A-2 N Leg with Rounded End

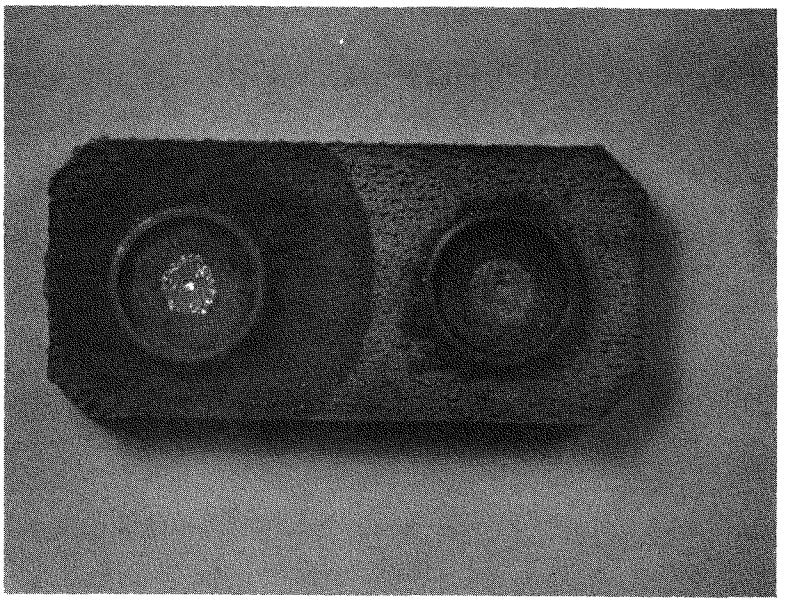

Figure 4-11. SNAP-23 Module A-2 Imprint of Legs in the Hot Electrode

The contact areas are small, approximately one-tenth of the leg area.

Reduction of the N leg contact area will affect the N leg resistance two ways:

- Increase the resistance of the N leg near the hot end by reduction in the effective cross-sectional area.
- Increase the contact resistance, which should be inversely proportional to the contact area.

It is a reasonable assumption that the contact resistance is inversely proportional to the area. Using additional data from SNAP-21 Prototype P-3, contact resistance is plotted as a function of the inverse square of contact diameter in Figure 4-12. The results support an inverse area relationship for contact resistance.

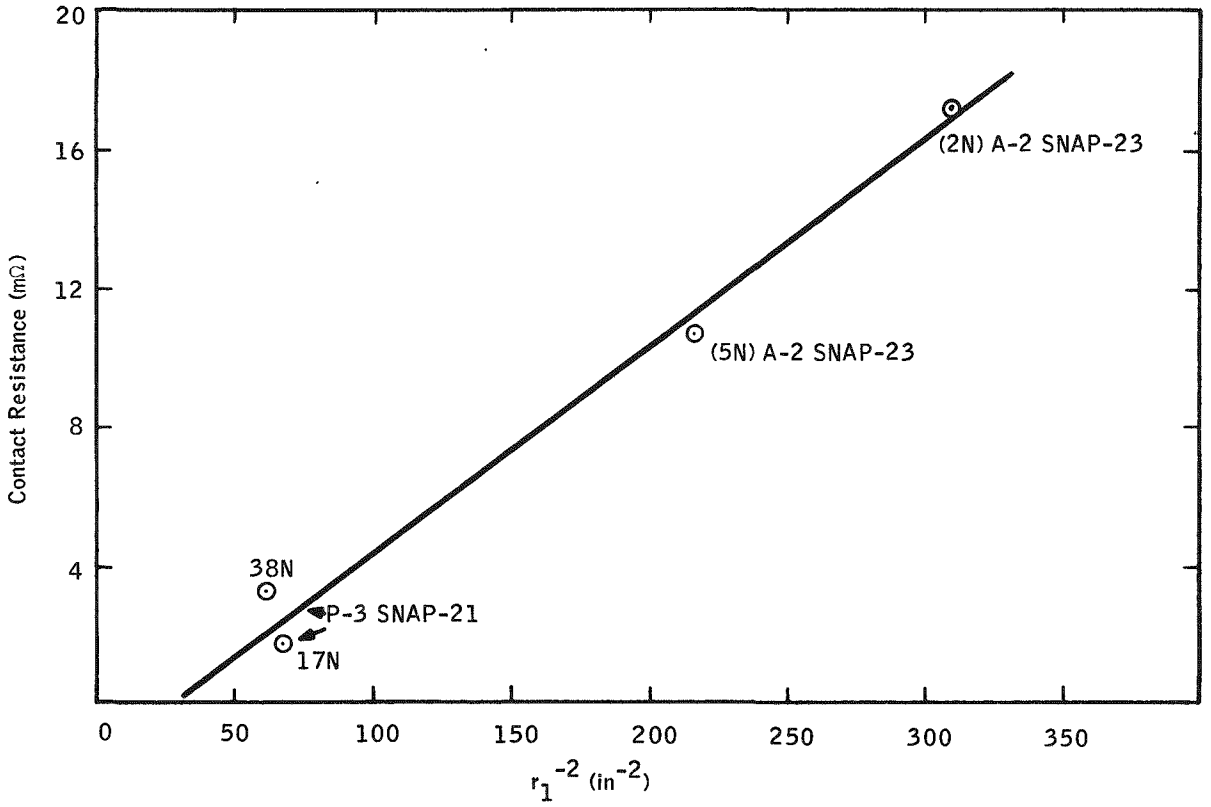

Figure 4-12. Extraneous Resistance (End of Testing) vs (Contact Diameter)$^{-2}$ for 2N, 5N of Module A-2 (SNAP-23) and N Leg 17 of P-3 SNAP-21 Prototype

4.4.4.2 Converter P-1

4.4.4.2.1 General Comments

Table 4-5 shows changes in circuit, couple, and leg resistances during various stages of disassembly. These variations were probably induced by mechanical disturbances during disassembly.

Resistance probing of various regions in the converter revealed no significant extraneous resistance except at the thermoelectric leg-hot electrode contact interface of all the P legs and a few N legs. There was no measurable extraneous resistance noted on the N legs from radial rows 1 through 11. The N legs from radial rows 12 through 14 had hot electrode contact resistances on the order of 40 to 60 mΩ. P leg hot contacts varied from 1 to 10 mΩ. The greatest contact resistances for the P legs occurred in the upper radial rows. The post-test contact resistance measurements were considerably greater than the extraneous resistance estimates during thermal gradient operation.

The contact resistance during operation for the instrumented N and P legs can be estimated by subtracting the expected resistance values from the actual resistance measurements. Expected nominal resistance values for N and P legs during operation were:

1) P leg (Radial Row 1) – 15 mΩ
2) P leg (Radial Row 14) – 16 mΩ
3) N leg (Radial Row 1) – 19 mΩ
4) N leg (Radial Row 14) – 20 mΩ

Using the resistance data from Figure 3-4, it follows that there was probably negligible contact resistance for the instrumented N legs from radial rows 1 and 14. The P legs had contact resistances on the order of 1 to 3 mΩ.

The contact resistances for the N and P legs in radial rows 12 through 14 were developed during cool down and subsequent mechanical disturbances to the converter. This can be seen by examining the relative resistances of the instrumented N and P legs during cool down as shown in Figure 4-13. Since the contact resistances for N and P legs in radial row 1 were small (1-3 mΩ for P legs and 0-2 mΩ for the N legs as shown in Figure 4-9), the relative resistances in Figure 4-13 can be

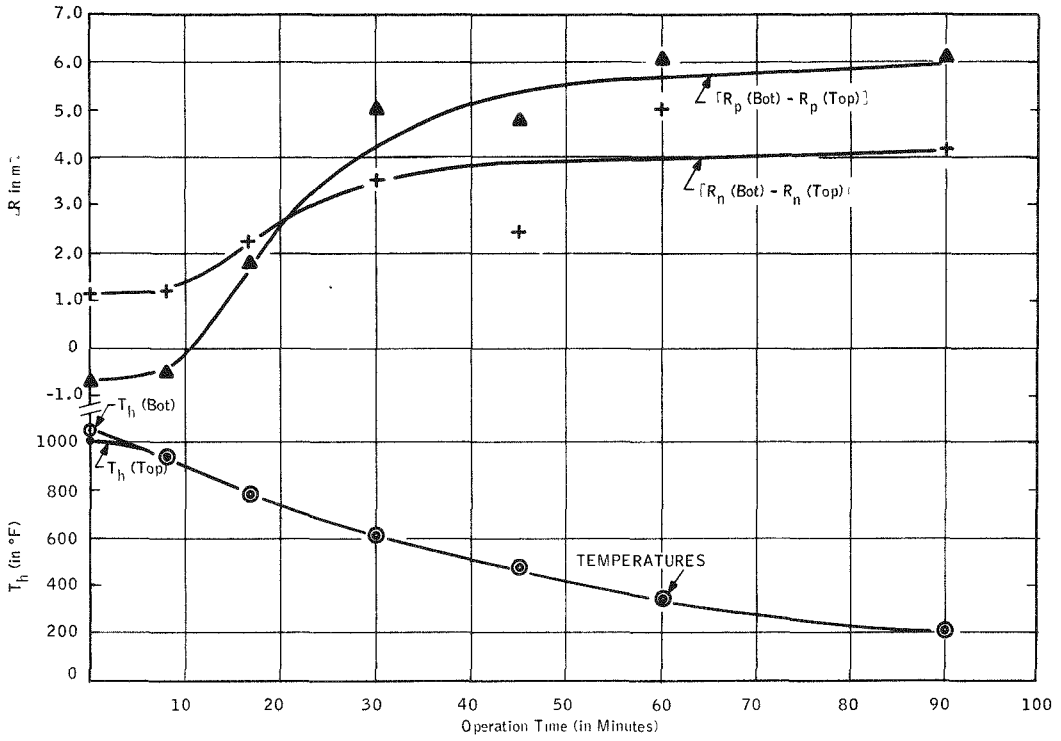

Figure 4-13. Hot Junction Temperature of the Top and Bottom of Converter During Cool Down. Relative Difference in Resistance of the Thermoelectric Legs During Cool Down

interpreted as approximately equal to the contact resistance of the N and P legs from radial row 14. The majority of the contact resistance developed during cool down occurred while decreasing the hot electrode temperatures from 900°F to 600°F.

4.4.4.2.2 Conclusions

Since the converter was thermal cycled three times during operation without adverse effects, the hot electrode contact resistances measured during post-test disassembly would probably have returned to normal low values if the converter had been energized to operating conditions.

The finite, but small, contact resistances for the P legs were probably due to sublimation effects. The P legs were rounded off at the edges, resulting in reducted contact areas; this effect is discussed in paragraph 4.4.4.1.2.

4.5 CONVERTER P-1 ALIGNMENT ANALYSIS

4.5.1 BACKGROUND

The leg alignment analysis on Converter P-1 consisted of determining the angular displacements, during and after operation, of the N and P legs from their normal positions.

Nominal cold frame-hot frame dimensional relationships for the SNAP 23 P-1 and P-2 converters are shown schematically in Figure 4-14.

As a result of machining discrepancies on the cold frame, the cold frame-hot frame relationship for Converter P-1 was altered, as shown in Figure 4-15. The discrepancy was noted and steps were taken to adjust for it, using the cold frame as it was. During final assembly, an induced error of 0.010 inch was recorded during welding when parts would not properly fit.

Figure 4-16 shows the relationship of the hot and cold frames after assembly and welding. The error was such that a 0.010 inch misalignment occurred. As a result, hot end hardware was properly located but the cold frame was displaced 0.010 inch toward the support cone end. A leg hot end contact angle of 1 degree would result from such a misalignment.

Because of the initial 0.010 inch displacement, it was expected that significant misalignment would be evident during disassembly.

4.5.2 ANALYTICAL PROCEDURES

Post-test alignment analysis was conducted following the general procedures described in paragraph 6.3 of Volume I. The following is a summary of the exact analysis procedure which was used.

After the bottom of the outer case was removed, axial and radial dimensional checks were taken on radial row 14. The upper support cone was then removed and complete axial and radial dimensional checks were performed on radial row 1 along with a few sample measurements from radial row 14. The legs were then

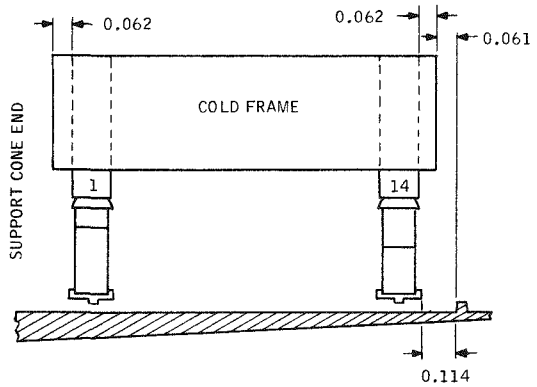

Figure 4-14. SNAP-23 Converter P-1 Nominal Design

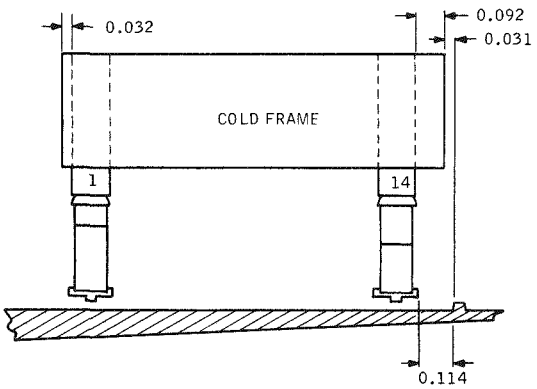

Figure 4-15. SNAP-23 Converter P-1 Actual Dimensions

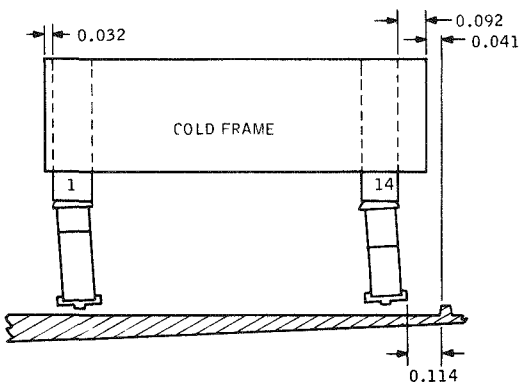

Figure 4-16. Misalignment in SNAP-23 Converter P-1 Prior to Energizing the Heaters

removed except for six axial rows located in double rows 120° apart which was necessary to maintain structural stability between the hot and cold frames. Axial measurements were then made on the remaining intact legs.

The above stated procedure determined the displacement of the legs after the converter cooled to room temperature. However, it was believed that leg displacement during thermal gradient operation was significantly different from the displacements measured during post-test disassembly.

In an effort, therefore, to describe ingradient displacement legs were physically examined and dimensioned. Visual examination disclosed that many legs still bore evidence at their hot ends of an angle not representative of nominal conditions. The hot end angle was determined by measuring the maximum and minimum leg lengths (shown in Figure 4-17).

Maximum and minimum leg length difference, C, was then used in the function, $\tan \phi = C/D$, to determine the displacement angle, ϕ.

It is believed that the angle, ϕ, represented the displacement of the legs from their normal position during operation.

The results of the thermal gradient displacements were based on measurements of the N legs only. This was done for two reasons:

1) N legs deform more readily in the thermal gradient environment. This can be seen from Figure 4-18.

2) The P legs had not completely seated into the hot electrode buttons as indicated by resistance determinations for P legs during operation. Extraneous resistance determined for the P legs was on the order of one to three milliohms, as previously discussed in paragraph 4.4.4.2.1.

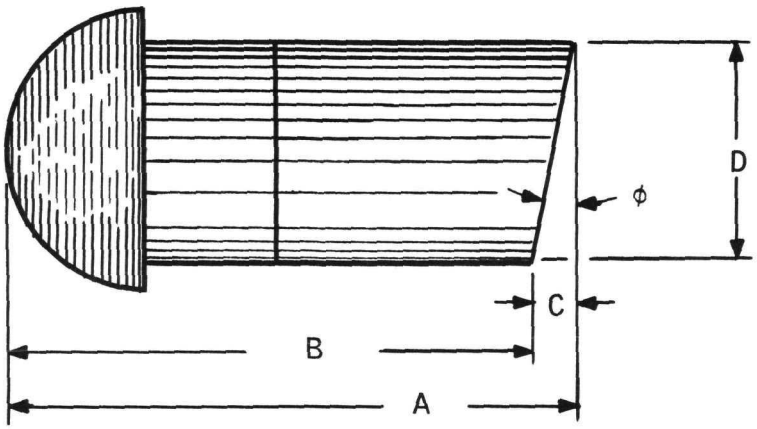

Figure 4-17. Using Post-Test Leg Geometry to Determine Displacement Angle ϕ

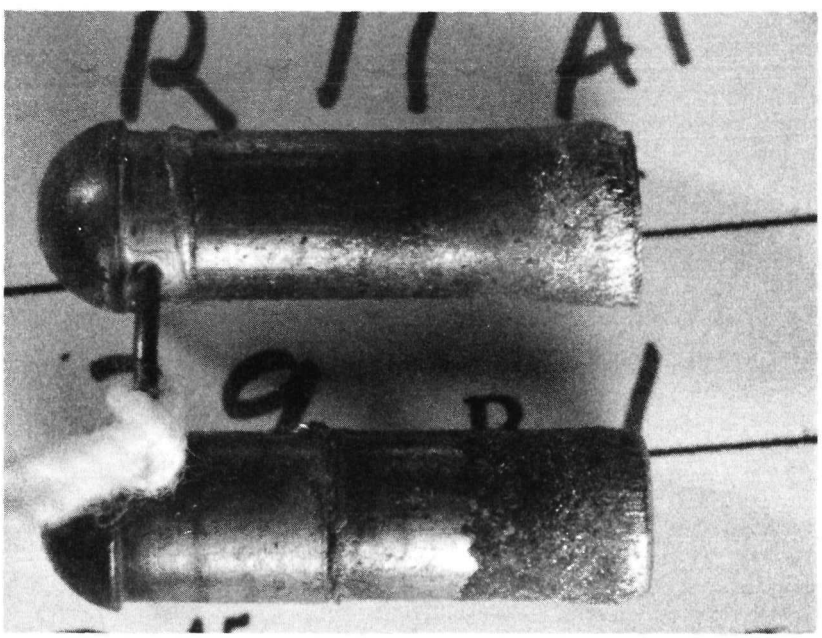

Figure 4-18. SNAP-23 Converter P-1 Leg Deformation

4.5.3 RESULTS

Post-test measurements of the actual hot end-cold end relationships during disassembly disclosed that the legs were displaced from their nominal position at both the top and bottom of the converter. In general, the hot electrodes were displaced downwards toward radial row 14. Figure 4-19 is a plot of the hot electrode displacement versus radial row number.

Average angular displacement during thermal gradient operation and during post-test disassembly are plotted as a function of radial row number (axial position) in Figure 4-20. The thermal gradient displacements are based on post-test leg measurements.

4.5.4 DISCUSSION OF RESULTS

Based on the alignment results, the electrical insulation strips (boron nitride) did not function as intended to restrict motion of the hot electrodes in the outer rows (1, 2, 3 and 14, 13, 12). During cool down, most of the hot electrode motion occurred in the region of the outer rows. This motion is reflected in the difference between thermal gradient and post-test angular displacements. An approximation of the actual hot electrode motion can be determined by equating a one-degree angular displacement with a 0.012-inch displacement of the hot electrode. Therefore, radial row 14 moved 0.03 inch and radial row 1 moved 0.01 inch during cool down.

An extension of the basic calculations presented in Section 3.3.24 titled "Couple Alignment Analysis" contained in the SNAP-23A Program Phase I Thermoelectric Converter Development Program Quarterly Report #2 (3M report MMM 3824-009) discloses that during heat-up, the hot frame should expand 0.039 inch relative to the cold frame at radial row 14. Conversely, the same amount of motion could be expected during cool-down. This is in agreement with actual alignment results.

It should be noted that post-test alignment measurements indicated that the legs in row 14 were displaced three degrees after cool down. This is contrary to the one degree displacement noted during assembly. It is possible that during thermal cycling, the individual boron nitride strips were sliding under the hot frame, forming a net displacement of the individual boron nitride strips outward away from the center of the converter.

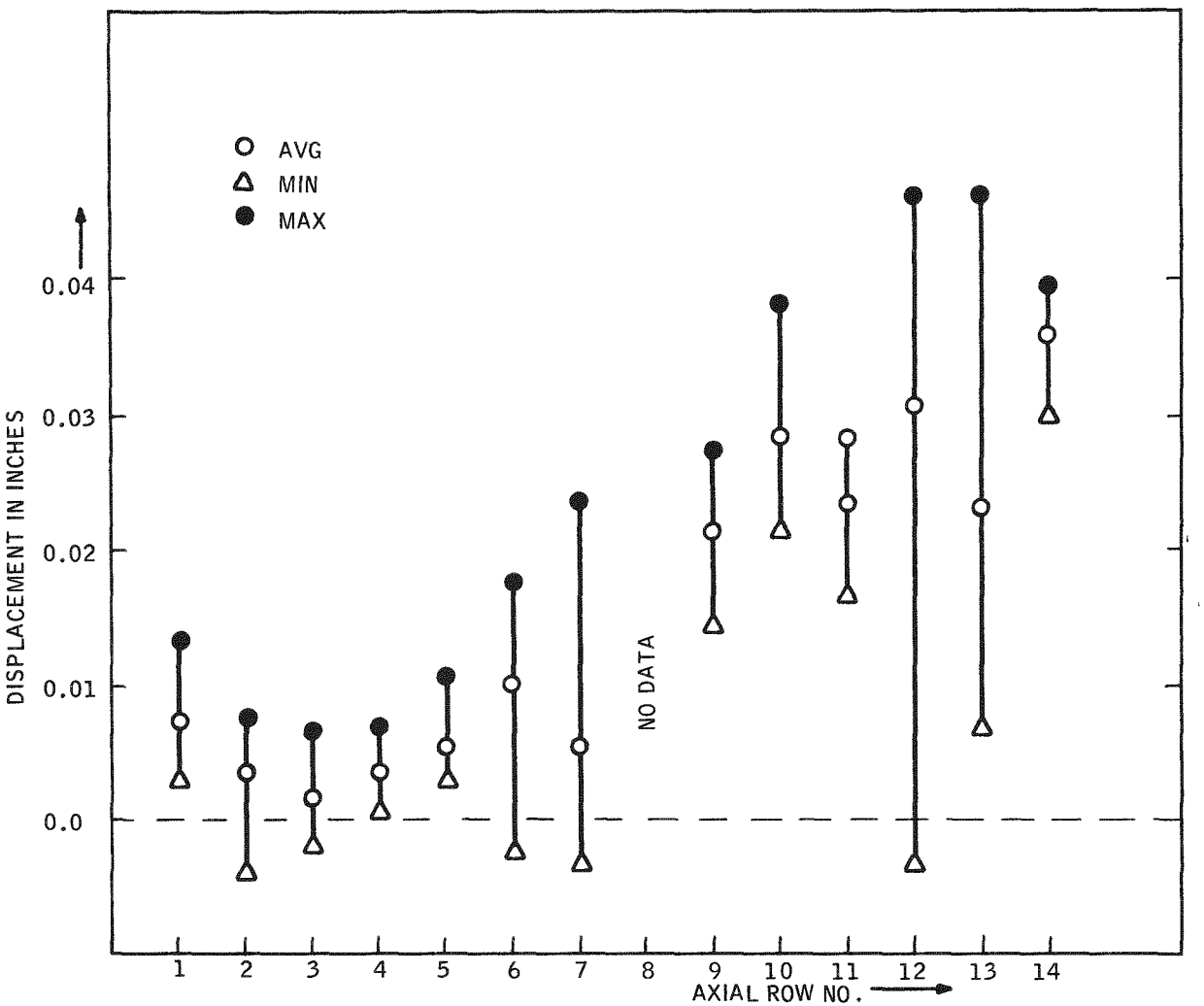

Figure 4-19. SNAP-23 Converter P-1 Displacement of Leg Hot End from Design Location

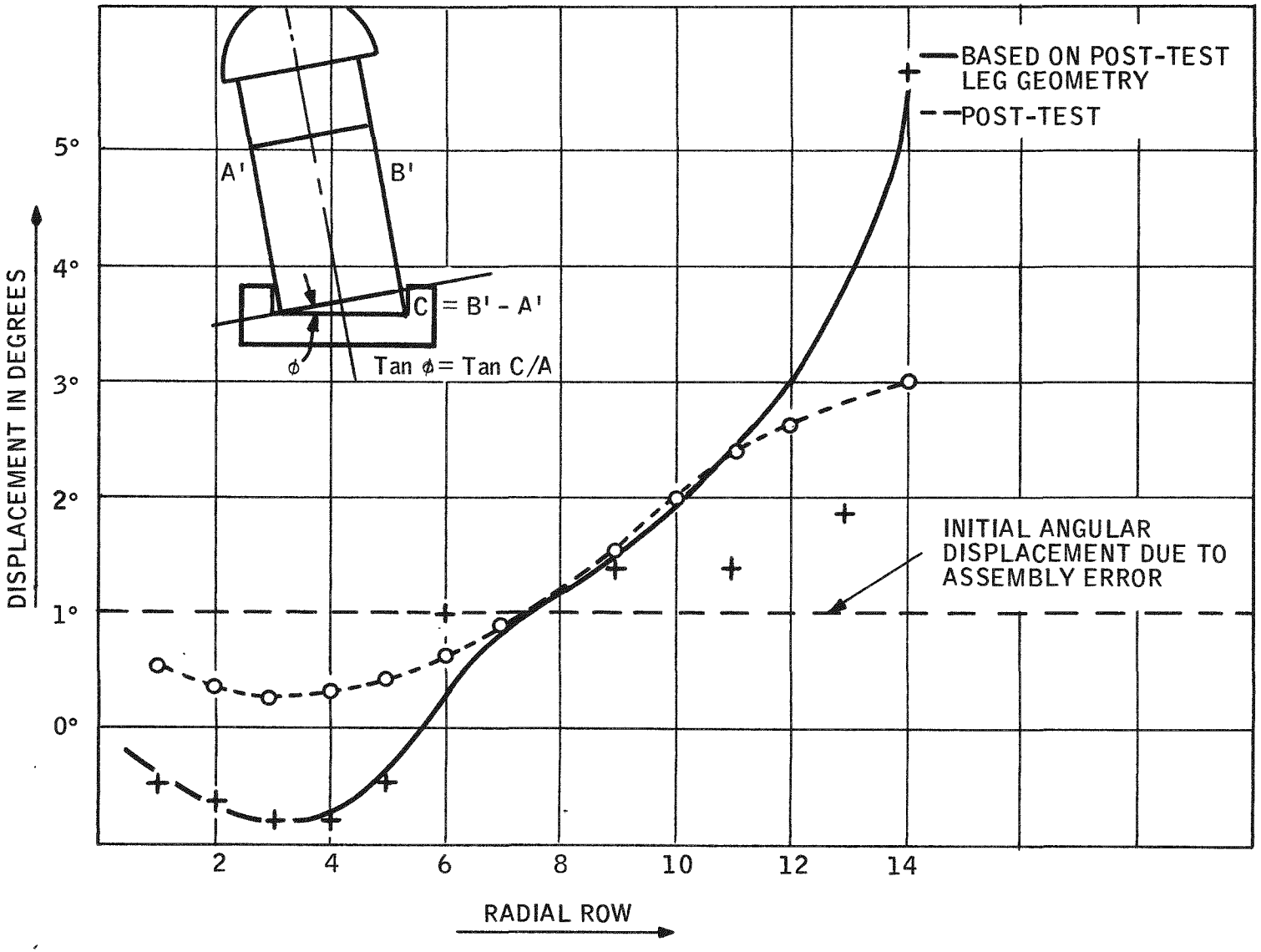

Figure 4-20. SNAP-23 Converter P-1 Post-Test and Ingradient Leg Displacement

The fact that the boron nitride strips did not restrict motion of the hot electrodes (relative to the hot frame) located in the outer rows is not surprising, since all of the boron nitride strips were broken into 8 to 12 pieces.

Since the thermal gradient alignment analysis is based on deformation of the legs during the long-term thermal gradient operation, the boron nitride strips probably broke up during an early stage of operation.

Since the converter operated stably for 10,800 hours and was thermal cycled four times without adverse effects to the output performance, the net effect of misalignment and hot electrode motion appeared to be negligible.

4.6 THERMAL CONDUCTANCE ANALYSIS

4.6.1 BACKGROUND

This section is primarily concerned with the thermal conductance changes that occurred between the cold cap and cold block of the converter (Figure 3-6). Both the SNAP-21 and SNAP-23 converters had similar cold cap-follower-cold frame systems. Therefore, the post-test cold end thermal impedance analysis of the SNAP-21 48-couple Prototype P-3 is relevant and will be included in this section. It is important to note that both SNAP-21 P-3 and SNAP-23 P-1 used silicon heat transfer grease at the follower-cold block and follower-cold cap interfaces.

The SNAP-21 prototype Converter P-3 demonstrated larger thermal conductance excursions than the SNAP-23 converter, as shown in Figure 4-21. Whatever time dependent heat transfer mechanism is involved at the cold end should be more readily apparent during the post-test analysis of the SNAP-21 Prototype P-3. Therefore, the majority of the cold end post-test thermal analysis was conducted on the SNAP-21 prototype.

During disassembly, it was noted that there were only traces of heat transfer grease between the two cold end interfaces for both the SNAP-21 and SNAP-23 converters. The residual grease was more viscous than fresh silicon grease. In addition, there was evidence that a reaction had occurred between the Min-K 1301 and the heat transfer grease on the followers and above the cold block.

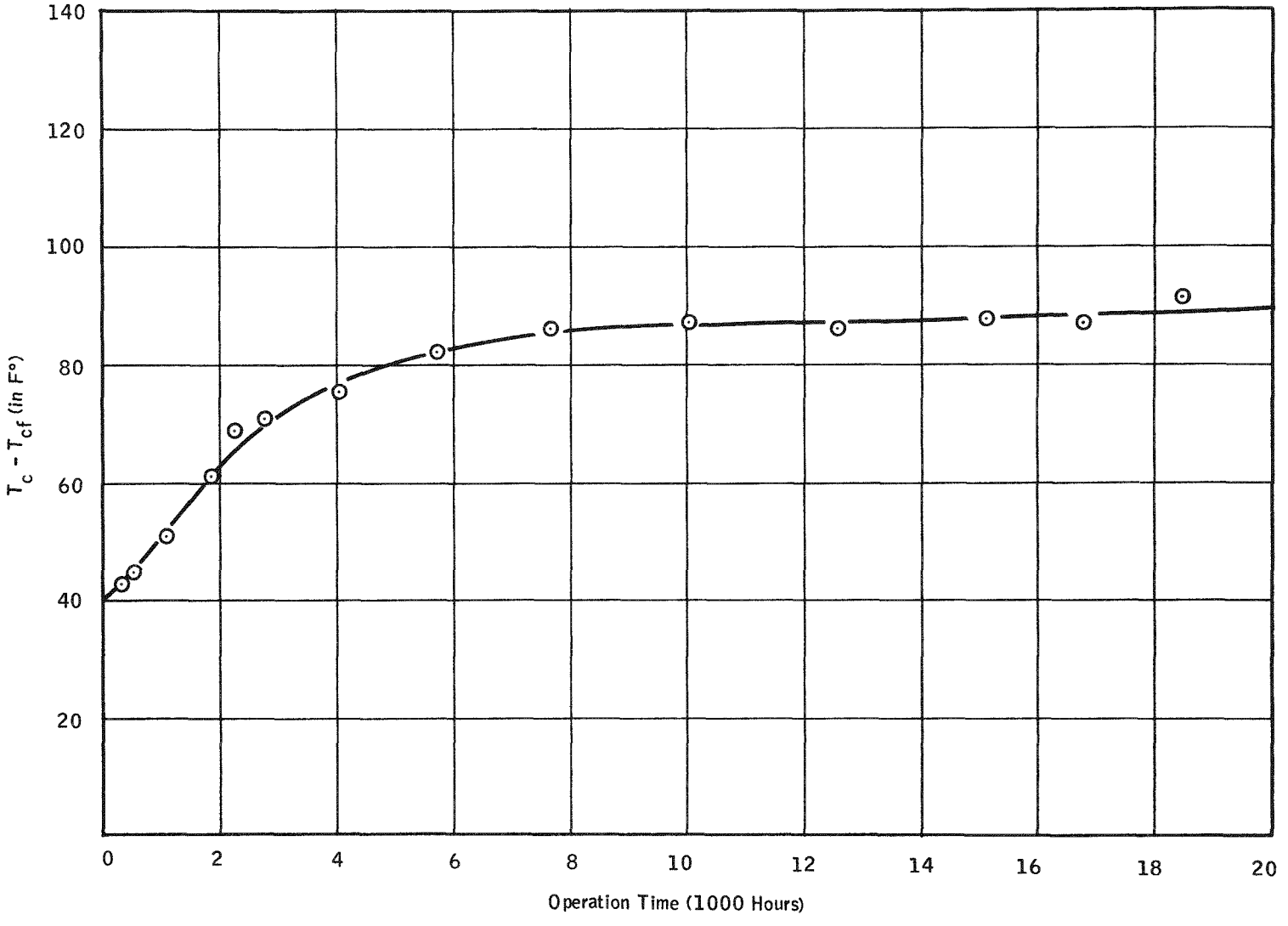

Figure 4-21. Temperature Drop Between Cold Cap (Average) and Cold Frame vs. Time for SNAP-21 Converter P-3

Visual examination suggested that a majority of the heat transfer grease was drawn from the cold end interfaces, while the remaining intact grease was changing in material characteristics. However, analytical tests were necessary to:

- Substantiate the heat transfer grease as the cause for the thermal instability.
- Determine why the SNAP-23 converter was thermally more stable than the SNAP-21 prototype.

4.6.2 ANALYTICAL PROCEDURES

Six N and six P legs with their respective followers were removed from the SNAP-21 prototype during post-test disassembly, and then tested in a bell jar under varying conditions. The bell jar fixture consisted of a hot and cold block in a parallel plate configuration capable of holding six couples and their respective followers. The old residue grease was removed from five N and P legs. The sixth N and P legs were tested in the bell jar with the old residual grease intact. Two of the other five N and P legs were tested without any grease in either interface. Fresh grease was applied to the remaining three N and P legs as follows:

1) Grease only at the follower-cold frame interface.

2) Grease only at the cold cap-follower interface.

3) Grease at both interfaces.

The twelve legs were then tested in the bell jar at a hot electrode temperature of 1100°F, cold block temperature of 80°F, with Min-K 1301 thermal insulation packed around the legs. The test was conducted both in a vacuum and in argon at an atmosphere pressure of 2 psig. Iron-constantan thermocouples were used to measure hot electrode, cold electrode, and cold frame temperatures. Refer to Figure 4-22.

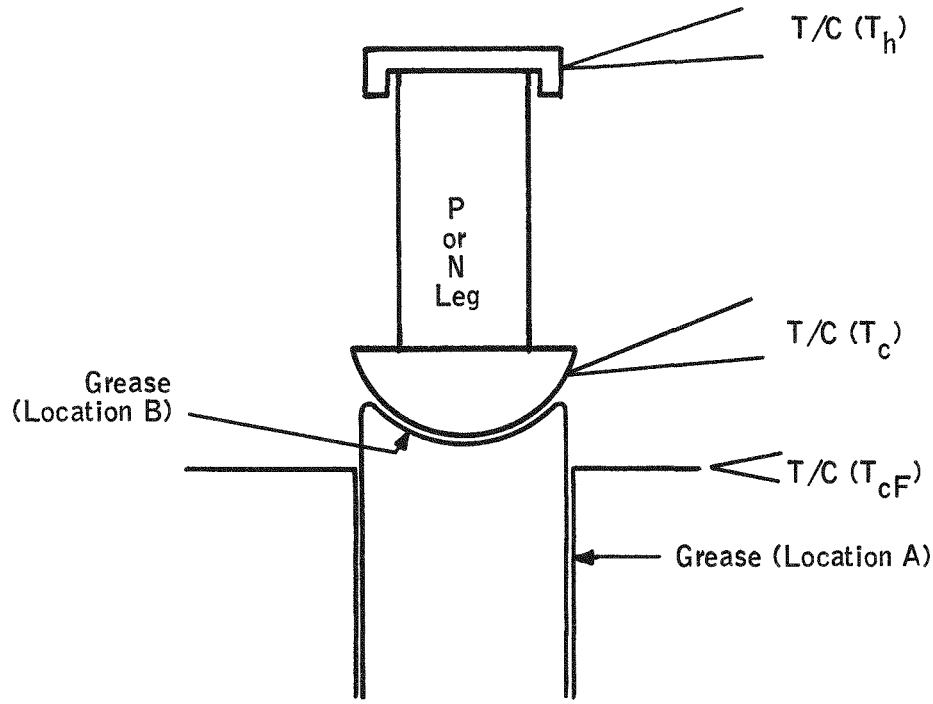

Figure 4-22. Location of Thermocouples and Grease in SNAP-21 Converter P-3 Cold End Heat Transfer Test

In addition to the bell jar testing, several SNAP-21 Converter P-3 and several SNAP-23 Converter P-1 followers and cold caps were inspected as follows:

- Surface roughness of cold cap and follower sockets.
- Deviation from round of caps and follower sockets.
- True radius of caps and follower sockets.

A total of ten N and ten P cold caps with their respective followers were examined from the SNAP-21 prototype. Four cold caps and followers were examined from SNAP-23 Converter P-1.

4.6.3 RESULTS

The results of bell jar testing are presented in Table 4-8. Grease locations A and B are identified in Figure 4-23. The thermoelectric leg identification numbers (e.g., P-14) identifies the leg such that it can be traced back to the original lot and batch material and pretest R vs L measurements.

Table 4-8. Cold End Heat Transfer Results for SNAP-21 Converter P-3 Hardware with (T_H = 1100°F; T_{CF} = 80°F)

Test Description	N Leg (T_C-T_{CF})		P Leg (T_C-T_{CF})	
	Vacuum $\Delta T' = T_C - T_{CF}$	2 PSIG (Ar) $\Delta T = T_C - T_{CF}$	Vacuum $\Delta T' = T_C - T_{CF}$	2 PSIG (Ar) $\Delta T = T_C - T_{CF}$
No grease P10; N9	185°F	76°F	366°F	146°F
No grease P12; N11	267°F	74°F	284°F	110°F
Grease (A) P14; N13	290°F	94°F	245°F	95°F
Grease (B) P6, N5	49°F	34°F	90°F	50°F
Grease (A+B) P27; N26	35°F	29°F	39°F	43°F
Old grease P39; N38	71°F	41°F	125°F	79°F

The results of the cold cap and follower inspection (dimensional and surface analysis) are in Table 4-9.

Table 4-9. Surface and Dimensional Inspection of Cold Caps and Follower Sockets for SNAP-21 Converter P-3 and SNAP-23 Converter P-1

Description	SNAP-21			SNAP-23		
	True Radius (in inches)	Deviation from Round (inches)	Surface Finish (μ inches)	True Radius (in inches)	Deviation from Round (inches)	Surface Finish (μ inches)
P Cold Caps	0.1232	No data	32	0.1066	±0.0002	4
N Cold Caps	0.1238	No data	16	0.1066	±0.0002	4
Followers	0.1307	±0.0013	8	0.1063	±0.0003	8

NOTE: Results are average values from all sockets and caps measured.

4.6.4 DISCUSSION OF RESULTS

4.6.4.1 General Comments

Based on the bell jar test, the temperature difference between cold cap and cold block can be reduced to 40°F by adding fresh heat transfer grease between the interfaces as can be seen in Table 4-8. A forty degree temperature difference agrees quite well with the temperature difference that existed in the SNAP-21 prototype at the beginning of thermal gradient test operation as shown in Figure 4-21.

It is significant to note that the greatest amount of improvement occurred when heat transfer grease was added to the cap-socket interface, suggesting that the majority of the cold end thermal impedance excursion during operation occurred across that interface. It should be noted that the results of the bell jar test dictated the dimensional and surface finish examination of the cold caps and follower sockets.

The following general comments can be made about the follower-socket and cold cap inspection for SNAP-23 Converter P-1 and SNAP-21 Converter P-3.

- The fit between the follower sockets and cold caps for the SNAP-23 converter was considerably better than for the SNAP-21 prototype.
- The surface finish on the cold caps and followers was better for the SNAP-23 Converter P-1.

In addition, it was noted during the cap-follower inspection that all of the followers for the SNAP-21 prototype had a flat spot near the center of the socket. Only a very small area will be in contact between the follower and cold cap. Refer to Figure 4-23.

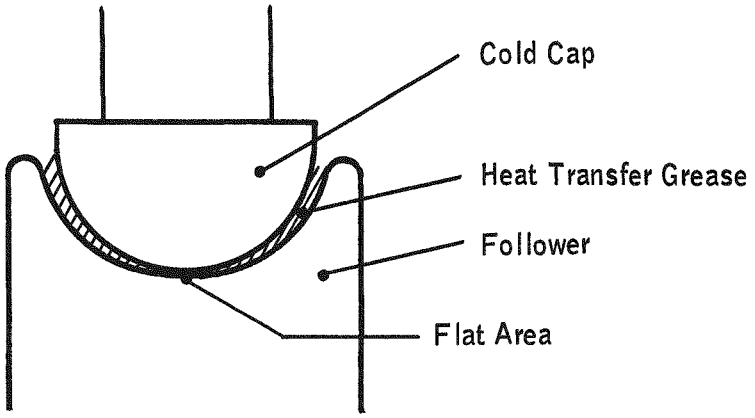

Figure 4-23. Follower-Socket Interface for SNAP-21 Converter P-1

4.6.4.2 Conclusions

The cold end thermal impedance increased during test operation because:

- A loss in effectiveness of the heat transfer grease to transfer heat across the cold cap-follower interface. This was due either to a change in heat transfer characteristics of the grease, or
- Withdrawing of the grease from out of the interface by capillary action.
- The extent to which the thermal impedance across the cap-follower interface increases is determined by the fit between the two surfaces. This is summarized in Table 4-10.

Table 4-10. Relationship of SNAP-21 Converter P-3 Cold Cap - Follower Mismatch and Total Observed Increase in ΔT Across Cold End

Description	True Radius of Follower Minus True Radius of Cold Cap	$T_C - T_{CF}$
SNAP-21	+0.0072	50°F
SNAP-23	-0.0003	14°F

4.7 SPRING PRESSURE ANALYSIS

4.7.1 BACKGROUND

During post-test analysis, the spring compressive load on each leg of couples numbered 5 and 6 in Module A-2 was determined. Because of the geometrical configuration of SNAP-23 Converter P-1 and the method used for retaining the springs in the cold frame, no attempt was made to determine the spring compressive load on sample legs from the converter.

Analysis of the spring load was deemed necessary because a loss of spring pressure was considered a possible potential major degrading mechanism within Module A-2.

4.7.2 ANALYTICAL METHOD

After the electrical continuity tests were completed, the snap rings that retain the springs were removed. Sufficient force was then applied to return the springs to their original position. The original position of the springs could be determined by aligning the base of the spring above the notches in the follower holes which retained the snap rings. The resulting compressive load was then measured.

After the legs were removed, the static friction of the followers from legs numbered 1N, 3P, 4N, 4P, 6P, and 6N were measured.

4.7.3 RESULTS

The spring compression on 5N, 5P, 4N and 4P are given in Table 4-11. The pressure data in Table 4-8 is defined as the spring compression divided by the cross sectional area of the leg.

Table 4-11. Contact Pressure on 4N, 4P, 5N, 5P of SNAP-23 Module A-2

Description	Compression (lbs)	Pressure (lb/in^2)
4N	4.05	147
4P	3.63	132
5N	4.05	147
5P	3.72	135

The static friction results for the followers are summarized in Table 4-12.

Table 4-12. Static Friction of Followers in Cold Block for SNAP-23 Module A-2

Follower Description	Static Friction (lbs)
1N	0.55
3P	0.45
4N	0.50
4P	0.45
6N	0.65
6P	0.50
Average	0.52

4.7.4 DISCUSSION OF RESULTS

The compressive load on the N legs were within 3 percent of their design value after 18,100 hours of test operation. The compressive loads on the P legs were slightly lower but still within 15 percent of their design values.

Static friction effects between the follower and cold block were an order of magnitude smaller than the spring loading forces. Therefore, it is likely that the majority of the spring forces were transferred to the hot electrode contact area. In addition, it is likely that the compressive loading at the leg-hot electrode interface was maintained throughout the thermal gradient test operation.

4.8 THERMOELECTRIC ANALYSIS

4.8.1 BACKGROUND

After removal from the SNAP-23 module and converter, the legs were tested to determine Seebeck coefficient and (room temperature) resistivity characteristics. The room temperature resistivity of all legs was then compared with pretest data for the same legs. Because Seebeck testing is destructive, only random samples from both thermopiles were taken and measured for Seebeck coefficient. Seebeck analysis was also performed on random samples of thermoelectric legs not used in any thermopile but from the same lots and batches used in the converter and module. It was then possible to compare the Seebeck characteristics of used legs with unused legs to determine if there had been any change in the Seebeck properties of the thermoelectric materials during the thermal gradient operation.

4.8.2 ANALYTICAL PROCEDURE

4.8.2.1 Resistivity Analysis

The resistivity was determined using a four-point probe resistance vs length technique in accordance with the general procedures described in Specification TPI-1B, presented in paragraph 6.3 of Volume I.

4.8.2.2 Seebeck Analysis

The Seebeck analysis was conducted in accordance with the general procedures described in Specification TPI-2A, procedure II, presented in paragraph 6.3 of Volume I. The following is a brief summary of the analysis procedure which was used:

Each N leg was divided into five (5) sections as illustrated in Figure 4-24. Sections numbered 1 through 3 were part of the hot segment, with approximate room temperature resistivity of 120 μΩ-inches. The other two sections, numbered 4 and 5, were part of the cold segment, with approximate room temperature resistivity of 400 μΩ-inches.

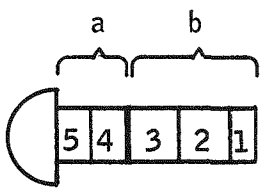

	a	b
Material	PbTe	PbTe
Segment	Hot	Cold
Resistivity	400 μΩ-inches	120 μΩ-inches

Figure 4-24. N-Leg Sections Measured for Seebeck

The sizes of the sections were approximately:

- number 1, 1 to 2 millimeters long
- numbers 2 and 3, 2 to 3 millimeters long
- numbers 4 and 5, 2 to 3 millimeters long

Because the P legs were shorter, each P leg from the converter was cut into four (4) sections as illustrated in Figure 4-25. The hot end segments (PbTe-SnTe) and cold end segments $(BiSb)_2$ Te_3 were divided approximately into equal sections.

However, it was deemed necessary to examine the P legs from Module A-2 more closely because of their voltage degradation during thermal gradient operation (shown in Figure 3-9). The P legs from Module A-2 were cut into five (5) sections as illustrated in Figure 4-25. The sizes of the sections were approximately:

- number 1, 1 millimeter long
- numbers 2 through 5, 2 millimeters long

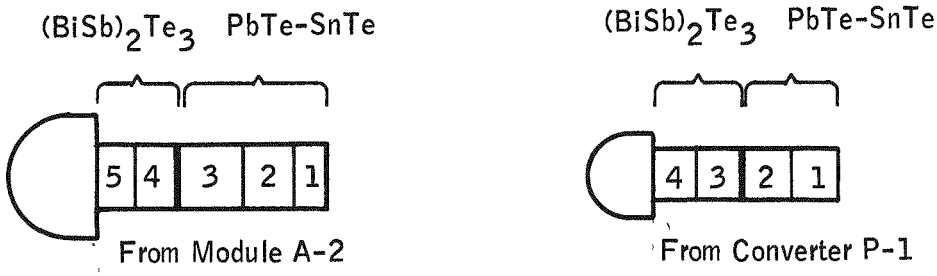

Figure 4-25. Sections of P Legs Measured for Seebeck

Seebeck analysis was then conducted on each section as follows:

One end of the section was held constant at 75°F and the hot end temperature was allowed to vary. The temperatures were varied as follows:

- For cold segment $(Bi\ Sb)_2\ Te_3$ material: 175° to 675°F.
- Remaining sections: 175° to 1075°F.

The Seebeck voltage and temperature differences were recorded on an x-y recorder. The Seebeck coefficient, as a function of temperature, was then determined by differentiating the curve obtained on the x-y recorder. The method of differentiating the curve from the x-y recorder was as follows:

1) The average slope of the Seebeck voltage was determined for every 100°F change in hot end temperature.
2) The slope was set equal to the Seebeck coefficient.
3) The temperature for a given Seebeck coefficient was set equal to the average hot end temperature over the 100°F temperature change.

Seebeck analysis was conducted on legs numbered 1N, 1P, 2N, 2P, 5N, and 5P from Module A-2. These legs were then compared with an unused N and P leg control sample from the same lot and batch used in the module, identified as follows:

- For N legs, SLP 34843 Lot-9, Batch 1.
- For P legs, SLP 34843 Lot-12, Batch 1.

Seebeck analysis was conducted on twenty N and P legs from Converter P-1. The location in the converter for the individual N and P legs is given in Table 4-13. The legs are identified by a letter-number combination. The letter (B, G, or R) refers to the lot and batch of materials that the leg originated from. The number identifies the couple number from the particular lot and batch. The lot and batch identification is as follows:

- B-SLP 34843, Lot-39, Batch 2.
- G-SLP 34843, Lot-39, Batch 2.
- R-SLP 34843, Lot-39, Batch 1.

Three unused N and P legs from lots and batches used in the converter were used as control samples. The lot and batch identification is:

- For N legs, SLP 34843, Lot-52, Batch 1.
- For P legs, SLP 34843, Lot-53, Batch 1.

The "control" N and P legs came from the same lots and batches as the instrumented N and P legs from the converter.

Table 4-13. Location of N and P Legs Used for Seebeck Analysis for SNAP-23 Converter P-1

P Legs		N Legs	
Description	Location	Description	Location
B-28	R1 A7	B-28	R1 A8
B-52	R1 A13	B-52	R1 A14
B-136	R1 A19	B-136	R1 A20
B-144	R1 A25	B-144	R1 A26
B-6	R1 A31	B-6	R1 A32
G-123	R5 A19	G-123	R4 A19
R-82	R4 A26	R-82	R5 A26
G-78	R3 A31	G-78	R2 A31
G-76	R5 A31	G-76	R4 A31
G-73	R7 A31	G-73	R6 A31
G-71	R9 A31	G-71	R8 A31
G-70	R11 A31	G-70	R10 A31
G-69	R13 A31	G-69	R12 A31
B-129	R14 A30	B-129	R14 A31
G-85	R7 A7	G-85	R6 A7
G-80	R11 A7	G-80	R10 A7
G-117	R9 A19	G-117	R8 A19
R-59	R14 A2	R-59	R14 A3
B-112	R-14 A18	B-112	R14 A19
B-74	R14 A6	B-74	R14 A7

4.8.3 RESULTS

4.8.3.1 Resistivity Results

Resistivity (R vs L) measurements conducted at room ambient temperature are accurate to about ±20 percent. Only very large changes in value should be considered in determining basic trends. All of the resistivity data will not be included in this report as over 2000 individual measurements were made in the analysis.

4.8.3.1.1 Module A-2

Although it was possible to determine lot and batch identification for the legs used in the module, traceability records were not available to determine leg location in the module, except for the P and N output terminal legs. A one-to-one correspondence between pre-test and post-test resistivity data was not possible.

The results for the pre-test resistivity analysis are given in Table 4-14.

Table 4-14. Pre-test Data for Module A-2 Legs Resistivity at Room Ambient Temperature (Micro-Ohm-Inches)

P Legs				N Legs	
Description	PbTe-SnTe Segment	BiTe-SbTe Segment	Description	PbTe ρ = 120 $\mu\Omega$-in	PbTe ρ = 400 $\mu\Omega$-in
**	316	~ 200*	**	120	420
**	310	310*	**	120	436
**	322	200*	**	100	400
**	344	162*	**	114	460
**	260	~260*	**	136	~300*
1P	316	234*	6N	126	400

*Noise level was high during R vs L (resistivity) measurements of the segment. The results given are estimates only (±50%).

**The actual location of the leg in Module A-2 was not documented.

The results for the post-test resistivity analysis are as follows:

1) Output terminal P leg (1P) had a high (1.5 mΩ) resistance zone located 0.05 inch from cold cap. This resistance zone was not detected during the continuity tests on the module, Section 4.4. A crack in the P leg was observed in the same zone. This crack was observed during the disassembly of the module and is shown in Figure 4-1.

2) A low resistivity (~ 120 μΩ-in.) region approximately 0.04 inch long located next to the cold cap existed on all P legs. The same region was dark purple in color compared to the normal light metallic color of bismuth-antimony-telluride (BiTe-SbTe) (Figure 4-26). The purple reaction zone is discussed in Section 4.8.3.2.2.

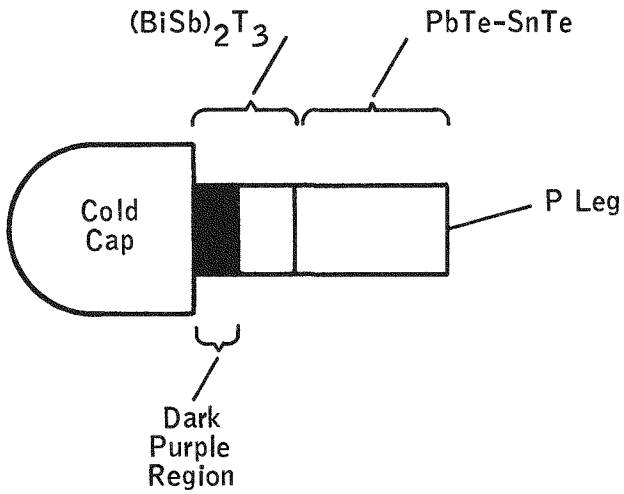

Figure 4-26. Post-Test P Leg with Purple Reaction Zone

The P-leg control samples did not have the purple reaction zone.

3) No difference in resistivity could be detected between the remaining portion of the bismuth-antimony-telluride (BiTe-SbTe) and the lead-tin-telluride (PbTe-SnTe) segments.

A summary of the post-test resistivity data is given in Table 4-15.

Table 4-15. Post-Test Data for Module A-2 Legs Resistivity at Room Ambient Temperature Micro-Ohm-Inches

P Legs			N Legs		
Description	Purple Region	Remaining Portion	Description	PbTe ρ = 120 $\mu\Omega$-in	PbTe ρ = 400 $\mu\Omega$-in
1P*	107	250	1N	120	395
2P	136	253	2N	115	410
3P	114	302	3N	130	No Data
4P	120	332	4N	120	385
5P	120	300	5N	110	390
6P	115	276	6N	120	388

*Cracked leg (cracked zone was 1.5 $\mu\Omega$)

4.8.3.1.2 Converter P-1

Within ±20 percent accuracy, there was no apparent difference between the pre-test and post-test resistivity results for the N and P legs.

4.8.3.2 Seebeck Results

The accuracy of the Seebeck voltage measurements is considered to be ±5 percent. Seebeck analysis is a very sensitive method for determining changes in thermo-electric properties.

4.8.3.2.1 Module A-2

A summary of the Seebeck analysis results of the legs for Module A-2 and the unused control samples are given in Table 4-16. The results are expressed in millivolts and represent the voltage across the sample when the cold side temperature is at 75°F, and the hot side temperature is at 675°F.

Refer to Figure 4-24 for the relative positions of the various leg sections.

Table 4-16. Seebeck Data for SNAP-23 Module A-2 (mv)
T_c = 75°F
ΔT = 600°F

Portion No.	Standard N	1N	2N	5N	Standard P	1P	2P	5P
1	52.1	58	57	60	35.2	28	28	28
2	54.0	54	51	56	33.7	31	31	31
3	53.0	52	51	53	31.7	28	27	27
4	87.0	82	77	86	51.0	28	50	44
5	82.5	83	80	82	56.9	21	23	30

4.8.3.2.2 Converter P-1

The Seebeck results for legs from Converter P-1 and the control samples are given in Table 4-17. All Seebeck voltage results were determined at a 675°F hot side and 75°F cold side on the leg sections. Relative positions of the numbered sections are illustrated in Figure 4-24 for the N legs and Figure 4-25 for the P legs.

In addition, Table 4-17 includes the locations of the various legs in the converter as to radial row number, along with an estimate of the average hot electrode temperature of the legs during thermal gradient performance.

Table 4-17. Seebeck Data for SNAP-23 Converter P-1 All with 600°F ΔT; T_c = 75°F (Seebeck in mv)

	ROW NUMBER																									
	Radial Row Number	1					2					3					4					5				
	Temperature (Hot Est)	1035°F					1039°F					1042°F					1046°F					1050°F				
	Leg Identification	Section Numbers					Section Numbers					Section Numbers					Section Numbers					Section Numbers				
		1	2	3	4	5	1	2	3	4	5	1	2	3	4	5	1	2	3	4	5	1	2	3	4	5
P Legs	B-28	34	34	32	42																					
P Legs	B-52	33	32	35	46																					
P Legs	B-136	33	33	32	46																					
P Legs	B-144			45	44																					
P Legs	B-6	33	34	44	45																					
P Legs	G-123																					32	32	46	44	
P Legs	R-82																	32	32	45	46					
P Legs	G-78											33	29	45	44											
P Legs	G-76																					33	33	46	43	
P Legs	G-73																									
P Legs	G-71																									
P Legs	G-70																									
P Legs	G-69																									
P Legs	B-129																									
P Legs	G-85																									
P Legs	G-80																									
P Legs	G-117																									
P Legs	R-59																									
P Legs	B-112																									
P Legs	B-74																									
N Legs	B-28	58	57	53	62	73																				
N Legs	B-52	56	58	57	56	76																				
N Legs	B-136	62	59	55	62	77																				
N Legs	B-144																									
N Legs	B-6	56	56	56	56	80																				
N Legs	G-123																62	59	59	66	86					
N Legs	R-82																					65	59	58	58	83
N Legs	G-78						62	58	58	60	82															
N Legs	G-76																64	59	58	73	86					
N Legs	G-73																									
N Legs	G-71																									
N Legs	G-70																									
N Legs	G-69																									
N Legs	B-129																									
N Legs	G-85																									
N Legs	G-80																									
N Legs	G-117																									
N Legs	R-59																									
N Legs	B-112																									
N Legs	B-74																									

	ROW NUMBER																									
	Radial Row Number	6					7					8					9					10				
	Temperature (Hot Est)	1054°F					1058°F					1062°F					1066°F					1070°F				
	Leg Identification	Section Numbers					Section Numbers					Section Numbers					Section Numbers					Section Numbers				
		1	2	3	4	5	1	2	3	4	5	1	2	3	4	5	1	2	3	4	5	1	2	3	4	5
P Legs	B-28																									
P Legs	B-52																									
P Legs	B-136																									
P Legs	B-144																									
P Legs	B-6																									
P Legs	G-123																									
P Legs	R-82																									
P Legs	G-78																									
P Legs	G-76																									
P Legs	G-73						33	34	43	44																
P Legs	G-71																34	32	42	45						
P Legs	G-70																									
P Legs	G-69																									
P Legs	B-129																									
P Legs	G-85						34	32	42	48																
P Legs	G-80																									
P Legs	G-117																34	32	44	45						
P Legs	R-59																									
P Legs	B-112																									
P Legs	B-74																									
N Legs	B-28																									
N Legs	B-52																									
N Legs	B-136																									
N Legs	B-144																									
N Legs	B-6																									
N Legs	G-123																									
N Legs	R-82																									
N Legs	G-78																									
N Legs	G-76																									
N Legs	G-73	62	57	57	61	84																				
N Legs	G-71											56	55	57	68	83										
N Legs	G-70																					69	59	57	68	85
N Legs	G-69																									
N Legs	B-129																									
N Legs	G-85	65	60	58	66	85																				
N Legs	G-80																					64	60	58	66	87
N Legs	G-117											63	58	59	69	85										
N Legs	R-59																									
N Legs	B-112																									
N Legs	B-74																									

	ROW NUMBER																				
	Radial Row Number	11					12					13					14				
	Temperature (Hot Est)	1074°F					1077°F					1081°F					1085°F				
	Leg Identification	Section Numbers					Section Numbers					Section Numbers					Section Numbers				
		1	2	3	4	5	1	2	3	4	5	1	2	3	4	5	1	2	3	4	5
P Legs	B-28																				
P Legs	B-52																				
P Legs	B-136																				
P Legs	B-144																				
P Legs	B-6																				
P Legs	G-123																				
P Legs	R-82																				
P Legs	G-78																				
P Legs	G-76																				
P Legs	G-73																				
P Legs	G-71																				
P Legs	G-70	33	33	29	45																
P Legs	G-69											32	33	48	47						
P Legs	B-129																34	33	42	44	
P Legs	G-85																				
P Legs	G-80	34	31	45	45																
P Legs	G-117																				
P Legs	R-59																33	34	43	46	
P Legs	B-112																28	34	45	42	
P Legs	B-74																34	33	48	47	
N Legs	B-28																				
N Legs	B-52																				
N Legs	B-136																				
N Legs	B-144																				
N Legs	B-6																				
N Legs	G-123																				
N Legs	R-82																				
N Legs	G-78																				
N Legs	G-76																				
N Legs	G-73																				
N Legs	G-71																				
N Legs	G-70																				
N Legs	G-69						63	58	58	58	84										
N Legs	B-129																63	59	56	67	79
N Legs	G-85																				
N Legs	G-80																				
N Legs	G-117																				
N Legs	R-59																69	59	55	57	82
N Legs	B-112																66	56	56	67	80
N Legs	B-74																67	60	55	65	83

	Ident.	1	2	3	4	5
Controls	P-11	34	34	35	47	
Controls	P-10	34	34	50	50	
Controls	P-9	34	33	44	52	
Controls	N-11	58	57	56	71	85
Controls	N-10	57	57	57	75	85
Controls	N-9	56	60	57	60	76

NOTE Controls come from SLP 34843 Lot 52 (N Legs), Lot 53 (P Legs) Batch 1. Legs in converter were given a color code Blue batch (B) is SLP 34843 Lot 39 Batch 2, Green Batch (G) Lot 39, Batch 2, Red Batch (R) Lot 39 Batch 1, and instrumented legs (N type) Lot 52 Batch 1 instrumented legs (P type) Lot 53 Batch 1.

4.8.4 DISCUSSION OF RESULTS

4.8.4.1 Resistivity

The following general comments can be made about the legs from Module A-2 and Converter P-1:

- There was no apparent change in resistivity of the N legs from either thermopile during thermal gradient performance.

- There was no apparent change in resistivity of the P legs from the converter, while the resistivity of the P legs from the module decreased markedly in a 0.04-inch region adjacent to the cold cap. Refer to Table 4-15.

The monitored P legs in Module A-2 were decreasing in resistance during the 18,100 hours of operation and had decreased to below the expected material resistance value. Refer to Figure 3-10.

4.8.4.2 Seebeck

The results of the Seebeck analysis on the N and P legs indicate the following:

4.8.4.2.1 N Legs

The Seebeck properties of the N legs changed in sections numbered 1 and 4 for both the module and the converter during thermal gradient performance. There was no apparent difference in Seebeck voltage between the control and operated legs in the other three leg sections.

For section number 1 near the hot electrode, the Seebeck voltage was greater in the operated legs of the converter and module than in the control sample. The extent to which the increase occurs, appears to be strongly temperature dependent as illustrated in Figure 4-27. Figure 4-27 is a plot of the difference in Seebeck voltage, for a 600°F ΔT, between sections numbered 1 and 2 as a function of radial row number in the converter. The differences in Seebeck voltage between sections 1 and 2 were plotted for the following two reasons:

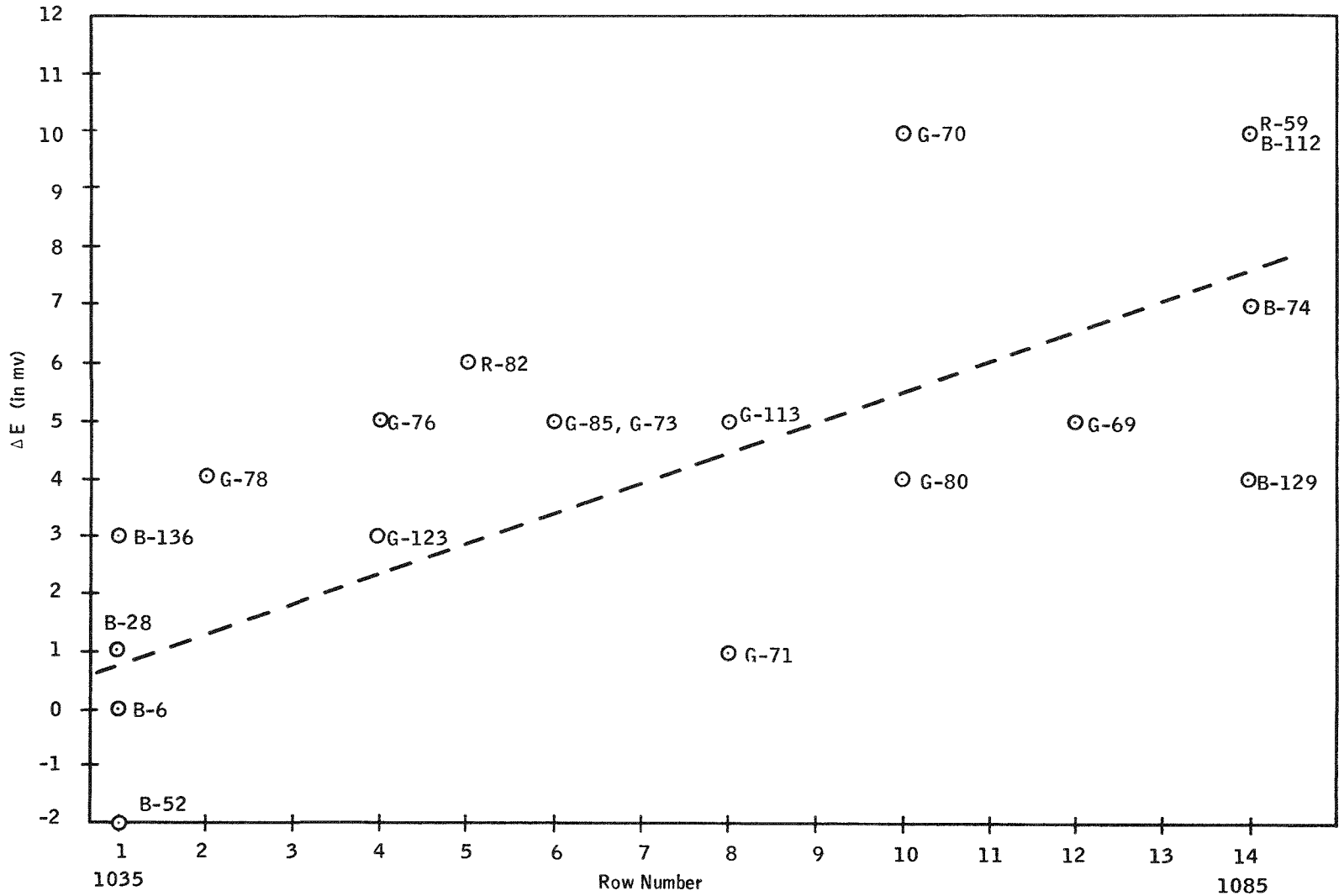

Figure 4-27. ΔE Between Segment No. 1 and No. 2 (E_1 - E_2) for N Legs Seebeck Voltage Measured for T_c = 75°F and ΔT = 600°F

- It is a gauge for measuring the inhomogeneity of the hot end thermoelectric material.

- If section number 2 has not changed, it can be used to determine the net change in Seebeck voltage of section number 1, assuming both sections had originally the same thermoelectric properties.

It is evident from Figure 4-27 that a strong correlation existed between radial row number and voltage difference (ΔE). Radial row 14 was at the base of the converter, which had an average hot electrode temperature of 1085°F during operation, compared to 1035°F average hot electrode temperature at radial row 1 near the top of the converter.

Although a change occurred in the thermoelectric properties of the N legs near the hot electrode, the change would not necessarily influence the performance of the N legs during operation. As a matter of fact, the majority of the evidence indicates that it had very little effect on the voltage performance of the N legs. This is based on two pieces of evidence:

1) Module A-2 and Converter P-1 N leg performance – the N legs' Seebeck voltages were stable throughout their performance lives.

2) Seebeck coefficient values for sections 1, 2, and 3 tend to converge above 1025°F (refer to Figure 4-28). Although the Seebeck coefficient of section 1 is greater than for sections 2 and 3 in the temperature range from 125°F to 1025°F, there is evidence from Figure 4-28 that all three coefficients may converge at some temperature above 1025°F. Since section 1 operated in the temperature region near and above 1000°F, it is likely that any possible increase in Seebeck voltage of the N legs due to section 1 was small. In addition, any increase in Seebeck voltage of the N legs due to section 1 may be negated by the observed decrease in Seebeck voltage of section 4.

For section number 4, adjacent to the hot segment interface, the Seebeck voltage was less in the operated legs of the converter and module than in the control legs.

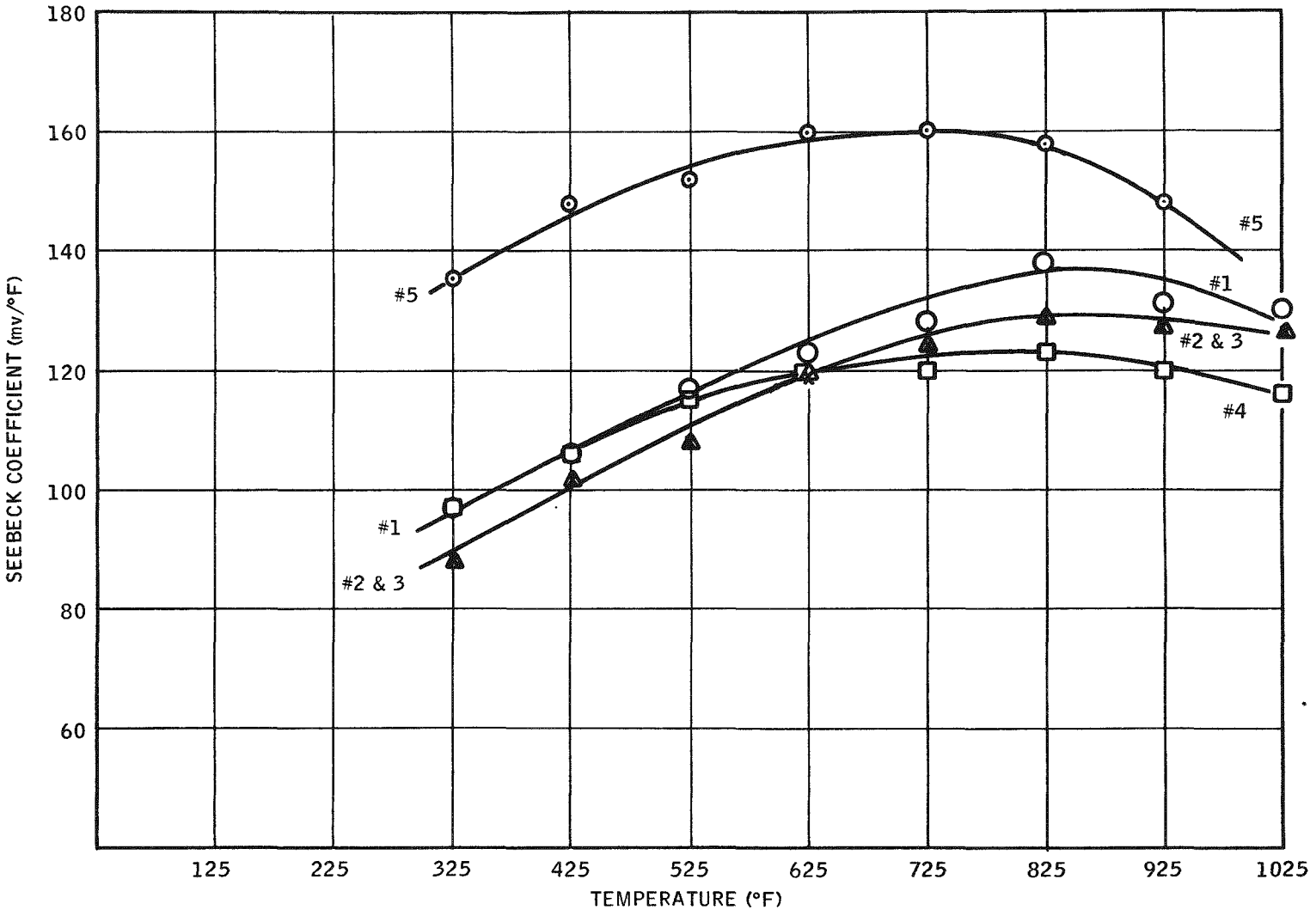

Figure 4-28. Seebeck Coefficient vs Temperature for G-73 (N leg) Converter P-1

4.8.4.2.2 P Legs

There was no apparent difference in Seebeck properties between the control and operated legs from Converter P-1. This paragraph will discuss the anomalies observed in the Seebeck characteristics of the operated P legs from Module A-2:

> The Seebeck voltage was less in the operated legs than in the control sample for all 5 sections. The greatest differences occurred in sections 1, 4, and 5. Refer to Table 4-16. For section 5 adjacent to the cold electrode, the Seebeck voltage values of the operated legs were only 35 to 55 percent of the control value, suggesting the possibility that the P legs were attacked by material adjacent to the cold end. Chemical analysis of the cold end material revealed that the bismuth-antimony telluride was contaminated with copper from the cold electrode. Refer to Section 4.10.4. The Seebeck voltage values for section 4 were higher than section 5, but still below the control sample value.

It is interesting to note that the low Seebeck voltage values near the hot end of the operated P legs (section 1) are consistent with those observed in the SNAP-27 Program (reference, Performance Test Report for 10-Couple Modules ST10B-1 and ST10C-3, SNAP-27 Program, Phase II B(U), Report No. MMM 8406-1604, dated 30 June 1967). Since the SNAP-27 Program uses the same P material as was used in the hot end P segments from Module A-2, it is not surprising that similar changes should occur in the Seebeck performance of the hot end segments from Module A-2.

4.9 DIMENSIONAL ANALYSIS

4.9.1 BACKGROUND

This paragraph is primarily concerned with changes in geometry of the legs from Module A-2 and Converter P-1 during operation. Leg geometry was determined for the operated legs and then compared with unused control samples. Many of the dimensional results for Converter P-1 are delineated in paragraph 4.4 and will not be duplicated here.

4.9.2 ANALYTICAL PROCEDURES

4.9.2.1 Module A-2

Using a micrometer, length and diameter were measured on all legs from the module. The leg geometry of the operated legs was then compared with an unused control sample from the same batch of manufactured legs used in the module.

4.9.2.2 Converter P-1

Immediately after converter disassembly, all available legs that had been removed were checked for post-test dimensions. An optical comparator was used, magnifying the legs 20X to facilitate accurate measurements. Measurements taken on both N and P legs were:

- Leg maximum length
- Leg minimum length
- Upper leg diameter
- Lower leg diameter (across sublimate buildup)

Legs were dimensioned in a random fashion, precluding to some extent, the possibility of a data trend influencing the operators measurements. Leg data was then sorted into axial and radial row groups.

4.9.3 RESULTS

The results for Module A-2 are given in Table 4-18.

Table 4-18. Dimensional Results for Module A-2

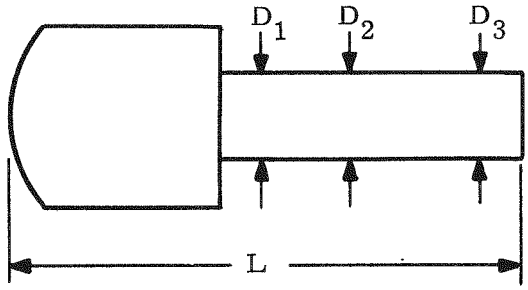

Identification	D_1	D_2	D_3	L
1N	0.200	0.196	0.196	0.876
2N	0.197	0.188	0.189	0.899
3N	0.199	0.189	0.189	0.876
4N	0.199	0.189	0.189	0.876
5N	0.199	0.189	0.191	0.877
6N	0.207	0.188	0.189	0.868
1P	0.198	0.192	0.206	0.891
2P	0.199	0.190	0.196	0.891
3P	0.199	0.190	0.195	0.887
4P	0.198	0.191	0.197	0.888
5P	0.195	0.191	0.194	0.885
6P	0.199	0.189	0.194	0.888
Control N	0.187	0.188	0.188	0.886
Control P	0.188	0.188	0.187	0.886

Both the N and P legs from the module showed evidence of sublimation. The N and P legs were rounded at the hot end corners with the greatest amount of rounding occurring for the N legs. Refer to Section 4. 4. 4. 2.

Converter P-1 results are summarized in Table 4-19. Post-test measurements at location A are not included, since they were unchanged from pre-test values.

It should be noted that all of the N legs from the converter had a tendency toward distortion of their geometry along their vertical axes. This is shown graphically in Figure 4-29 and to a lesser extent in Figure 4-18. All of the N legs accommodated themselves to the angular displacements of the hot electrodes. Refer to Section 4. 4. The P legs were considerably less distorted than the N legs and showed evidence of rounding at the hot end edges.

4. 9. 4 DISCUSSION OF RESULTS

The N legs from the converter showed the greatest evidence of material creep. This may be due, in part, to the higher contact pressure (250 psi) for the legs in the converter. The P legs, being harder, demonstrated greater resistance to creep.

It is interesting to note that the contact areas for the N legs from the module were reduced to approximately 10 percent of the leg's initial cross-sectional area. Refer to Section 4. 4. 4. 2. This means that (based on measured spring forces and measured contact areas) the effective contact pressures were about 1500 psi at the time of post-test disassembly. It is likely that most of the N leg material creep occurs during the early hours of operation. This is based on two reasons:

- N leg resistance stability –

  The resistance of the N legs from the converter was stable throughout the test duration, suggesting that any geometrical change in the N legs occurred during the pre-test processing and early "run in" of the converter.

Table 4-19. Average Dimensions of P and N Legs Versus Axial Position for Converter P-1

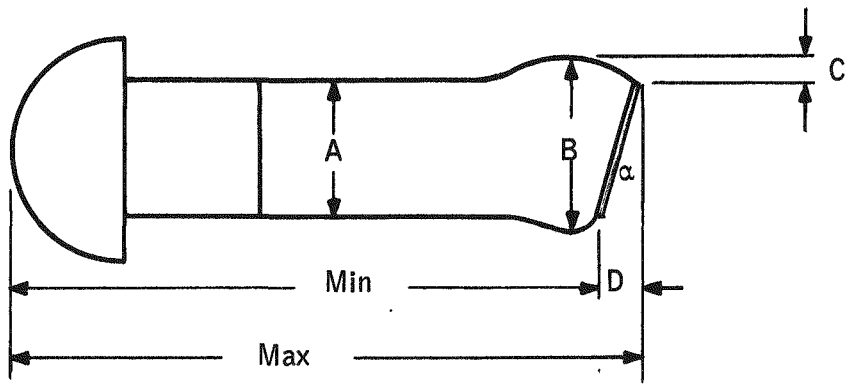

A and B = Pre-test

Standard = 0.187 inch

Pre-test Average = 0.6764 inch for N legs; 0.6777 inch for P legs.

Radial Row a Type (Average)	Maximum	Minimum	Average	Difference (Max - Min)	$\frac{C}{\frac{B-A}{2}}$
1N	0.6665	0.6654	0.6660	0.0011	0.0047
1P	0.6733	0.6702	0.6717	0.0031	0.0023
2N	0.6645	0.6621	0.6633	0.0024	0.0045
2P	0.6726	0.6707	0.6717	0.0019	0.0020
3N	0.6659	0.6634	0.6647	0.0025	0.0041
3P	0.6731	0.6711	0.6721	0.0020	0.0023
4N	0.6639	0.6618	0.6629	0.0021	0.0047
4P	0.6713	0.6694	0.6704	0.0019	0.0022

Table 4-19. Average Dimensions of P and N Legs Versus Axial Position for Converter P-1 (Continued)

Radial Row a Type (Average)	Maximum	Minimum	Average	Difference (Max - Min)	C $\frac{B - A}{2}$
5N	0.6653	0.6636	0.6645	0.0017	0.0041
5P	0.6715	0.6699	0.6707	0.0016	0.0025
6N	0.6646	0.6609	0.6628	0.0037	0.0052
6P	0.6711	0.6683	0.6697	0.0028	0.0021
7N	0.6656	0.6625	0.6641	0.0031	0.0045
7P	0.6719	0.6687	0.6703	0.0032	0.0029
8N	0.6651	0.6601	0.6626	0.0050	0.0056
8P	0.6698	0.6655	0.6677	0.0043	0.0026
9N	0.6671	0.6624	0.6648	0.0047	0.0047
9P	0.6720	0.6686	0.6703	0.0034	0.0025
10N	0.6653	0.6576	0.6615	0.0078	0.0060
10P	0.6709	0.6662	0.6686	0.0047	0.0030
11N	0.6674	0.6614	0.6644	0.0060	0.0050
11P	0.6698	0.6673	0.6686	0.0025	0.0032
12N	0.6656	0.6537	0.6597	0.0119	0.0066
12P	0.6702	0.6638	0.6670	0.0064	0.0030
13N	0.6651	0.6576	0.6614	0.0075	0.0053
13P	0.6724	0.6680	0.6702	0.0044	0.0036
14N	0.6632	0.6429	0.6531	0.0203	0.0074
14P	0.6725	0.6563	0.6644	0.0162	0.0044

*All dimensions are in inches

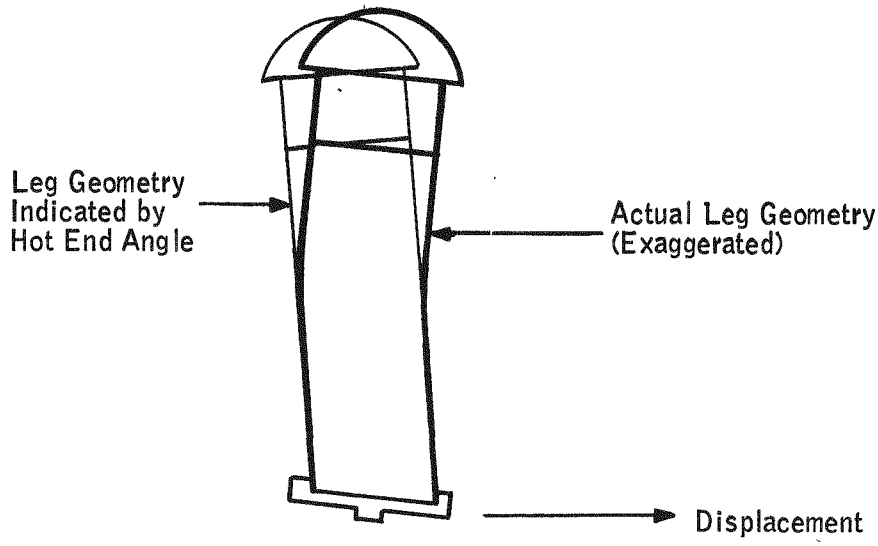

Figure 4-29. Axial Deformation of N Legs

- Module A-2 contact pressure –

  There were no noticeable material creep effects for the N legs from the module, even though they had extremely large contact pressures during the latter stages of operation.

4.10 CHEMICAL ANALYSIS OF COUPLES

4.10.1 BACKGROUND

After the module and converter were disassembled, chemical analyses were performed on three couples from the converter and two couples from the module. Unused control samples were analyzed in a similar manner and then compared with the operated couples to determine if there had been any changes in the chemical properties of the thermoelectric materials due to the extended thermal gradient operation.

Three couples were analyzed from the following three positions in the converter:

- Extreme top (radial row 1)
- Near the center of the thermopile (radial rows 6 and 7)
- Extreme bottom (radial row 14)

These three couples had operated at three different average hot electrode temperatures during operation ranging from 1035° F to 1085° F. A tabulation of the history of these couples, along with the control sample, is given in Table 4-20.

Table 4-20. Converter H Couple History and Control Sample

Identification				Location		Time on Test (Hrs)	Nominal Temperatures			
							T_h (° F)		T_c (° F)	
Couple #	Slp #	Lot #	Batch #	P	N		P	N	P	N
B-22	34843	39	2	R1A3	R1A4	10,800	1035	1035	200	200
R-30	34843	39	2	R7A13	R6A13	10,800	1058	1054	207	207
B-115	34843	39	1	R14A24	R14A25	10,800	1085	1085	214	214
C-133	34843	49	1	-	-	-	-	-	-	-

Couple 133 was the control sample

Converter P-1 N and P legs were segmented. That is, the hot and cold ends have different compositions which are designed to give optimum performance in their respective temperature ranges. The N legs contain 3N PbTe (ρ=120$\mu\Omega$-in. @ 75° F) at the hot end and a lighter doped 4N (ρ=400$\mu\Omega$-in. @ 75° F) at the cold end. The P legs have 3P (PbSnTe) at the hot end and bismuth-antimony-telluride at the cold end. In addition, the copper cold caps in the converter were nickel plated.

Two couples, numbers 3 and 4, from Module A-2 were analyzed in the same manner as an unused control sample. The control sample came from the same lot and batch as the operated A-2 couples. A history of the operated and control legs is given in Table 4-21.

Table 4-21. Module A-2 Couple and Control Sample

Identification	Slp-Lot-Batch		Time on Test (In Hours)	Temperatures	
	N	P		T_h (° F)	T_c (° F)
Couple #3	34843-9-1	34843-12-1	18,100	1100	190
Couple #4	34843-9-1	34843-12-1	18,100	1100	190
Control	34843-9-1	34843-12-1	18,100	-	-

Module A-2 legs were segmented with hot and cold end materials as in Converter P-1. In the P legs, the $(BiSb)_2Te_3$ and 3P materials were separated by a stainless steel barrier disc which is intended to prevent diffusion across the $(BiSb)_2Te_3$ / 3P interface.

The subject of this section of the report is a comparison of the chemical differences between the control and operated legs. This is a full report of all observations obtained during the analyses.

4.10.2 ANALYTICAL PROCEDURES

The N and P elements in the control and operated couples were analyzed for composition changes, phase changes, and diffusion effects by electron microprobe, emission spectrographic and x-ray diffraction techniques. Both the electron microprobe and emission spectrographic data are semi-quantitative since corrections necessary for quantitative analyses were not made. The microprobe data are generally within ±15 percent of the amount present, while the emission spectrographic results are accurate to within a factor of 1/2 to 2 times the amount present. X-ray diffraction analyses were restricted to qualitative identification of the species present.

4.10.3 RESULTS

4.10.3.1 Converter P-1

The chemical results for operated and control samples from Converter P-1 are as follows:

4.10.3.1.1 N Legs

With reference to the diagram of the N legs in Figure 4-30, the results of the analyses start at the cold junction and proceed through the hot junction.

1. Microprobe analyses of both the control and operated legs showed a thin (5 microns – 0.0002 in.) Cu-Sn alloy at the nickel plated copper cold cap-tin solder interface. In both the control and operated legs, the solder was about 15-50 microns (0.0006 – 0.002 in.) thick with only an

occasional intrusion of tin extending into the leg. These intrusions of tin extended about 50 microns (0.002 in.) away from the cold cap. Several small voids and fractures were evident at the Sn-PbTe interface in all legs studied. Random droplets of free lead were observed from the cold junction to the midsection of the control leg.

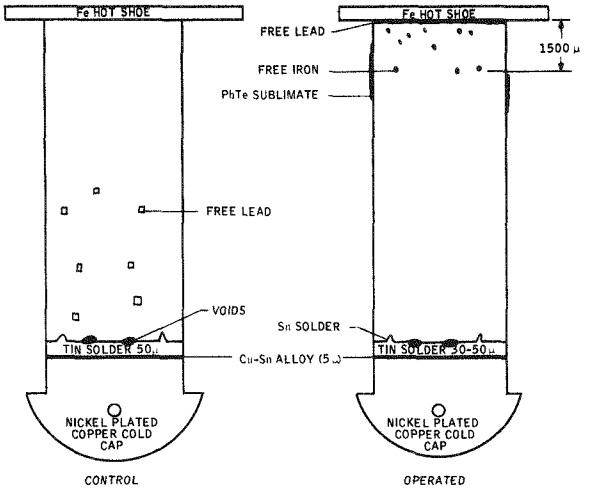

Figure 4-30. Diagram of SNAP-23 Converter P-1 Leg N-Microprobe

2. Sublimed PbTe, identified by x-ray diffraction and microprobe measurements, was observed along the edges and on the surface near the hot junction of the operated legs. These sublimates had about the same composition as the bulk of the leg.

3. Random areas of high lead concentrations were observed by the microprobe along the hot shoe-PbTe interface in the B-115 operated leg. X-ray diffraction analysis of the hot end of a typically operated leg showed a high ratio of free lead to PbTe.

4. At the hot junction of the operated leg and about 1500 microns (0.060 in.) into the PbTe, there are randomly distributed grains of free iron.

5. The N legs were analyzed for diffusion and contamination effects by taking microdrillings and analyzing these drillings spectrographically. The concentrations, in ppm, at various positions shown in Figure 4-31, are given in Table 4-22.

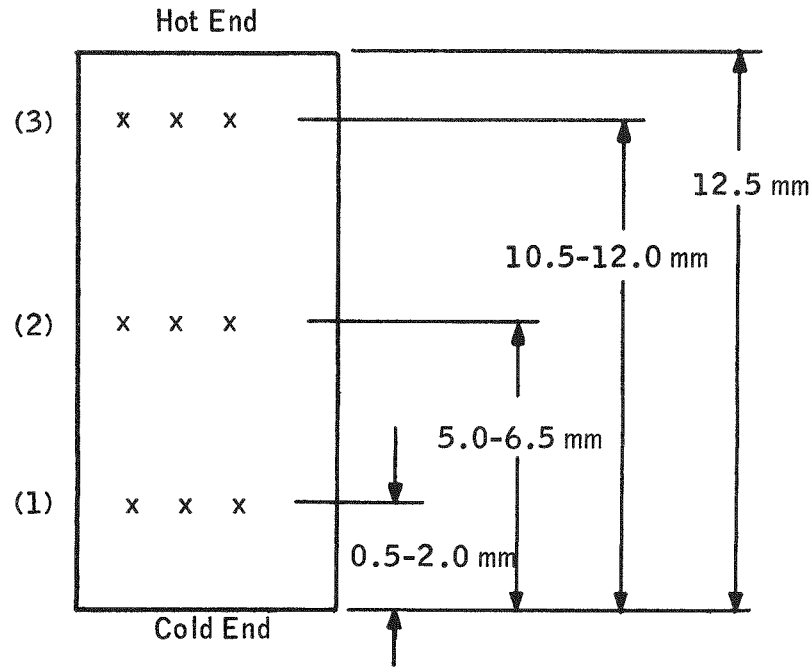

Figure 4-31. Relative Position of Microdrilling Samples in N Legs of Converter P-1

Table 4-22. Emission Spectrographic Results for N Legs From Converter P-1 (All concentrations in PPM)

Element	Control			Operated		
	Position Number			Position Number		
	3	2	1	3	2	1
Fe	250	300	3	600	350	3
Si	5	10	30	10	20	30
Ni	350	330	100	40	300	100
Cu	3	30	5	<1	<1	3
Sn	3	2	<1	150	2	3
Mn	3	3	<3	20	<3	<3

6. Concentration gradients across the 3N and 4N segments could not be evaluated by the microprobe because the segments differ by only small amounts of lead to which the microprobe is insensitive.

The Be, B, Na, Cr, Bi, and Sb concentrations were all below the level of detection in both the control and operated legs.

4.10.3.1.2 P Legs

With reference to the diagram of the P legs in Figure 4-32, the results of the analyses start at the cold junction and proceed through the hot junction.

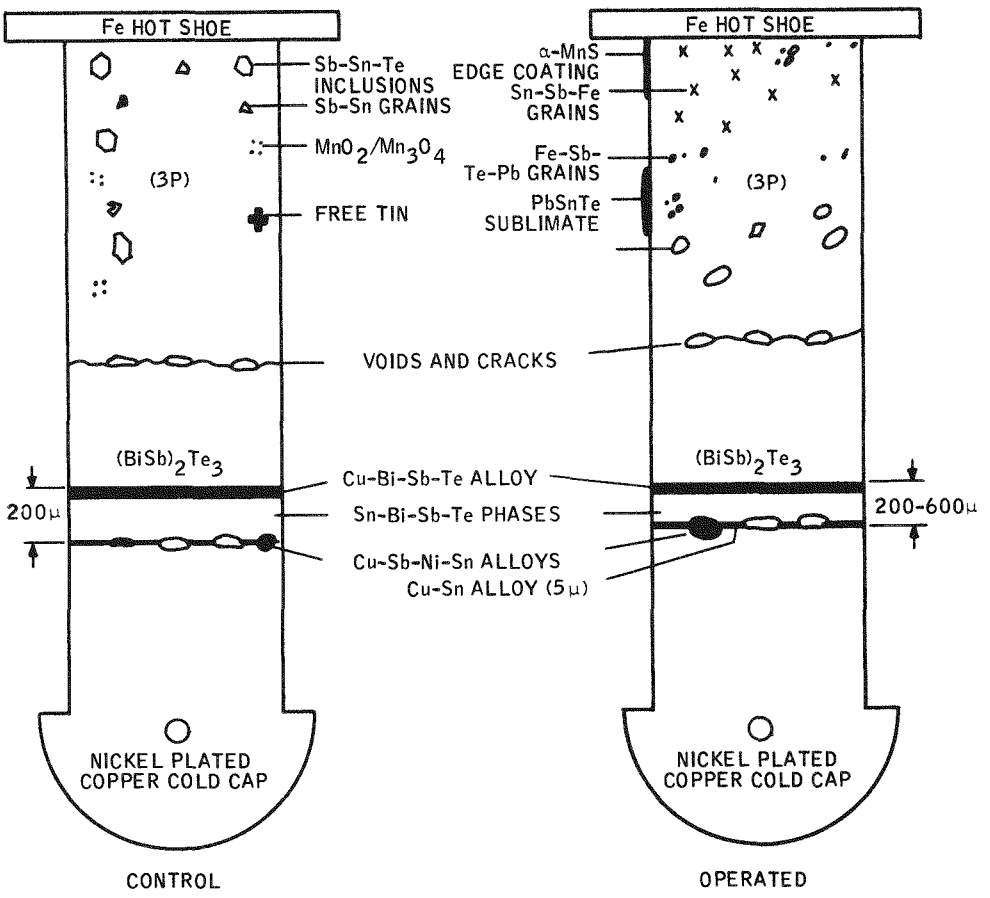

Figure 4-32. Diagram of Converter P-1 P-Segmented Element

1. At the nickel-plated copper cold cap-tin solder interface in all the legs, there are several craterlike phases of Sn-Cu-Sb-Ni which extend into the copper cold cap. The approximate average weight percent composition as determined by the microprobe is:

   18Sn/32Cu/5Bi/40Sb/5Ni

   There are cracks and fractures at the Cu-Sn solder interface and at Sn-$(BiSb)_2Te_3$ interface in all control and operated legs.

2. In all the elements, the microprobe identified several phases of (a) Sn/Bi/Sb/Te and a single phase of (b) Cu/Bi/Sb/Te at the $(BiSb)_2Te_3$-tin solder interface and extending 200-600 microns (0.008 – 0.024 in.) into the $(BiSb)_2Te_3$. Phase (b) is about 100 microns (0.04 in.) thick and forms a band centered about 300 microns (0.012 in.) from the cold cap in the B-22 and B-115 operated legs and in the C-133 control. However, in the R-30 operated leg, the phase "b" is located about 600 microns (0.024 in.) into the $(BiSb)_2Te_3$. The approximate weight composition of these different phases, as measured by the microprobe, are:

control:	a:	34Sn/8Bi/30Sb/28Te
	b:	28Cu/5Bi/25Sb/42Te
operated:	a)	35Sn/8Bi/30Sb/27Te
	b)	20Cu/5Bi/25Sb/50Te

3. To evaluate possible diffusion effects at the $(BiSb)_2Te_3$/PbSnTe interface, microprobe scans across a 120 micron (0.0048 in.) area between the $(BiSb)_2Te_3$/3P interface were made on both the operated and control legs. There was no significant difference between the two. Figure 4-33 shows the concentration variation of Pb, Sn, Te, and Sb across this interface, along with the respective slopes (dc/dx). The slopes are the same for both the control and operated legs, indicating diffusion probably did not occur during operation.

4. At the $(BiSb)_2Te_3$/3P interface in both the control and operated legs, there are several cracks and voids. In the control there is complete

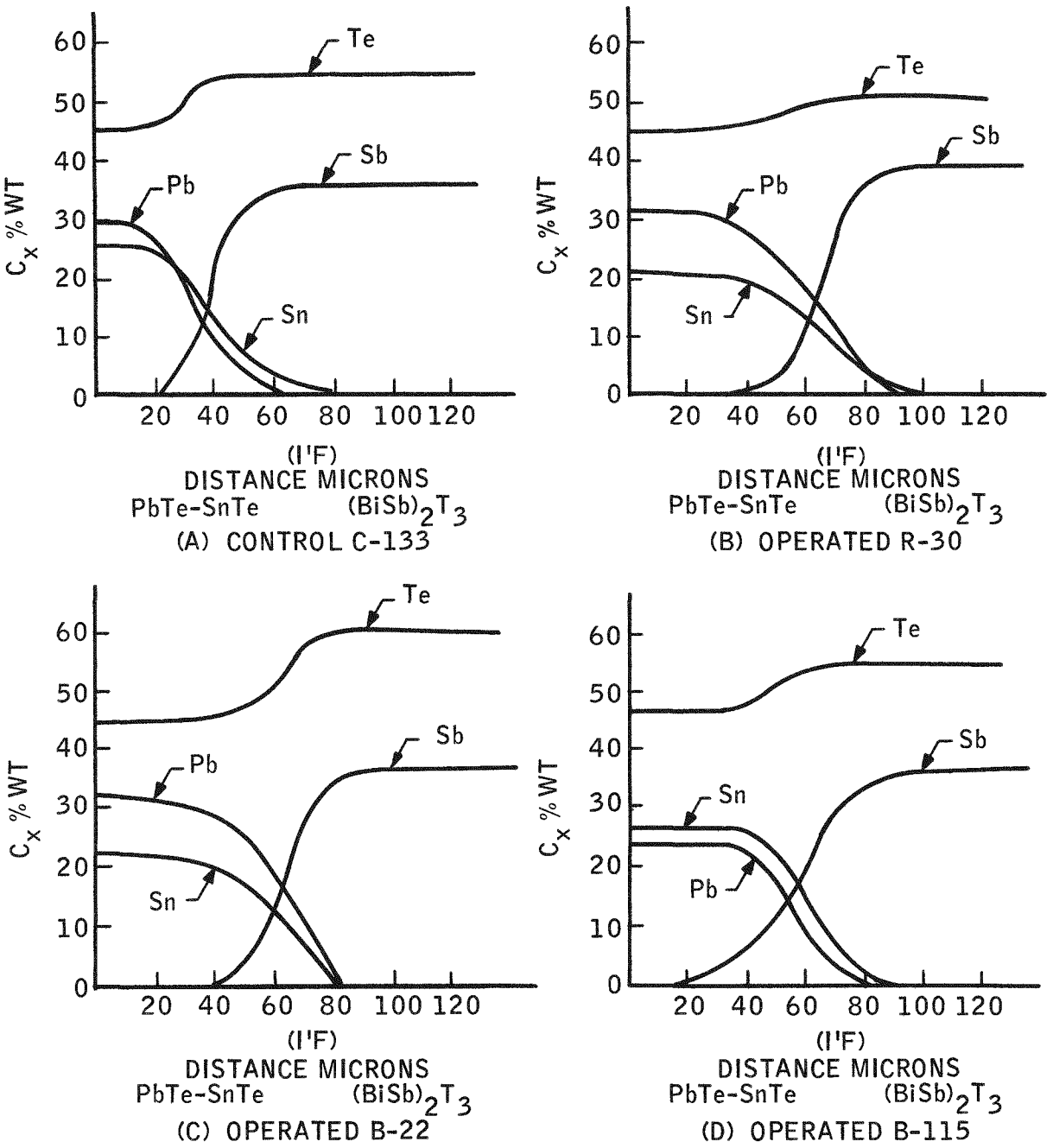

SLOPES = dc/dx

	Te	Sn	Sb	Pb
(A)	0.13	-0.26	0.43	-0.36
(B)	0.12	-0.18	0.29	-0.26
(C)	0.13	-0.18	0.30	-0.26
(D)	0.14	-0.27	0.38	-0.25

Figure 4-33. Diffusion Plots at $(BiSb)_2T_3$ – 3P Interface

separation between the $(BiSb)_2Te_3$ and the 3P. Generally, the voids within the $(BiSb)_2Te_3$ bulk are smaller and more numerous than those in the 3P bulk.

5. A few clusters of discreet grains of $MnO/MnO_2/Mn_3O_4$ were observed throughout the 3P segment of all legs. No significant differences were observed in the occurrence of these clusters between the operated and the control legs. Exact identification of this compound is complicated by the uncertainty in the microprobe oxygen analysis.

6. X-ray diffraction and microprobe analyses identified an α-MnS coating along the edges near the hot junction of the operated P legs.

7. Several sizes of (a) Sn/Sb/Fe grains and (b) Sb/Sn/Fe/Te alloy were observed at the hot junction and about 2500 microns (0.100 in.) into the 3P segment of the operated legs. Microprobe measurements indicated the approximate weight compositions of these inclusions to be:

   a: 61Sb/3Sn/36Fe

   b: 49Sb/10Sn/38Fe/2Te/1Pb

8. Pure Sb grains are randomly distributed throughout the operated 3P segment. In the control leg, there are grains of Sb/Sn along with Sb/Sn/Te inclusions scattered throughout the 3P segment but no free Sb is observed. The approximate weight compositions, measured on the microprobe, of (a) Sb/Sn and (b) Sb/Sn/Te are:

   a) 86Sb/14Sn

   b) 50Sb/49Sn/1Te

9. There are lead-rich and tin-deficient sublimates (relative to the PbSnTe bulk material) along the PbTe-SnTe segment edges near the hot junctions. The approximate weight percent composition of these sublimates, as determined by the microprobe, is:

   43Pb/13Sn/44Te

10. The P legs were examined for diffusion and contamination by the emission spectrographic techniques used for the N legs. The concentrations in ppm at various positions as shown in Figure 4-34 are given in Table 4-23.

4.10.3.2 Module A-2

The chemical results for operated and control samples from Converter P-1 are as follows:

4.10.3.2.1 N Legs

With reference to the diagram of the N elements, Figure 4-35, the results start at the cold junction and proceed through the hot junction.

1. Microprobe analysis of both the control and operated legs showed a thin (<5 microns or 0.0002 in.) Cu-Sn alloy at the copper cold cap-tin solder interface. In both the control and operated legs, the solder itself was about 15-50 microns (0.0006 – 0.002 in.) thick with only an occasional intrusion of tin extending into the leg. These intrusions of tin extended about 50 microns (0.002 in.) away from the cold cap. Several small voids and fractures were evident at the Sn-PbTe interface in all of the control and operated legs. Small lobes of solder were detected along the edges adjacent to the Sn-PbTe interface in all the legs.

2. Sublimed PbTe, identified by x-ray diffraction and microprobe measurements, was observed along the edges and on the outer skin (see Figure 4-36) near the hot junction of the operated legs. These sublimates had about the same composition as the bulk of the leg.

3. Randomly dispersed droplets of free lead were observed by the microprobe at the cold junction and the midsection of both operated and control N legs.

4. The N legs were analyzed for diffusion and contamination effects by taking microdrillings and analyzing these drillings by emission spectroscopy. The concentrations, in ppm at various positions shown in Figure 4-37, are given in Table 4-24.

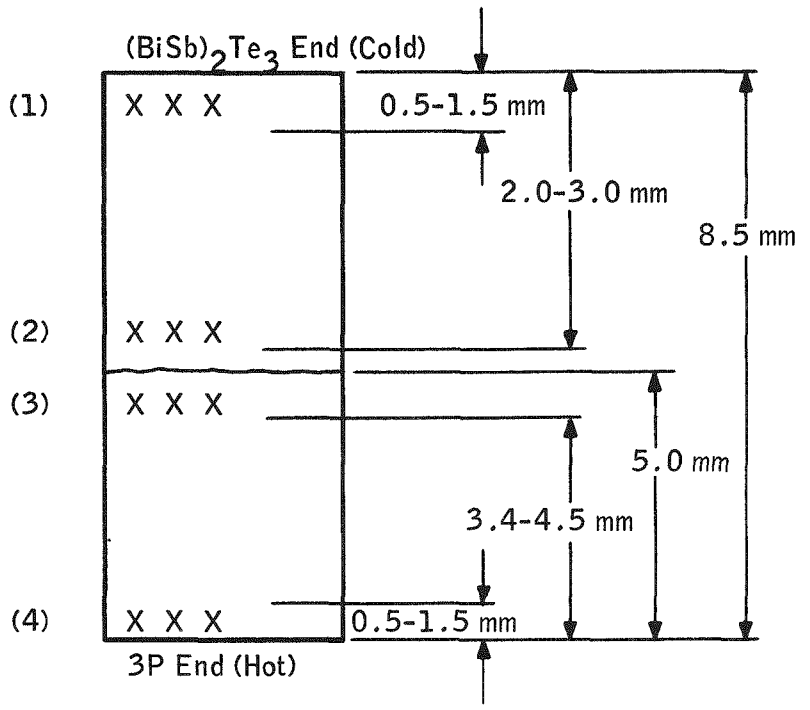

Figure 4-34. Relative Position of Microdrilling Samples in Converter P-1 P-Segment Legs

Table 4-23. Emission Spectrographic Results for N Legs From Converter P-1 (All concentrations in PPM)

Control					Operated			
Position Number					Position Number			
BiTe-SbTe			3P		BiTe-SbTe		3P	
Element	1	2	3	4	1	2	3	4
Fe	<1	<1	1	3	<1	<1	3	900
Si	5	3	<1	3	5	5	40	40
Cu	>1000	5	5	5	900	400	5	5
Bi	-	-	30	5	-	-	300	50
Sb	-	-	>1000	>1000	-	-	>1000	>1000
Na	<10	<10	750	800	<10	<10	700	700
Sn	>1000	>1000	-	-	500	200	-	-
Mn	3	100	-	-	3	3	-	-
Pb	150	>1000	-	-	150	150	-	-
Ni	3	<1	<1	<1	3	<1	<1	<1

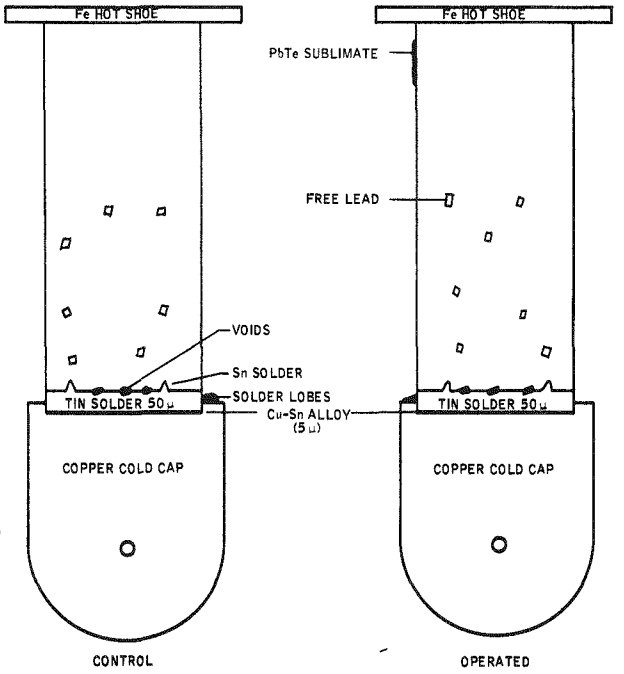

Figure 4-35. Diagram of Module A-2 N Element

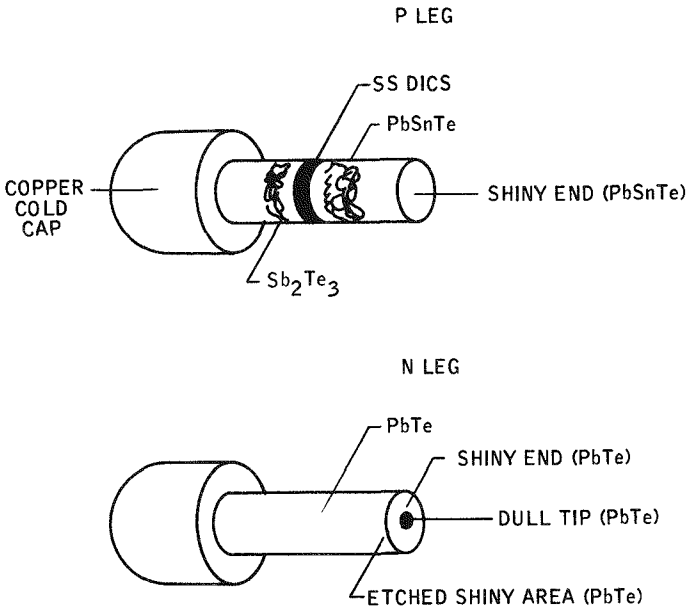

Figure 4-36. Diagram of Skin Sublimates on Operated N and P Elements From Module A-2

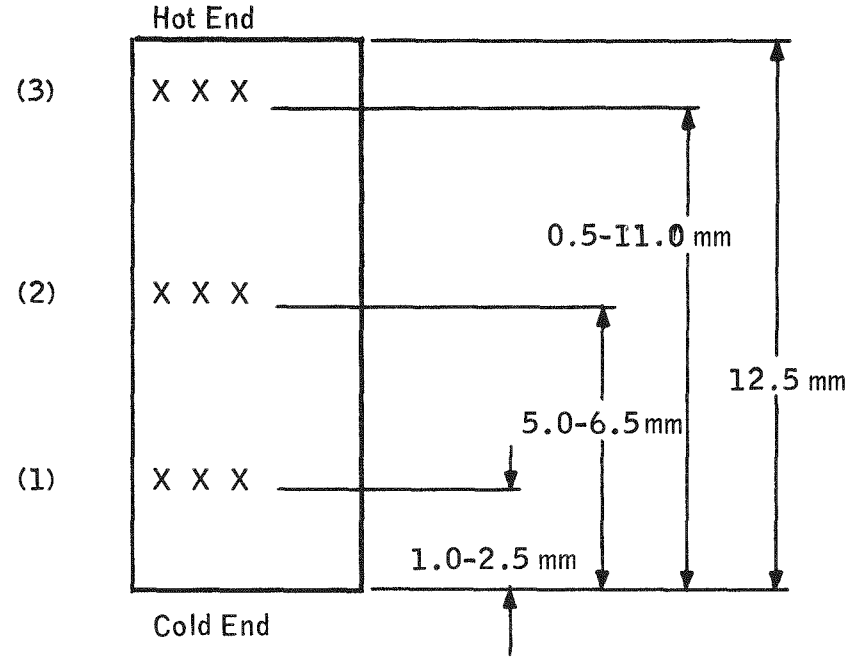

Figure 4-37. Relative Position of Microdrilling Samples in Module A-2 N Legs

Table 4-24. Emission Spectrographic Analysis of N Legs and Control Sample for Module A-2 (Concentrations in PPM)

	Control			Operated		
	Position Number			Position Number		
Element	3	2	1	3	2	1
Fe	<1	<1	1	330	1	<1
Si	5	5	10	20	10	10
Cu	3	5	3	1	1	5
Sn	<1	<1	<1	10	<1	25
Mn	<3	<3	<3	20	<3	5

The Be, B, Na, Ni, Cr, Sb, and Bi concentrations were all below the level of detection in both the control and operated legs.

4.10.3.2.2 P Legs

With reference to the diagram of the P legs (Figure 4-38), the results of the analyses start at the cold junction and proceed through the hot junction.

1. The following are common to control and operated legs: at the cold cap-tin solder interface, the thin Cu-Sn alloy observed in the N legs was observed.

   There are several cracks and fractures at the Sn solder – $(BiSb)_2Te_3$ interface and small lobes of solder along the edges.

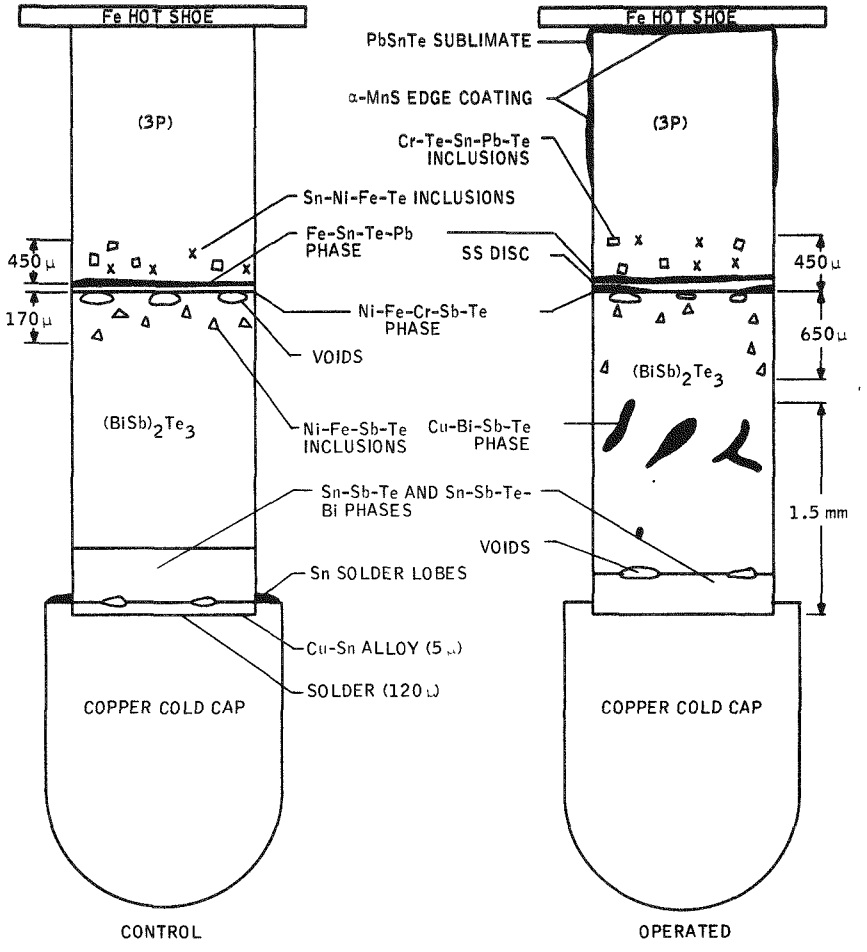

Figure 4-38. Diagram of Module A-2 P-Segmented Element

2. Microprobe measurements on operated and control legs indicated several phases of (a) Sn-Bi-Sb-Te and (b) Sn-Sb-Te which extend 200-400 microns (0.008 – 0.016 in.) into the $(BiSb)_2Te_3$. The approximate weight compositions, averaged over several regions of each phase, as measured by the microprobe, are:

	(a)	(b)
Sn	40	52
Te	42	25
Sb	15	33
Bi	3	-

3. Microprobe measurements on operated legs identified a Cu-Sb-Bi-Te veinlike phase covering about 1/3 to 1/2 of the internal (metallographically polished) surface area of the $(BiSb)_2Te_3$. This veinlike phase starts about 200 microns (0.008 in.) from the cold cap and extends about 1500 microns (0.060 in.) into the $(BiSb)_2Te_3$. The approximate weight percent composition of this phase, determined by the microprobe, is 32Cu-22Sb-5Bi-41Te.

4. Emission spectrographic data on microdrillings taken near the midsection of the bulk of the operated $(BiSb)_2Te_3$ segment gave the following gross weight percent composition of the $(BiSb)_2Te_3$ leg:

Cu	20
B	0.05
Sb	>30
Bi	15
Sn	0.2
Ca	0.02
Te	>30
Si	0.01

5. On the $(BiSb)_2Te_3$ side and adjacent to the stainless steel disc in both operated and control legs, there are phases of Sb-Te-Fe-Cr-Ni. At this

location several fractures are evident. The approximate averaged weight composition of these phases, as measured by the microprobe, is:

Ni	2
Fe	17
Te	55
Sb	19
Cr	7

Ni-Fe-Sb-Te inclusions migrated from the stainless steel barrier disc into the $(BiSb)_2Te_3$ about 170 microns (0.0068 in.) in the control and about 650 microns (0.026 in.) in the operated. The approximate weight composition, as determined by the microprobe is:

Ni	3
Fe	14
Sb	20
Te	62

No significant diffusion of the 3P components into the $(BiSb)_2Te_3$ was observed.

6. On the PbTe-SnTe side and adjacent to the stainless steel disc in both operated and control legs, there are phases of Fe-Te-Pb-Ni-Cr-Sn. At this locale, several minute voids were observed. The approximate averaged weight percent composition, as determined by the microprobe is:

Ni	5
Fe	40
Te	25
Cr	3
Sn	17
Pb	10

Also, Sn-Pb-Te-Cr (a) and Sn-Ni-Fe-Te (b) inclusions migrated about 450 microns (0.018 in.) into the PbTe-SnTe in both the control and operated legs. The phase (a) is more plentiful than phase (b).

Generally, these inclusions are smaller than those observed on the $(BiSb)_2Te_3$ side. The approximate weight compositions, as measured by the microprobe are:

	(a)		(b)
Sn	9	56	56
Pb	7		--
Te	68		12
Cr	14		--
Ni	--		20
Fe	2		12

No significant diffusion of the $(BiSb)_2Te_3$ components into the PbTe-SnTe was observed.

7. X-ray diffraction (Figures 4-36 and 4-39) and microprobe analyses identified an edge coating of α-MnS at the hot junction-hot shoe interface and along the edges of the operated elements. A lesser amount of the α-MnS, along with graphite, was detected by x-ray diffraction in the hot shoe of the operated N elements. Microprobe measurements showed a decrease in the Mn content at the hot junction of the operated elements but not at the hot junction of the control.

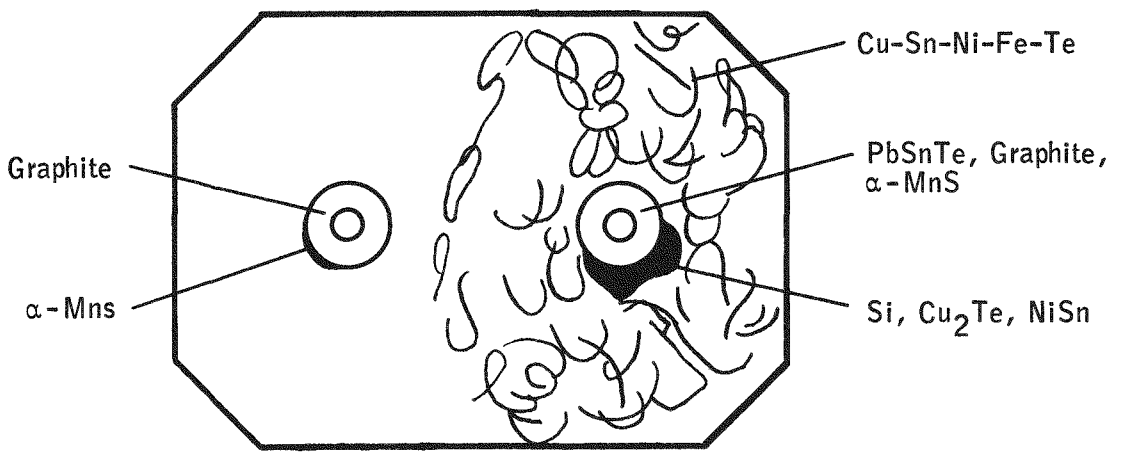

Figure 4-39. Diagram of Hot Shoe From Module A-2

8. There are lead-rich, tin-deficient sublimates along the PbTe-SnTe segment edges near the hot junction of the operated P elements. The approximate weight composition of these sublimates, as determined by the microprobe, is:

Pb	43
Sn	16
Te	41

9. The P elements were examined for diffusion and contamination by emission spectroscopy. The respective concentrations, ppm at various positions shown in Figure 4-40, are given in Table 4-25.

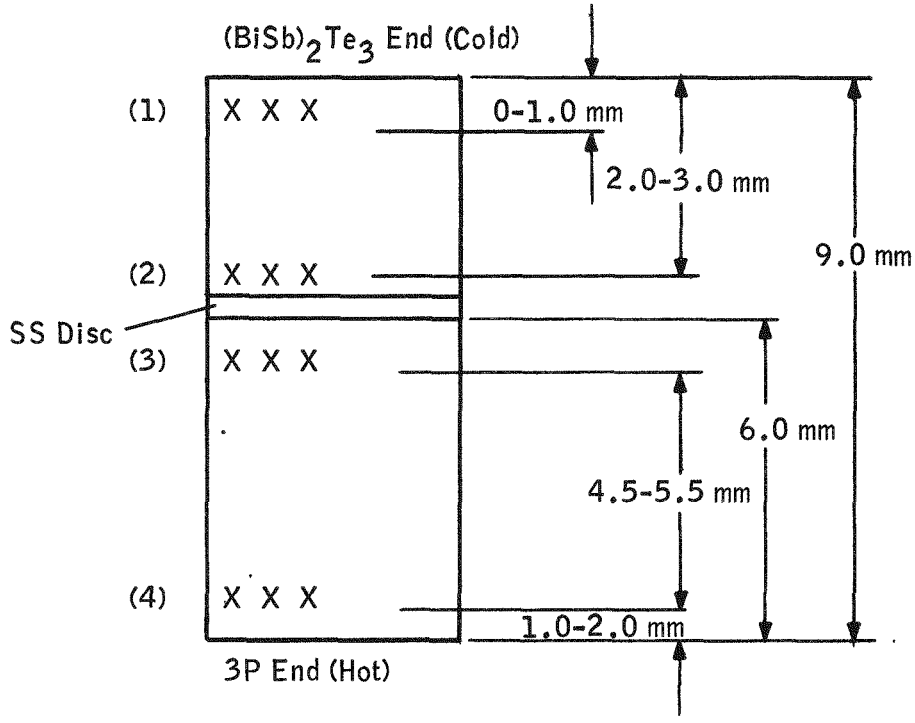

Figure 4-40. Relative Position of Microdrilling Samples in P-Segmented Elements From Module A-2

Table 4-25. Emission Spectrographic Results of P Legs and Control Sample from Module

(Concentration in PPM)

Elements	Control				Operated			
	3P		$(BiSb)_2Te_3$		3P		$(BiSb)_2Te_3$	
	4	3	2	1	4	3	2	1
Fe	3	800	20	<1	700	900	1000	1
Si	15	<1	20	20	200	15	20	40
Cu	5	10	5	500	5	5	>1000	>1000
Bi	<3	10	--	--	<3	50	--	--
Sb	50	300	--	--	50	500	--	--
Na	750	800	<10	<10	800	800	<10	<10
Sn	--	--	15	>1000	--	--	200	900
Mn	--	--	<3	<3	--	--	50	<3
Pb	--	--	200	200	--	--	250	200
Ni	10	1000	<1	<1	5	900	700	2
Cr	5	150	<1	<1	<1	150	250	50

4.10.4 DISCUSSION OF RESULTS

The observed differences between the control and operated couples common to both thermopiles were the following:

1) Pb Te Sublimate deposits were found on the surface near the hot junction of all operated N legs.

2) A lead-rich/tin-deficient sublimate deposit was found along the edges near the hot junction of the operated P legs. The Pb-rich/Sn-deficient sublimate may reflect the higher vapor pressure of PbTe vs PbSnTe, resulting in Pb enrichment of the sublimate by PbTe vaporizing from the N legs.

3) Traces of iron had diffused from the hot electrodes into the hot ends of both the N and P operated legs.

4) α-MnS is observed at the hot junction interface and along the edges of the operated P legs. The α-MnS coating is probably the result of a reaction between Mn from the 3P bulk material and S from the Min-K 1301 thermal insulation.

Observed differences between the control and operated couples not common to both thermopiles were the following:

1) Large grains of Sb are distributed throughout the PbTe-SnTe segments of the converter P legs only.

2) Sb-Sn-Te and Sb-Sn inclusions are distributed throughout the PbTe-SnTe segment of the control sample for the converter. The inclusions are not observed in the operated converter P legs.

3) There was free lead randomly distributed at the hot junction and in the hot shoes of the N operated legs from the converter but was not observed in the control samples or in the module N legs.

4) A Cu-Bi-Sb-Fe veinlike phase was found throughout the BiTe-SbTe segment of the operated P legs from the module. It is believed that the diffusion of the copper into the cold end was the cause of the reduced

resistivity and Seebeck coefficient in the operated $(BiSb)_2Te_3$ segments. Refer to Section 4.8.4. It is suspected that the nickel plating may have hindered copper diffusion in the converter.

5) There was a decrease in Mn content near the hot junction of the operated P legs from the module. No decrease was noted for the control or converter P legs.

6) Stainless steel components from the barrier disc had diffused about 0.026 in. into the $(BiSb)_2Te_3$ material of the operated P legs from Module A-2 and about 0.0068 in. into the control sample.

5.0 CONCLUSIONS

Because Module A-2 and Converter P-1 operated so differently, the conclusions drawn from the two thermopiles will be discussed separately.

5.1 MODULE A-2

Module A-2 had large fluctuations in output performance during operation. The output increased over the first 2000 hours from 1.46 watts to 1.75 watts. Thereafter, the power decreased to 1.23 watts after 18,000 hours.

The initial increase in power was due to a decrease in resistance across the P legs primarily in the hot electrode contact region. In addition, an actual reduction of P leg material resistivity was also evident.

The final power degradation from 1.75 watts to 1.23 watts was caused by two factors:

- A decrease in output voltage due to a decrease in P leg Seebeck voltage.
- An increase in internal resistance due to an increase in resistance across the N leg hot electrode contacts.

The principal cause for the gradual decrease in P leg open circuit voltage was from copper migration into the P leg $(BiSb)_2Te_3$ material. A secondary cause was the loss of manganese, principally near the hot end of the 3P (lead-tin-telluride) segment. Based on data from the converter, a nickel coating on the cold electrodes appears to prevent the migration of copper into the $(BiSb)_2Te_3$ material.

Material sublimation effects near the N leg hot junction interfaces caused an increase in N leg contact resistance and appear to be the major cause of N leg performance degradation. The N legs were rounded off at the hot end from sublimation producing a reduced hot end contact area and a correspondingly large contact resistance.

The Seebeck voltage outputs of the N legs were stable during operation. However, changes in Seebeck characteristics of the N legs were noted during post-test analysis. The changes occurred in two regions:

1) An increase in Seebeck coefficient near the hot electrode.

2) A decrease in Seebeck coefficient in the cold segment (PbTe-3N) material near the segment interface.

The two effects appear to have negated each other producing little change in Seebeck voltage for the N legs.

5.2 CONVERTER P-1

Converter operation was stable except for small thermal changes and a ±5 percent output power fluctuation during the first 2000 hours.

The output power fluctuations were due mainly to the P legs. The N legs operated stably. The post-test analysis did not reveal the cause for the small power fluctuations.

During test operation, the thermal impedance between the cold cap and cold frame increased. This was due to a change in heat transfer characteristics of the grease located between the cap-follower interface and/or a withdrawing of the grease from out of the interface by some sort of capillary action. To what extent the thermal impedance across the cap-follower interface increases is determined by the fit between the two surfaces.

Post-test analysis revealed no apparent change in the thermoelectric properties of the P leg materials. The small changes in Seebeck characteristics of the N legs from Module A-2 were also apparent in Converter P-1. In addition, it was

noted that the increase in Seebeck coefficient near the N leg hot junction was strongly dependent on hot electrode temperature with the greatest increase occurring in the hotter bottom portions of the converter.

Alignment analysis revealed that the legs near the bottom of the converter (rows 13 and 14) had their hot electrodes misaligned approximately 5.5° or 0.066 inch during operation. During cool down the hot electrodes from the bottom couples moved approximately 0.03 inch, decreasing the misalignment to approximately 3.5° or 0.036 inch. All of the boron nitride strips were broken into 8 - 12 pieces and did not appear to restrain the movement of the hot electrodes. The boron nitride strips were probably broken during an early stage of operation.

Since the converter was thermal cycled four times without adverse effects to the output performance, the net effect of misalignment and hot electrode motion appeared to be negligible.

5.3 COMPARISON OF CONVERTER P-1 AND MODULE A-2

The environmental conditions were different in the two thermopiles. The principal differences were:

- Spring pressure – 250 psi for P-1, 150 psi for A-2
- Hot electrode temperature – 1035°F to 1085°F for P-1, 1100°F for A-2

Both spring pressure and hot electrode temperature significantly affected the performance of the two thermopiles. Sublimation was considerably more evident in Module A-2 than in Converter P-1. Higher spring pressure in conjunction with lower hot electrode temperatures produced larger hot electrode contact areas in P-1, resulting in lower contact resistance and higher output power.

Both the converter and the module showed little evidence of oxygen being present. It is significant to note that MnS rather than MnO had formed on the edges of the P legs near the hot end. (A specific re-examination of similar samples analyzed for the SNAP-27 10-Couple Module showed that MnS was present in small amounts along with a larger amount of MnO.)